MULTIFUNCTIONAL REGULATORS OF CARDIAC DISEASE AND DEVELOPMENT

APPROVED BY SUPERVISORY COMMITTEE

Eric N. Olson, Ph.D.

Jane E. Johnson, Ph.D.

Michelle D. Tallquist, Ph.D.

Woodring E. Wright, M.D., Ph.D.

To my supportive friends and family,
especially my mom.

Acknowledgements

I have been blessed to be around many great people that I should be thankful to throughout my graduate school training.

First of all, my deepest appreciation goes to my mentor Dr. Eric N. Olson. It has been my great honor to be a member of his lab. I appreciate him for giving me opportunities to work on exciting projects with great people in an extraordinary environment. I am also very grateful for his constant great support, guidance, and encouragement. I am certain that I will never forget the question that he always asked me, "anything hot?" I will always remember and try to learn his never-ending enthusiasm and love for science. Being a part of the Olson lab has been one of the most memorable and enjoyable experiences of my life.

Dr. Rhonda Bassel-Duby has been like a loving mom throughout my graduate school. I am extremely grateful for her kindness and support, especially after my car accident in January 2008. I greatly appreciate her and Dr. Allan Duby's loving care during the difficult time.

I would like to thank to my thesis committee members, Drs. Jane Johnson, Michelle Tallquist, and, Woodring Wright for their advice and encouragement during my training.

I am grateful to my former mentors in Korea Advanced Institute of Science and Technology Drs. Gou Young Koh and Dae Sik Lim for their constant support.

I am also thankful to Dr. James Richardson, John Shelton, and the histology core members for their great help on histolocial sections and discussion. I would like to thank Dr. Joseph Hill, Yongli Kong, Dr. Andrew Blagg, and Dr. R. Haris Naseem for their help on surgical procedures and cardiac remodeling studies. My deep gratitude goes to Department of Molecular Biology staff members, especially Alisha Tizenor for graphics and Jennifer Brown for help with manuscripts and travel. I am grateful to Xiaoxia Qi for her excellent work on gene targeting in

ES cells, Cheryl Nolen for her endless help on mouse studies, John McAnally for his transgenic work, Evelyn Tennison and Kathy Mercer for her technical support, Gaile Vitug for her help on genotyping, and Jonathan Guevara for his tremendous technical assistance.

In addition, there have been numerous people who have influenced me greatly and helped me achieve my successful graduate study over the years. I would like to thank the former and current Olson lab members, especially Jay Schneider, Rusty Montgomery, Bryan Young, Michael Arnold, Masao Murakami, Dillon Phan, Eva van Rooij, Ning Liu, Andrew Williams, Lillian Sutherland, Matthew Potthoff, Jiyeon Oh, Mayssa Mokalled, Eric Small, Mei Xin, Jens Fielitz, Johaness Backs, Ana Barbosa, Mi-Sung Kim, Shurong Chang, Chris Li, Drazen Sosic, Michael Haberland, Shusheng Wang, Kunhua Song, Arin Aurora, Mark Hatley, and Osamu Nakagawa.

I am very thankful to my special friends whom I met in Dallas, Liliana Carbajal, Anne Marie Corgan, Norma Romero, and Kristen Tolson. I am also very thankful to my friends in Korea who have always supported me from long distance, especially Minjeong Koh, Dalah Yoo, and Eunjeong Bae. Finally, I would like to thank my entire family for their endless love and support.

MULTIFUNCTIONAL REGULATORS OF CARDIAC DISEASE AND DEVELOPMENT

by

Yuri Kim

DISSERTATION

Presented to the Faculty of the Graduate School of Biomedical Sciences

The University of Texas Southwestern Medical Center at Dallas

In Partial Fulfillment of the Requirements

For the Degree of

DOCTOR OF PHILOSOPHY

The University of Texas Southwestern Medical Center at Dallas

Dallas, Texas

July, 2008

MULTIFUNCTIONAL REGULATORS OF CARDIAC DEVELOPMENT AND DISEASE

Yuri Kim

The University of Texas Southwestern Medical Center at Dallas, 2008

Eric N. Olson, Ph.D.

Embryogenesis requires delicate regulatory mechanisms. A single cell embryo divides into millions of daughter cells to form an organism comprised of various organs with different shapes and function. Organogenesis is mainly controlled by genes that are expressed in a tissue-specific manner. Thus, regulation of gene expression is a critical step in development. In this thesis, I present my findings on two cardiac transcription factors MEF2 and Yap that play multiple roles in development.

First, I show a novel function of myocyte enhancer factor 2 (MEF2) transcription factors in development of endochondral bone. MEF2 proteins are widely known as essential regulators of development of various tissues such as striated muscle and brain. Based on expression patterns of *Mef2* genes and skeletal defects present in *Mef2c*$^{+/-}$*; Mef2d*$^{+/-}$ mice, I hypothesized that MEF2

is an important regulator of skeletogenesis and generated mice lacking MEF2C and MEF2D in chondrocytes using *Mef2c* and *Mef2d* conditional mutant alleles. From this study, I demonstrated that MEF2 proteins are also critical regulators of chondrocyte hypertrophy at least partly through their regulation of *procollagen, type X, alpha 1* (*Col10a1*). I also explored another function of MEF2 protein, which is to mediate stress-dependent cardiac remodeling. *Mef2d* null mice show impaired response to cardiac remodeling stresses such as pressure overload and chronic β-adrenergic stimulation; hypertrophy, chamber dilation, fibrosis, and fetal gene activation were blunted in the absence of MEF2D. Conversely, overexpression of MEF2D is sufficient to drive pathological remodeling of the heart. These findings reveal an important role of MEF2D in stress-dependent cardiac growth and reprogramming of gene expression in the adult heart. Finally, I demonstrate that yes-associated protein (Yap) serves as a critical regulator of cardiac function and angiogenesis by generating a *Yap* conditional mutant allele. Deletion of *Yap* in cardiomyoctes leads to lethal cardiomyopathy resulting from compromised cardiac angiogenesis and ischemia. I also identify Yap as a coactivator of GATA4, a trascription factor that functions as a regulator of angiogenesis in the heart. Moreover, my studies on deletion of *Yap* in other tissues suggest the possible role of Yap as a global angiogenic factor.

Collectively, these studies show that key transcriptional regulators of cardiogenesis play a significant role not only in heart development, but also in development of other organs. These findings imply that combinatorial actions of transcriptional regulators in a tissue-specific manner are critical in embryogenesis.

Table of Contents

List of Publications

Kim, Y., Murakami, M., Qi, X., Richardon, J.A., Bassel-Duby, R., Olson, E.N. Cardiomyocyte Yap is a critical regulator of angiogenesis and maintenance of myocardial function. Manuscript in preparation.

Kim, Y.[*], Phan, D.[*], van Rooij, E., Wang, D.Z., McAnally, J., Qi, X., Richardson, J.A., Hill, J.A., Bassel-Duby, R., Olson, E.N. (2008). The MEF2D transcription factor mediates stress-dependent cardiac remodeling. J. Clin. Invest. *118*, 124-132.

Liu, N., Williams, A.H., **Kim, Y.**, McAnally, J., Bezprozvannaya, S., Sutherland, L.B., Richardson, J.A., Bassel-Duby, R., Olson, E.N. (2007). An intragenic MEF2-dependent enhancer directs muscle-specific expression of microRNAs 1 and 133. Proc. Natl. Acad. Sci. USA *104*, 20844-20849.

Arnold, M.A.[*], **Kim, Y.**[*], Czubryt, M.P., Phan, D., McAnally, J., Qi, X., Shelton, J.M., Richardson, J.A., Bassel-Duby, R., Olson, E.N. (2007). MEF2C transcription factor controls chondrocyte hypertrophy and bone development. Dev. Cell *12*, 377-389.

Haberland, M., Arnold, M.A., McAnally, J., Phan, D., **Kim, Y**., Olson, E.N. (2007). Regulation of HDAC9 gene expression by MEF2 establishes a negative-feedback loop in the transcriptional circuitry of muscle differentiation. Mol. Cell. Biol. *27*, 518-525.

[*]equal contribution

List of Figures

List of Tables

List of Abbreviations

Acta1	actin, alpha 1, skeletal muscle
Agc1	aggrecan
αMHC	α-myosin heavy chain
Angpt1	angiopoietin1
ANP	atrial natriuretic peptide
BAC	bacterial artificial chromosome
bHLH	basic helix-loop-helix
BMP	bone morphogenetic protein
BNP	brain natriuretic peptide
CaMKII	calcium/calmodulin-dependent protein kinase II
CAMTA	calmodulin-binding transcription activator
cDNA	complementary DNA
CMV	cytomegalovirus
Col10a1	procollagen, type X, alpha 1
Col1a2	procollagen, type I, alpha 2
Col2a1	procollagen, type II, alpha 1
Col3a1	procollagen, type III, alpha 1
Ctgf	connective tissue growth factor
DEPC	diethyl pyrocarbonate
DMEM	Dulbecco's Modified Eagle's Medium
DNA	deoxyribonucleic acid
E	embryonic day
ES	embryonic stem
FBS	fetal bovine serum
FS	fractional shortening
GAPDH	glyceraldehyde-3-phosphate dehydrogenase
GATA	GATA binding protein
GSK-3	glycogen synthase kinase-3
HAND	heart and neural crest derivatives expressed transcript

H&E	hematoxylin and eosin
HDAC	histone deacetylase
hGH	human growth hormone
Hif1α	hypoxia inducible factor 1, alpha subunit
HMG	high-mobility group
HOS	Holt-Oram syndrome
Hpo	hippo
HR	heart rate
HW	heart weight
Ihh	indian hedgehog
ISO	isoproterenol
KOH	potassium hydroxide
LVIDd	left ventricular end-diastolic diameter
LVIDs	left ventricular end-systolic diameter
MADS	MCM1, agamous, deficiens, SRF
MAPK	mitogen-activated protein kinase
MEF2	myocyte enhancer factor 2
$MgCl_2$	magnesium chloride
MHC	myosin heavy chain
miRNA	microRNA
MRF	myogenic regulatory factor
Myh6	myosin, heavy polypeptide 6, cardiac muscle, alpha
Myh7	myosin, heavy polypeptide 7, cardiac muscle, beta
n.s.	non-significant
NFAT	nuclear factor of activated T cells
P	postnatal day
PBS	phosphate buffered saline
PCR	polymerase chain reaction
PKD	protein kinase D
Ppr	parathyroid hormone-related peptide receptor
Ptc-1	patched-1

PTHrP	parathyroid hormone-related peptide
Q-PCR	quantitative PCR
RISC	RNA-induced silencing complex
RNA	ribonucleic acid
RT-PCR	reverse transcriptase-polymerase chain reaction
Runx	runt related transcription factor
Sav	salvador
Smo	smoothened
Sox	SRY-box containing gene
Sprk	serine arginine protein kinase
TAC	thoracic aortic constriction
Taz	transcriptional coactivator with PDZ-binding motif
TL	tibia length
UTP	uridine triphosphate
VEGF	vascular endothelial growth factor
Wts	warts
Yap	yes-associated protein
Yki	yorkie

Chapter I

Introduction

The development of multicellular organisms starts from a fertilized egg. The egg undergoes numerous divisions to give rise to millions of cells with different functions, which form complex structures such as heart, brain, and limbs. These developmental processes are mainly controlled by spatiotemporal regulated expression of the genome. One critical step in controlling expression of genes is at the transcriptional level. Extensive research on transcriptional networks has demonstrated that tissue-specific gene expression is often regulated by different combinations of common transcription factors and their coactivators in a tissue-specific manner. One example of well-studied combinatorial transcriptional regulatory networks involves the myogenic regulatory factors (MRFs), which are basic helix-loop-helix (bHLH) transctiption factors. The MRF family members, MyoD, myogenin, myf5, and MRF4, are expressed exclusively in skeletal muscle, and they form heterodimers with ubiquitously expressed bHLH proteins known as E-proteins to control skeletal muscle development (Olson, 1993).

Here I will review how development of different organs is controlled through the combination of various transcriptional regulators. First, I will give a review of the current work on transcriptional regulation of cardiac development and remodeling. Then, I will summarize current knowledge on how endochondral bone development is regulated at a transcription-level.

Transcriptional regulation of cardiac development

The circulatory system consisting of heart, blood vessels, and blood cells is the first functional system to form in developing embryos. Its importance in development is bolstered by the fact that congenital heart disease is the most common human birth defect,

affecting about 1% of the world population (Hoffman and Kaplan, 2002). The mammalian heart consists of four chambers, two ventricles and two atira that are separated by atrial and ventricular septa (Srivastava and Olson, 2000). Mesodermal precursor cells that are derived from anterior lateral plate mesoderm, which is known as the cardiac crescent, differentiate into cardiomyocytes soon after gastrulation. This differentiation occurs in response to bone morphogenetic proteins (BMPs) and Wnts, which are secreted from adjacent endoderm (Redkar et al., 2001; Schultheiss et al., 1995). Cardiac muscle cells migrate toward the ventral midline of the embryo to form a linear heart tube, which is composed of an interior layer of endocardial cells and an exterior layer of myocardial cells. The first heartbeat is observed at the linear heart tube stage. As development progresses, the linear heart tube undergoes rightward looping, and each cardiac chamber develops in a segmental fashion accompanied by trabeculation and cushion formation (Fig. I.1) (Bruneau, 2008; Buckingham et al., 2005; Olson and Srivastava, 1996).

Homeobox proteins A homeobox protein Nkx2-5 is one of the earliest markers of cardiac progenitor cells. The Nkx2-5 ortholog in Drosophila, *tinman*, is required for the formation of the primitive heart in the fruit fly while deletion of *Nkx2-5* in mouse leads to embryonic lethality at E9.5 accompanied by defective heart looping and abnormal ventricle formation (Bodmer, 1993; Lyons et al., 1995). These findings demonstrate that a conserved transcriptional regulatory mechanism controls cardiogenesis in different species. Recent studies reinforced the important relationship between Nkx2-5 and the specification of cardiac progenitor cells. Most Nkx2-5 expressing cells isolated from E9.5 embryos are capable of differentiating into cardiac conduction system and

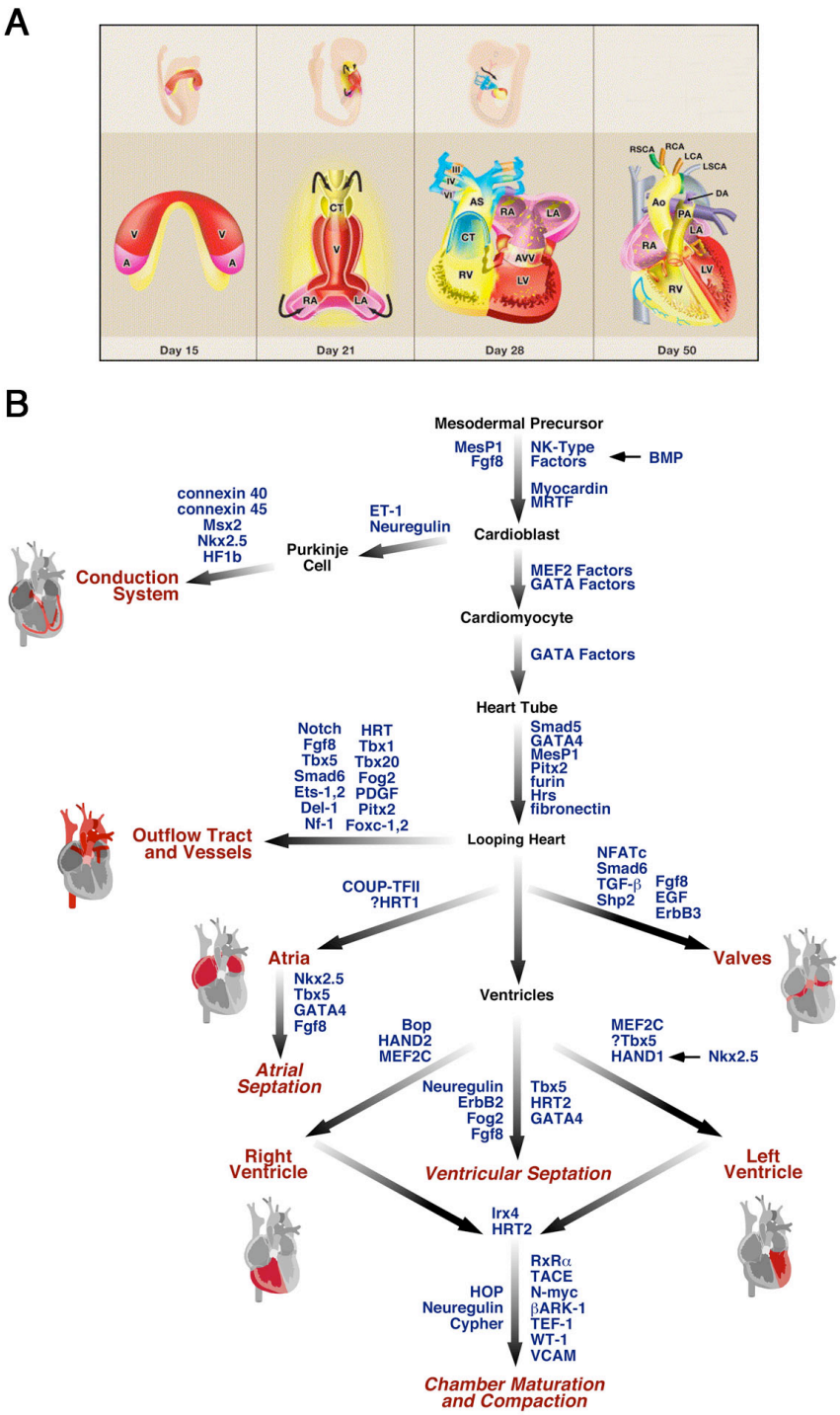

Figure I.1 Transcriptional regulation of mammalian heart development. (A) A diagram describing human heart development. A/a, atrium; Ao, aorta; AS, aortic sac; AVV, atrioventricular valves; CT, conotruncus; DA, ductus arteriosus; LA, left atrium; LCA, left carotid artery; LSCA, left subclavian artery; LV/lv, left ventricle; RA, right atrium; PA, pulmonary artery; RCA, right carotid artery; RSCA, right subclavian artery; RV/rv, right ventricle. (B) A schematic of cardiac morphogenesis illustrating distinct processes and transcriptional regulators that are involved in each process. (Adapted from Srivastava, 2006; Srivastava and Olson, 2000)

cardiomyocytes (Wu et al., 2006). Furthermore, $Isl1^{+}/Nkx2\text{-}5^{+}/Flk1^{+}$ cells are defined as embryonic stem cell-derived cardiovascular progenitors that give rise to cardiac muscle, smooth muscle, and endothelial cells in vitro (Moretti et al., 2006).

MEF2 factors MEF2 family members belongs to the MADS (MCM1, agamous, deficiens, SRF) family of transcription factors, which bind to the consensus sequence CTAWWWWTAG as homo- or heterodimers. There are four MEF2 factors in vertebrates, Mef2a, -b, -c, and -d, while there is a single Mef2 in *Saccharomyces cerevisiae*, *Drosophila melanogaster*, and *Caenorhabditis elegans* (Black and Olson, 1998; Gossett et al., 1989). MEF2 proteins are important regulators of cardiomyocyte differentiation. Cardiomyoblasts do not differentiate into mature cardiomyocytes in flies when D-MEF2, the MEF2 ortholog in *Drosophila*, is deleted (Lilly et al., 1995). In addition, disruption of MEF2C in mouse causes defective cardiac looping resulting in lethality at E9.5 (Lin et al., 1997). The fact that cardiomyocytes still form in these *Mef2c* mutant mice suggests that other MEF2 proteins possibly play redundant roles in cardiomyocyte differentiation in mouse embryos. It is interesting to note that deletion of *Mef2a* and *Mef2d* leads to neonatal cardiac sudden death accompanied by mitochondrial deficiency and compromised cardiac remodeling in response to stress, implying that each MEF2 protein plays both redundant and distinct roles in cardiogenesis (Kim et al., 2008; Naya et al., 2002).

GATA factors GATA family members are zinc finger transcription factors and can be divided into two subgroups: GATA1, GATA2, GATA3 that are expressed predominantly in hematopoietic cells and GATA4, GATA5, GATA that are expressed in endodermal and mesodermal-derived tissues such as lung, gonad, gut, liver, and heart

(Molkentin et al., 2000; Orkin et al., 1998). Deletion of the *Drosophila Gata4* ortholog, *pannier*, zebrafish *Gata5*, or mouse *Gata4* leads to defects in early cardiogenesis (Kuo et al., 1997; Molkentin et al., 1997; Reiter et al., 1999). Recent studies utilizing *Gata4* conditional alleles in mouse demonstrate that GATA4 is not only important in early cardiogenesis, but also in stress-dependent hypertrophy and angiogenesis (Heineke et al., 2007; Oka et al., 2006; Zeisberg et al., 2005). GATA factors share similar protein structures and overlapping expression patterns suggesting their possible redundant functions; the existence of sensitivity toward the dosage of GATA4 and GATA6 factors has been recently demonstrated (Xin et al., 2006).

T-box proteins T-box proteins share a characteristic sequence-specific DNA binding motif called the T-box, which binds to the consensus sequence TCACACCT, and act as transcriptional activators, repressors, or both depending on cellular context (Naiche et al., 2005). T-box transcription factor family members are important in specification of heart progenitor cells in *Drosophila* and mammals. *Drosophila Tbx4/5/6* triple mutants (*Doc*) have no heart (Reim and Frasch, 2005). Moreover, the importance of combinatorial regulatory mechanisms in cardiac specification is evidenced by the fact that T-box proteins interact with the Nkx2-5 ortholog Tinman and the Gata ortholog Pannier (Reim et al., 2005). Seven members of the T-box transcription factor family are expressed in developing mammalian heart: *Tbx1*, *Tbx2*, *Tbx3*, *Tbx4*, *Tbx5*, *Tbx18*, and *Tbx20*. Genetic analysis of T-box proteins in model organisms and human patients has shown that these factors are critical regulators of early cardiac lineage determination, chamber formation, valvuloseptal development, and conduction system specialization.

Especially, mutation in *TBX1* and *TBX5* has been implicated in DiGeorge syndrome and Holt-Oram syndrome, respectively (Basson et al., 1997; Merscher et al., 2001).

HAND proteins Heart and neural crest derivatives expressed transcript (HAND) proteins consist of a bHLH family of transcrtiption factors. *Hand1* and *Hand2* are expressed in a complimentary and chamber-specific manner, left ventricle and right ventricle, respectively (Srivastava et al., 1995). Genetic analysis in zebrafish and mouse model systems demonstrates that HAND1 and HAND2 are key regulators of cardiac morphogenesis. Disruption of zebrafish *Hand* leads to defective ventricular development (Yelon et al., 2000). Cardiac-specific deletion of *Hand1* using its conditional allele in mouse causes defects in the left ventricle and endocardial cushions while *Hand2* null mice die at E10.5 with hypoplasia of the right ventricle (McFadden et al., 2005; Srivastava et al., 1997). In addition to their roles in cardiac morphogenesis, HAND proteins are likely to regulate cardiac development through maintaining the balance between proliferation and differentiation in the developing heart. Loss of *Hand1* leads to elevated differentiation of embryonic stem (ES) cell-derived cariomyocytes, while a gain of HAND1 results in delayed and reduced cardiomyocyte differentiation (Risebro et al., 2006).

Transcriptional regulation of cardiac remodeling

The heart is a dynamic organ that undergoes remodeling even after its development is complete. Under circumstances with mechanical unloading such as weightlessness and bed rest, the heart becomes atrophic. On the other hand, the adult heart undergoes cardiac remodeling accompanied by an increase in cardiomyocyte size, thickening of the

ventricular wall, loss of cardiomyocytes with fibrotic replacement, and higher organization of sarcomeres under mechanical or neurohormonal stress. In addition to structural changes, protein synthesis is enhanced and the fetal gene program is activated, including upregulation of *atrial natriuretic peptide* (*ANP*), *brain natriuretic peptide* (*BNP*), *myosin, heavy polypeptide 7, cardiac muscle, beta* (*Myh7*), and *actin, alpha 1, skeletal muscle* (*Acta1*) (Frey and Olson, 2003; Hill and Olson, 2008). Cardiac remodeling can be either physiologic or pathologic depending on the circumstances. Beneficial physiologic hypertrophy usually results from exercise and pregnancy. However, under stress, the heart undergoes pathological hypertrophy progressing to dilated cardiomyopathy and possible death (Fig. I.2). The prevalence of pathological hypertrophy and the necessity of finding its treatment are highlighted by the fact that heart disease is the number one killer of adult men and women in the industrialized world and affects an estimated five million Americans (Rosamond et al., 2008). Although hypertrophic growth was traditionally considered as a beneficial compensatory mechanism, recent studies have demonstrated that the cardiac hypertrophic process is not entirely beneficial; the inhibition or regression of cardiac hypertrophy has been shown to lower the risk for heart failure and death (Mathew et al., 2001). Elucidating molecular mechanisms that control cardiac hypertrophy will facilitate discovery of new drug targets for cardiac hypertrophy and heart failure.

Calcineurin and NFAT One of molecular pathways in cardiac remodeling that has been extensively studied involves calcineurin and nuclear factor of activated T cells (NFAT). Calcineurin is a Ca^{2+}/calmodulin-dependent serine-threonine phosphatase that consists of a catalytic A subunit and a regulatory B subunit. It dephosphorylates NFAT,

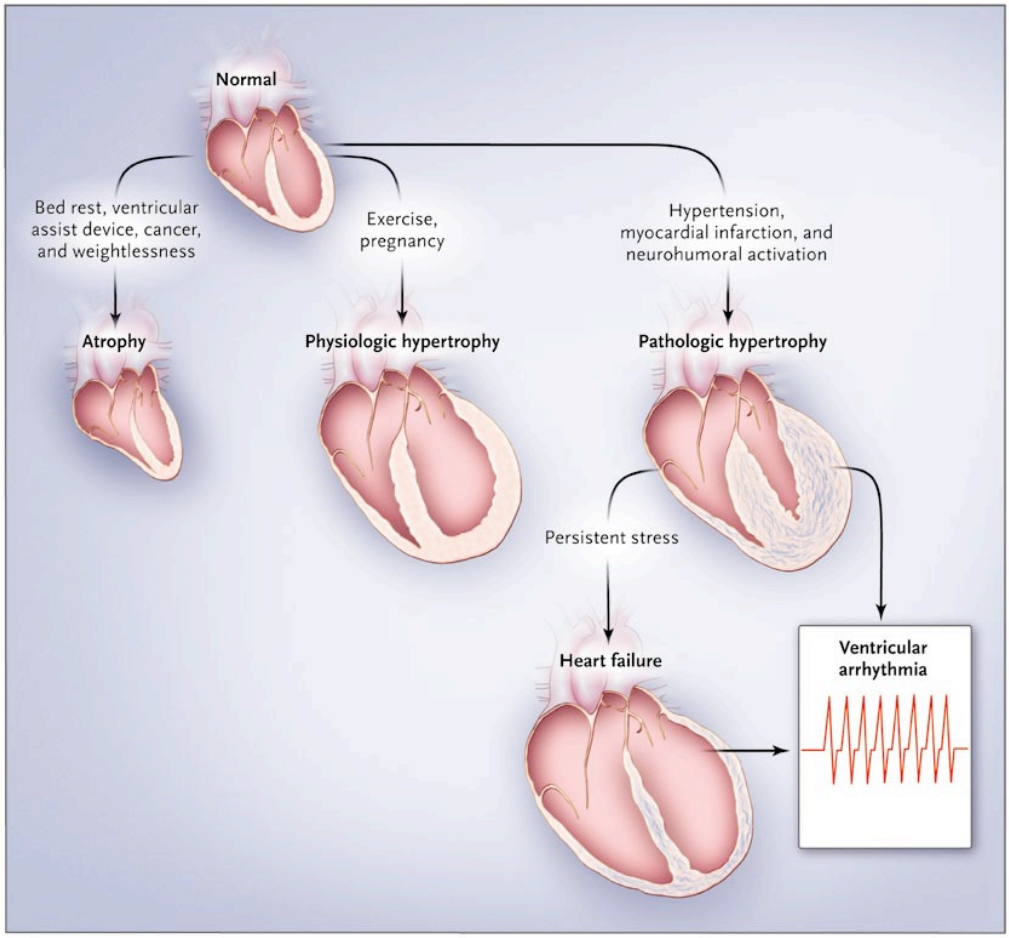

Figure I.2 Remodeling of the heart under different conditions. The adult heart undergoes different modes of remodeling depending on the circumstances. Hypertophy can be either physiologic, which is beneficial, or pathologic, which eventually results in heart failure and ventricular arrhythmia. (Adapted from Hill and Olson, 2008)

which leads to nuclear localization of NFAT and activation of its downstream targets (Fig. I.3). Conversely, glycogen synthase kinase-3 (GSK-3) phosphorylates NFAT proteins and induces their nuclear export. The importance of the calcineurin and NFAT pathway is underscored by the fact that overexpression of an active form of calcineurin and nuclear NFAT3 stimulates cardiac hypertrophy and heart failure (Molkentin et al., 1998; Shimoyama et al., 1999). Furthermore, a hypertrophic response to pressure overload and β-adrenergic stimulation is impaired when GSK-3β is constitutively activated in the heart

(Antos et al., 2002). Genetic analysis of *CnAβ* null mice and *NFATc3* null mice demonstrates that the calcineurin-NFAT pathway is not only sufficient but also necessary for cardiac remodeling upon stress (Bueno et al., 2002; Wilkins et al., 2002). Nuclear NFATs and GATA factors interact and synergetically activate cardiac fetal genes suggesting that the combination of various transcription factors regulates both development and remodeling of the heart (Molkentin et al., 1998).

Class II HDACs and MEF2s Class II histone deacetylases (HDACs), HDAC4, HDAC5, HDAC7, and HDAC9, bind to MEF2 and repress its transcriptional activity. Phosphorylation of class II HDACs by HDAC kinases such as protein kinase D (PKD) and calcium/calmodulin-dependent protein kinase II (CaMKII) leads to their nuclear export and derepression of MEF2 activity (Fig. I.3) (Backs et al., 2008; Lu et al., 2000b). The importance of the class II HDAC-MEF2 pathway in cardiac remodeling was first demonstrated in a study of *Hdac9* null mice. Deletion of *Hdac9* in mice results in development of cardiac hypertrophy and augmented response to pathological stress (Zhang et al., 2002). Moreover, transcriptional activity of MEF2 in the heart increases under hypertrophic conditions suggesting that MEF2 plays an important role in cardiac remodeling (Passier et al., 2000). This notion is further supported by the fact that *Mef2d* null mice show an impaired stress-dependent cardiac remodeling response while forced overexpression of MEF2D is sufficient to reactivate the fetal gene program and drive pathological remodeling of the heart (Kim et al., 2008). The presence of the residual hypertrophic response in *Mef2d* null mice implies that other MEF2 factors, especially MEF2A, are likely to be involved in stress-dependent cardiac remodeling in addition to MEF2D.

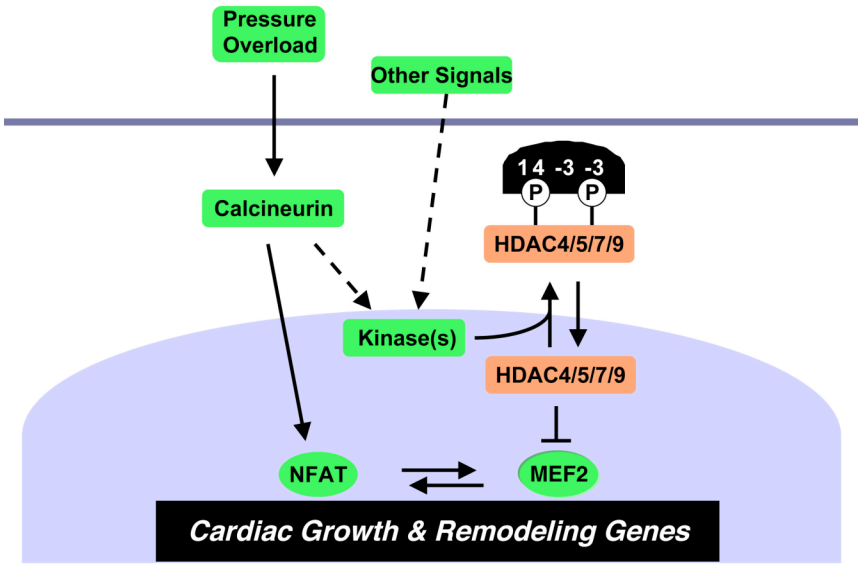

Figure I.3 Molecular signaling pathways involved in cardiac remodeling. The heart responds to chronic and acute injury by undergoing cardiac growth and remodeling. Various transcription factors involved in cardiac remodeling such as MEF2 and NFAT and their upstream molecules have been identified.

MicroRNAs Recent studies have revealed another level of regulation in stress-dependent cardiac remodeling. MicroRNAs (miRNAs) are initially transcribed by RNA polymerase II as a pre-miRNA, processed in the nucleus by the RNase Drosha into 70 to 100 nucleotide-long pre-miRNAs, and finally processed by RNA-induced silencing complex (RISC) into mature forms, which are single-stranded RNA molecules that are approximately 22 nucleotides in length (Denli et al., 2004; Lee et al., 2003). miRNAs share sequence complementarity with their target genes and generally downregulate their expression by either translational repression or mRNA degradation (Bagga et al., 2005; Lim et al., 2005). Recent reports have identified miRNAs that are sufficient and necessary for cardiac remodeling, suggesting that miRNAs are fine-tuners of stress-induced responses. Overexpression of miRNA-195 is sufficient to drive hypertrophic growth and myocyte disarray in primary cardiomyocytes, while its cardiac-specific

overexpression in mice results in dilated cardiomyopathy and heart failure (van Rooij et al., 2006). In addition, analysis of *miRNA-208* null mice demonstrates that miRNA-208 is required for stress-dependent cardiac growth and gene expression (van Rooij et al., 2007). These findings reveal a novel regulatory mechanism of cardiac remodeling and possibly of other developmental processes.

Transcriptional regulation of endochondral bone development

The skeleton consists of two different types of bones depending on which developmental pathway it undergoes: intramembranous and endochondral bone. The developmental process of skeleton formation starts from mesenchymal cells migrating into presumptive skeletogenic sites and condensing in both cases. In intramembranous bone development, condensed mesenchymal cells directly differentiate into osteoblasts without going through a cartilaginous intermediate step; this process generally forms flat bones of the skull and craniofacial structures. On the other hand, condensed mesenchymal cells differentiate into cartilaginous chondrocytes during endochondral bone development. Chondrocytes first flatten and proliferate to form columnar proliferating chondrocytes, which contribute to the longitudinal growth of bones. Cells at the bottom of the column exit the cell cycle and become hypertrophic. These hypertrophic chondrocytes undergo apoptosis and are replaced by invading osteoblasts and blood vessels to form ossified bones (Fig. I.4). Differentiated chondrocytes express characteristic extracellular matrix and regulatory markers along the developmental process; columnar chondroblasts express *procollagen, type II, alpha 1* (*Col2a1*) and *SRY-box containing gene* (*Sox*) genes, and hypertrophic chondrocytes express *procollagen, type X, alpha 1* (*Col10a1*), *runt related transcription factor 2* (*Runx2*), and *vascular endothelial growth factor* (*VEGF*). Recent

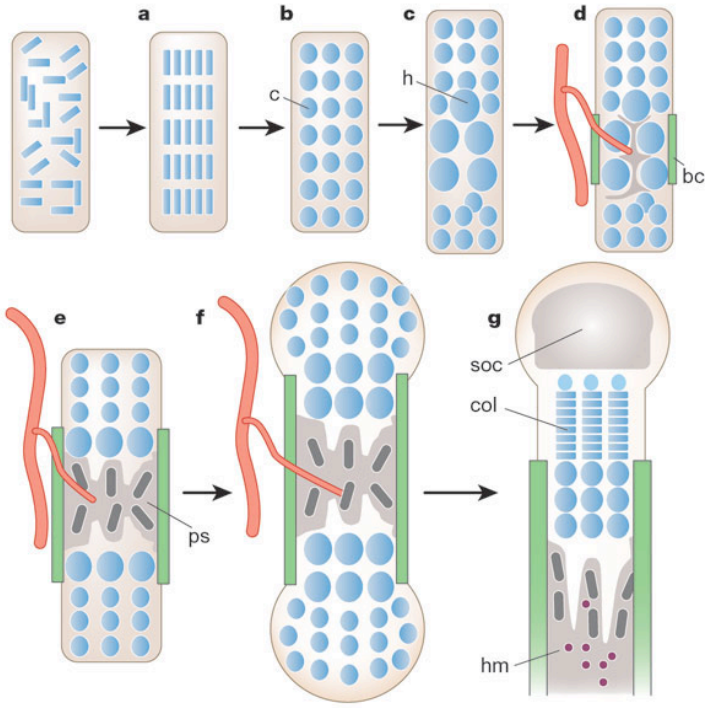

Figure I.4 Endochondral bone development. (a) Mesenchymal cells condense. (b) Condensed cells differentiate into chondrocytes. (c) Chondrocytes at the bottom of the columnar proliferating stack of cells become hypertrophic. (d) Hypertophic chondrocytes undergo apoptosis, attract blood vessels, and stimulate formation of bone collar of osteoblasts from perichondrial cells. bc, bone collar; c, chondrocytes; col, columns of proliferating chondrocytes; h, hypertrophic; hm, haematopoietic marrow; ps, primary spongiosa; soc, secondary ossification center. (Adapted from Kronenberg, 2003)

reports have identified a number of transcriptional regulators in this process and how they are intertwined to coordinate skeletogenesis.

Sox proteins The Sox family of transcription factors possess a high-mobility group (HMG) box DNA binding domain whose sequence is about 50% identical to that of the sex-determining factor SRY (Wegner, 1999). Analysis of *Sox9* heterozygous mice reveals that Sox9 is an important regulator of mesenchymal cell condensation and early chondrocyte differentiation. The mutant mice show larger zones of hypertrophic chondrocytes and premature mineralization suggesting that Sox9 also controls the rate at which chondrocytes differentiate into hypertrophic chondrocytes (Akiyama et al., 2002;

Bi et al., 2001). Moreoever, Sox9 plays a critical role in successive steps of chondrocyte differentiation as well by controlling the expression of Sox5 and Sox6, which are necessary for late chondrocyte differentiation (Akiyama et al., 2002; Smits et al., 2001). These Sox proteins are not only required but also sufficient for chondrocyte differentiation; coexpression of Sox9, Sox5, and Sox6 leads to expression of cartilage markers such as *Col2a1* and *Aggrecan* (*Agc1*) in non-chondrogenic cells underscoring their importance in endochondral bone development (Ikeda et al., 2004).

Ihh and PTHrP *Indian hedgehog (Ihh)*, a member of the hedgehog family of secreted ligands, is synthesized by prehypertrophic chondrocytes and early hypertrophic chondrocytes. It binds to its receptor Patched-1 (Ptc-1) leading to activation of a cell membrane protein Smoothened (Smo), which further controls expression of downstream target genes. *Ihh* null mice and cartilage-specific *Smo* null mice show decreased proliferation of chondrocytes demonstrating that Ihh signaling is an important regulator of chondrocyte proliferation (Long et al., 2001; St-Jacques et al., 1999). In addition, *Ihh* mutant mice also show an absence of osteoblasts in either the primary spongiosa or the bone collar of endochondral bones, indicating that Ihh controls the differentiation of osteoblasts and the location at which it occurs. Furthermore, Ihh regulates synthesis of parathyroid hormone-related peptide (PTHrP) (St-Jacques et al., 1999). PTHrP is a secreted protein that is produced by perichondrial cells and early proliferative chondrocytes. The role of PTHrP and its receptors PTH/PTHrP receptors (Pprs) is to keep proliferating chondrocytes in the proliferative stage as demonstrated by analysis of *PTHrP* null mice and *Ppr* null mice (Karaplis et al., 1994; Lanske et al., 1996). This notion is supported by the fact that overexpression of PTHrP or a constitutively active

Ppr results in delayed appearance of hypertrophic chondrocytes (Schipani et al., 1997; Weir et al., 1996). Ihh and PTHrP together determine when chondrocytes leave the proliferative stage and become hypertrophic. Chondrocytes start synthesizing Ihh when stimulation by PTHrP is no longer sufficient at the bottom of columns of proliferating chondrocytes. Ihh then stimulates proliferating chondrocytes at the top of the proliferative zone to produce PTHrP, forming a feedback loop, which determines the lengths of proliferative columns in individual bones (Vortkamp et al., 1996).

Runx2, HDAC4 and MEF2 proteins Runx2 is highly expressed in chondrocytes in the late condensation stage, in the prehypertrophic zone, and in the hypertrophic zone. It is also expressed in perichondrial cells and osteoblasts. An essential role of Runx2 in endochondral bone development is revealed by the observation that *Runx2* null mice lack osteoblasts and show abnormalities of chondrocyte maturation (Komori et al., 1997; Otto et al., 1997). In addition, transgenice mice overexpressing Runx2 in proliferating and prehypertrophic chondrocytes exhibit premature and ectopic ossification (Takeda et al., 2001). The transcriptional activity of Runx2 is inhibited by HDAC4, a class II HDAC whose expression pattern in prehypertrophic endochondral cartilage coincides with that of Runx2. The interaction between the two molecules is evident in vivo by the fact that deletion of *Hdac4* in mice leads to premature and ectopic ossification of developing bones, which is very similar to what is observed in Runx2 transgenic mice (Vega et al., 2004b). Runx2 and HDAC4 have been thought to be the major transcriptional regulators of chondrocyte hypertophy. However, a recent report has identified MEF2 as another critical regulator in this process. Analysis of *Mef2* mutant mice demonstrates that MEF2 proteins genetically interact with HDAC4 and play a critical role during chondrocyte

hypertrophy (Arnold et al., 2007). This finding highlights the notion that a transcriptional regulator can serve multiple roles in the developmental processes of various organs.

In this dissertation, I will describe my studies using transgenic mouse model systems to investigate and understand transcriptional regulators of endochondral bone development, cardiogenesis, and cardiac remodeling. My specific aims are:

1) To investigate the potential function of MEF2 factors in endochondral bone development utilizing chondrocyte-specific *Mef2* mutant mice;

2) To characterize *Mef2d* mutant mice and analyze the in vivo function of MEF2D in stress-dependent cardiac remodeling;

3) To generate a conditional *Yap* null allele in mice and study its function in cardiac development.

Chapter II

MEF2 in Endochondral Bone Development

Chondrocyte hypertrophy is essential for endochondral bone development. We discovered that MEF2C, a transcription factor that regulates muscle and cardiovascular development, unexpectedly, controls bone development by activating the gene program for chondrocyte hypertrophy. Genetic deletion of *Mef2c* or expression of a dominant negative MEF2C mutant in endochondral cartilage impairs hypertrophy, cartilage angiogenesis, ossification and longitudinal bone growth in mice. Conversely, a super-activating form of MEF2C causes precocious chondrocyte hypertrophy, ossification of growth plates and dwarfism. Endochondral bone formation is exquisitely sensitive to the balance between MEF2C and the co-repressor histone deacetylase 4 (HDAC4), such that bone deficiency of *Mef2c* mutant mice can be rescued by an *Hdac4* mutation, and ectopic ossification in *Hdac4* null mice can be diminished by a heterozygous *Mef2c* mutation. These findings reveal unexpected commonalities in the mechanisms governing muscle, cardiovascular and bone development with respect to their regulation by MEF2 and class II HDACs.

INTRODUCTION

The vertebrate skeleton is comprised of endochondral and membranous bones, which form through different mechanisms (Karsenty, 2003; Kronenberg, 2003; Nakashima and de Crombrugghe, 2003; Olsen et al., 2000). Endochondral bones, which account for all the bones of the body with the exception of the craniofacial bones and the clavicle, develop from a cartilaginous template. In contrast, membranous bones are derived from mesenchymal cells, which differentiate directly into osteoblasts without a cartilaginous intermediate. There are also permanent cartilaginous structures throughout the body, such as in ears, nose, throat, joints, and segments of the ribs. Why the cartilage in these regions fails to undergo ossification is unknown.

Endochondral bone formation begins with the aggregation of mesenchymal cells and their differentiation into chondrocytes. Chondrocyte hypertrophy, which initiates in the center of cartilaginous skeletal elements, drives longitudinal bone growth. This process is coupled to exit from the cell cycle and is marked by the expression of specific extracellular matrix molecules, such as α_1(X) collagen (Col10a1). Chondrocyte hypertrophy is followed by apoptosis, invasion of blood vessels, osteoclasts and other mesenchymal cells from the perichondrium and production of the mature bone matrix. The ultimate sizes and structures of endochondral bones depend on the coordinated regulation of chondrocyte proliferation, maturation and hypertrophy in response to multiple extracellular signals. Indian hedgehog (Ihh) and Parathyroid hormone-related peptide (PTHrP) play critical roles in coordinating these processes (Karaplis et al., 1994; Lanske et al., 1996; St-Jacques et al., 1999; Vortkamp et al., 1996; Weir et al., 1996). Ihh produced by pre-hypertrophic chondrocytes induces the expression of PTHrP, which

regulates the rate at which chondrocytes exit the cell cycle and undergo hypertrophy. Ihh also stimulates chondrocyte proliferation and controls the differentiation of mesenchymal cells into osteoblasts within the bone collar. VEGF expressed by hypertrophic chondrocytes is required for chondrocyte survival and cartilage angiogenesis (Zelzer et al., 2004).

Several transcription factors that control the patterning and maturation of the endochondral skeleton have been identified (Karsenty, 2003; Lefebvre and Smits, 2005; Zelzer and Olsen, 2003). Runx2 and Runx3, members of the Runt family of transcription factors, are necessary for chondrocyte hypertrophy and osteoblast differentiation (Komori et al., 1997; Yoshida et al., 2004). Chondrocyte hypertrophy is arrested during the late stages of maturation in *Runx2* null mice, and is completely blocked in mice lacking Runx2 and Runx3, suggesting redundant roles for these factors in chondrocyte differentiation. The zinc finger transcription factor osterix acts downstream of Runx2 and is required for osteoblast differentiation and bone formation (Nakashima et al., 2002; Nishio et al., 2006). Mice lacking the HMG-box transcription factor Sox9 display hypoplasia of endochondral skeletal elements, resembling the defects associated with campomelia dysplasia in humans (Bi et al., 2001). Sox5 and 6 have also been implicated in chondrocyte differentiation (Smits et al., 2001).

Recently, we reported that histone deacetylase 4 (HDAC4) acts as a negative regulator of chondrocyte hypertrophy (Vega et al., 2004b). *Hdac4* null mice die during the perinatal period due to premature and ectopic chondrocyte hypertrophy and ossification of endochondral cartilage. HDAC4 and other class II HDACs establish co-repressor complexes with DNA-binding transcription factors (Lu et al., 2000a; Miska et

al., 1999; Verdin et al., 2003), including myocyte enhancer factor-2 (MEF2), a MADS (MCM1, Agamous, Deficiens, serum response factor)-box factor implicated in muscle and cardiovascular development (Black and Olson, 1998; McKinsey et al., 2002). There are four mammalian *Mef2* genes, *Mef2a, b, c* and *d*, which are expressed in complex and overlapping patterns in embryonic and adult tissues (Edmondson et al., 1994). *Mef2c* null mice die by E9.5 from abnormal cardiovascular development (Lin et al., 1998; Lin et al., 1997), whereas *Mef2a* null mice die perinatally from a spectrum of heart defects (Naya et al., 2002).

We demonstrate the previously undescribed expression of *Mef2* genes in developing chondrocytes, and show that MEF2C plays an unexpected role in endochondral bone development. Conditional deletion of *Mef2c* or expression of a dominant negative mutant of MEF2C in developing cartilage impairs chondrocyte hypertrophy and subsequent growth plate vascularization and endochondral ossification. Conversely, a super-activating form of MEF2C promotes precocious chondrocyte hypertrophy and ossification of endochondral bones. Deletion of *Hdac4* restores normal bone formation in heterozygous *Mef2c* mutant mice, and deletion of a single *Mef2c* allele prevents excessive and ectopic bone formation in *Hdac4* mutant mice. We conclude that MEF2C acts as an essential, early regulator of bone development by orchestrating transcriptional and cell-cell signaling events involved in chondrocyte hypertrophy. These findings highlight the partnership of MEF2 and class II HDACs as a nodal point in the control of the seemingly unrelated processes of muscle, cardiovascular and bone development.

RESULTS

Expression of *Mef2* genes in the developing skeleton

While analyzing the expression of *Mef2* genes during mouse embryogenesis, we found that *Mef2c* was expressed in the mesenchymal primordium of the endochondral cartilage at E12.5 (Fig. II.1Ac) and that both *Mef2c* and *Mef2d* were expressed in prehypertrophic and hypertrophic chondrocytes, a well as the spongiosa of developing endochondral bones at later stages of bone development (Fig. II.1A). It is noteworthy that the level of *Mef2c* and *Mef2d* expression in hypertrophic chondrocytes was comparable to that in surrounding skeletal muscle (Fig. II.1A). *Mef2a* transcripts were detectable at lower levels and *Mef2b* expression was not detectable in the developing skeleton (Fig. II.1A).

A heterozygous *Mef2c* mutation impairs bone development

Mice homozygous for a *Mef2c* null mutation die at E9.5 from defects in cardiovascular development (Lin et al., 1997), precluding an analysis of potential functions of *Mef2c* at later developmental stages. In light of the expression of *Mef2c* in the developing endochondral skeleton, we analyzed $Mef2c^{+/-}$ mice for possible skeletal abnormalities and noticed a lack of ossification within the sternum at postnatal day (P) 1 (Fig. II.1B, compare a and b). Typically, the sternum contains trabeculated bone within each sternabra with growth plates at both ends. In contrast to wild-type mice in which the sternebrae and xiphoid process are ossified by P1, these structures remained cartilaginous in mutant mice (Fig. II.1B). Histological analysis and von Kossa staining, which detects calcium deposits within the mineralized cartilaginous matrix, showed only residual hypertrophic chondrocytes and almost a complete absence of trabeculated bone in the

sternum of *Mef2c*$^{+/-}$ mutants at P1. We did not detect abnormalities in other endochondral skeletal elements of *Mef2c*$^{+/-}$ mutants, indicating that the sternum is most sensitive to levels of *Mef2c* expression.

Mice homozygous for a *Mef2d* null allele are viable and show no skeletal abnormalities (Kim et al., 2008). In light of the expression of *Mef2d* in the developing skeleton, we generated *Mef2c*$^{+/-}$*; Mef2d*$^{+/-}$ double heterozygous mutant mice to test for potential functional redundancy of these genes in skeletal development. Indeed, *Mef2c*$^{+/-}$*; Mef2d*$^{+/-}$ mutants displayed a deficiency in ossification of the sternum more severe than that of *Mef2c*$^{+/-}$ mutants (Fig. II.1B). Histological analysis revealed almost no hypertrophic chondrocytes in the sternum of *Mef2c*$^{+/-}$*; Mef2d*$^{+/-}$ mice. *In situ* hybridization showed *α_1(II) collagen (Col2a1)* expression, a marker of proliferating chondrocytes, throughout the sternum of *Mef2c*$^{+/-}$*; Mef2d*$^{+/-}$ mice at P1, whereas *Col2a1* expression was excluded from the hypertrophic and mineralized regions of the wild-type sternum (Fig. II.1C). In contrast, *Col10a1*, *Col1a1* and *bone sialoprotein*, which are markers of hypertrophic chondrocytes, trabeculated bone, and differentiated osteoblasts, respectively, were not expressed in the mutants (Fig. II.1C). *Mef2c*$^{+/-}$*; Mef2d*$^{+/-}$ mutant mice died within a day after birth so we were unable to analyze them for possible skeletal abnormalities later in postnatal development. These findings suggested that MEF2C played an essential role in bone development and that MEF2D augmented this function of MEF2C.

Generation of a conditional *Mef2c* allele

To further investigate the potential involvement of *Mef2c* in bone development, we

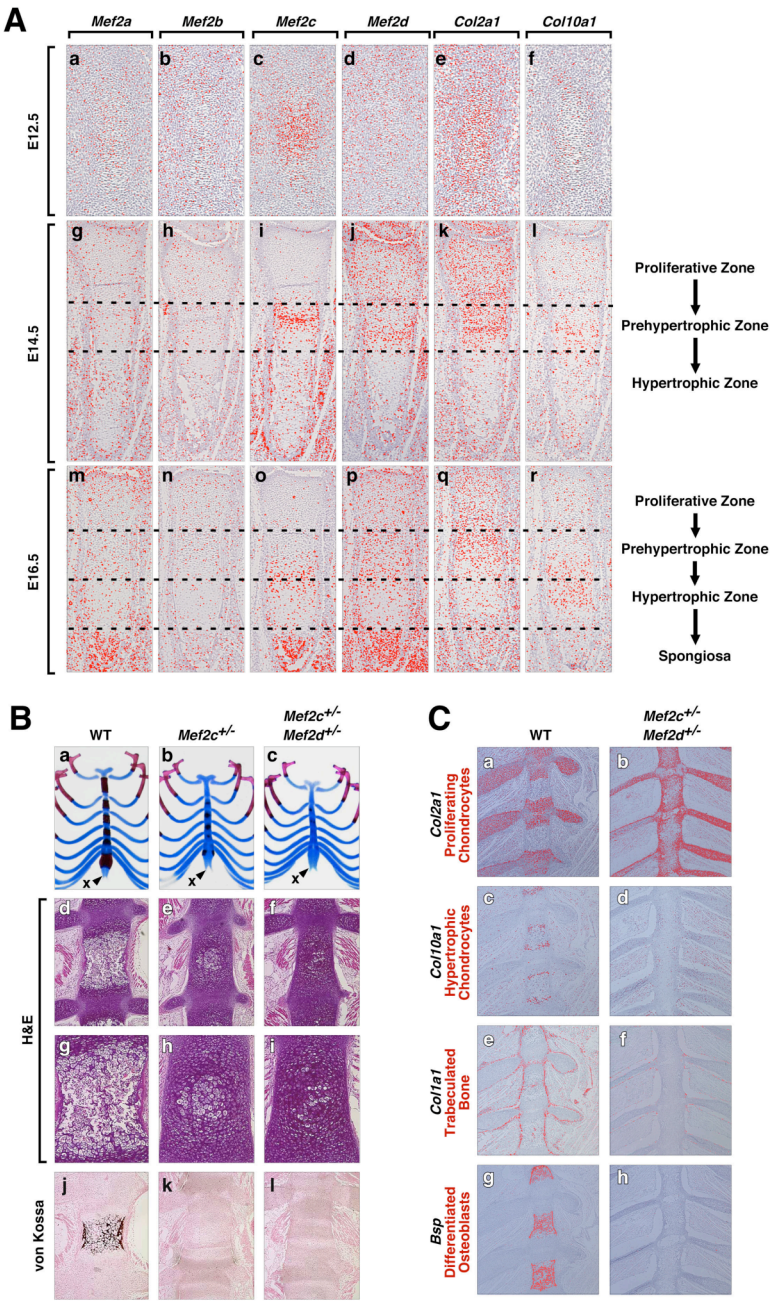

Figure II.1 Mef2 expression in developing endochondral bones and skeletal defects in heterozygous *Mef2* mutant mice. (A) Detection of Mef2 transcripts by in situ hybridization to sections of the developing radius at E12.5 (a - d), E14.5 (g - j) and E16.5 (m - p). Expression of *Mef2c* is initially observed in the cartilage primordium at E12.5. *Mef2c* and *d* are expressed in prehypertrophic and hypertrophic chondrocytes at later stages. Expression of *Col2al* (e, k, q) and *Col10al* (f, l, r) are also described to show chondrocyte differentiation. (B) Anterior views of the sternum and ribs of mice stained for bone (red) and cartilage (blue) at P1 (a – c). The xiphoid process (x) is indicated. Note the reduction in ossification of the sternum in b and the complete absence of ossification in c. Hematoxalin and eosin (H&E) stained sections are shown (d – f) with a high magnification view of the sternabrae below (g – i). Note the absence of hypertrophic chondrocytes and trabeculation in the mutants. Von Kossa stained sections are shown at the bottom (j – l). (C) Detection of markers of bone development by *in situ* hybridization to sections of sternum from wild-type and *Mef2c*$^{+/-}$; *Mef2d*$^{+/-}$ mice at P1.

generated a conditional *Mef2c* null allele, called *Mef2c*^{loxP}, containing loxP sites in the introns flanking the second coding exon, which encodes the MADS and MEF2-specific domains, which mediate DNA binding, dimerization and cofactor interactions. Deletion of the genomic region between the loxP sites inactivates the gene (Fig. II.2). A similar genomic region was deleted in our original *Mef2c*^{KO} null allele (Lin et al., 1997). Mice homozygous for the *Mef2c*^{loxP} allele or trans-heterozygous for this allele and the *Mef2c*^{KO} allele showed no apparent abnormalities, indicating that the *Mef2c*^{loxP} allele functioned normally.

Conditional deletion of *Mef2c* disrupts bone development

We used two mouse lines that express Cre recombinase in different skeletal elements and their precursors to conditionally delete *Mef2c in vivo*. We deleted *Mef2c* from the early precursors of all cell types of the developing bone by using the *Twist2-Cre* knock-in (Long et al., 2001; Yu et al., 2003), or we deleted the gene specifically in the cartilaginous template of endochondral bones by using *Col2-Cre* (Long et al., 2001). The expression of *Mef2c* was effectively reduced as a result of Cre expression (Fig. II.2D).

Mef2c$^{loxP/KO}$*; twist2-Cre* mice were readily identifiable at birth by their shortened limbs (Fig. II.3A and B). A fraction of these conditional *Mef2c* mutants also displayed difficulty breathing, evidenced by gasping and accumulation of air in their intestines, and none survived beyond the first week of postnatal life. Analysis of the skeletons of *Mef2c*$^{loxP/KO}$*; twist2-Cre* mice revealed severe defects in ossification of nearly all endochondral bones (Fig. II.3A and B). This phenotype was especially pronounced in the sternum (Fig. II.3B, compare a and e). Similarly, the vertebral bodies failed to ossify, as

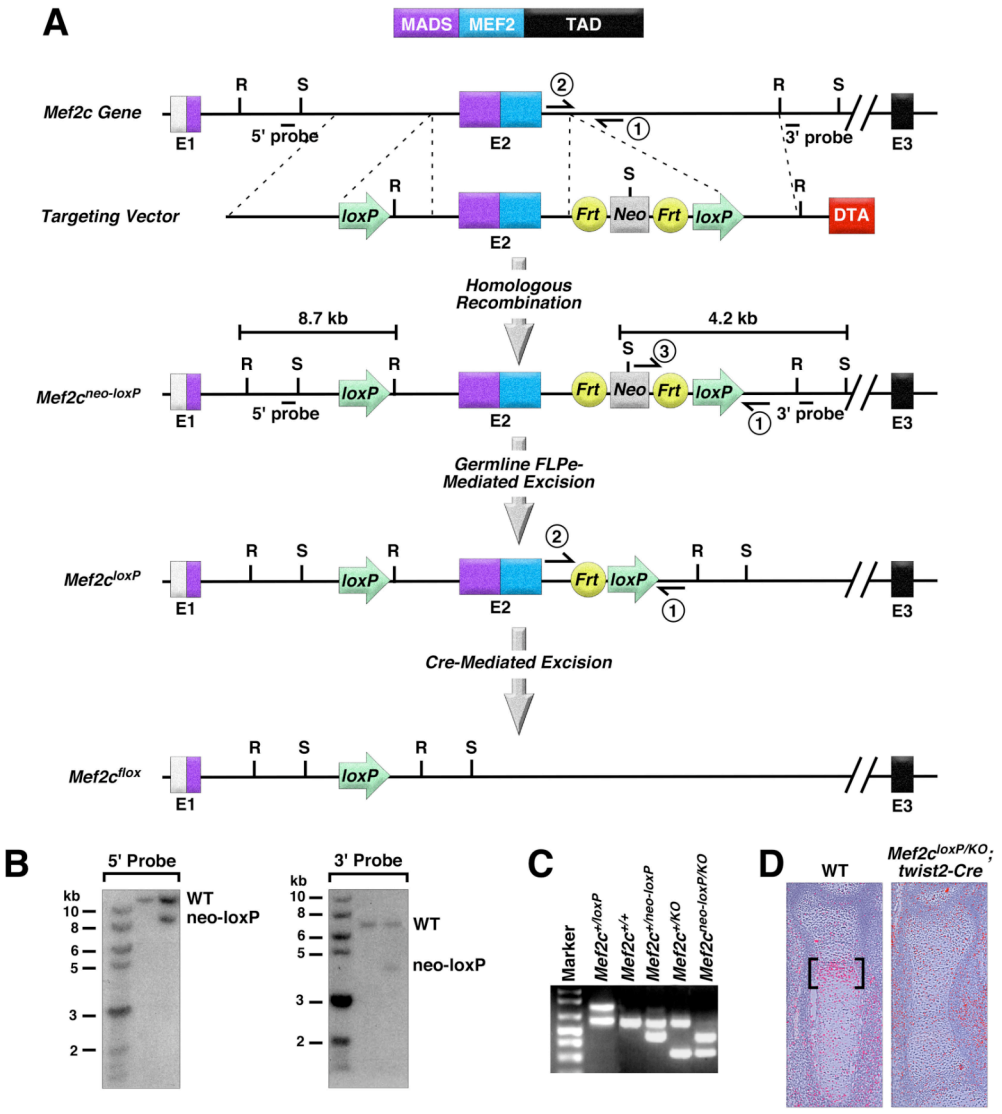

Figure II.2 Generation of mice with a conditional *Mef2c* mutation. (A) Schematic representation of the *Mef2c* locus, targeting vector, targeted locus and alleles resulting from FLPe and Cre mediated recombination. LoxP sites were inserted into the introns flanking the second coding exon (E2) of the *Mef2c* locus. The neomycin resistance cassette was removed in the mouse germline by breeding heterozygous mice to *hACTB::FLPe* transgenic mice. Tissue-specific deletion of exon 2 was achieved by breeding $Mef2c^{loxP/loxP}$ mice to mice harboring various Cre transgenes. Positions of the probes used for Southern analysis are shown. R, EcoRI; S, SacI. (B) Southern blot analysis of representative targeted ES cell clones. In the left panel, DNA was digested with EcoRI and hybridized to the 5'probe, yielding bands of 11.5 kb and 8.7 kb for the wild-type and mutant alleles, respectively. In the right panel, DNA was digested with SacI and hybridized to the 3' probe, yielding bands of 7.0 kb and 4.2 kb for the wild-type and mutant alleles, respectively. (C) PCR genotyping to distinguish the resulting alleles of *Mef2c* on genomic DNA of mice of the indicated genotypes. PCR products corresponding to the wild-type (586bp), loxP (773bp), neo-loxP (412 bp) and previously generated KO (253bp) alleles of *Mef2c* are detected. The positions of oligonucleotide primers that produce the corresponding PCR product for each allele are marked in panel A as 1, 2 and 3. (D) Detection of *Mef2c* transcripts in the radius of mice of the indicated genotypes at E14.5. *Mef2c* transcripts are enriched in prehypertrophic and hypertrophic chondrocytes of WT mice (bracket) and are present at background levels in the presence of *Twist2-Cre*. In contrast, expression of *Mef2c* transcripts in surrounding skeletal muscle is comparable in mice of both genotypes.

did the supraoccipital bone, which defines the dorsal margin of the foramen magnum (Fig. II.3A arrows in panel d). There was also obvious foreshortening of the ossified regions of the bones of the fore and hindlimbs and lack of ossification in many phalangeal bones of the digits (Fig. II.3B). Truncation of the tibia and fibula was particularly severe (Fig. II.3B, compare d and h). Ossification of the bone collar also appeared disorganized in these mutant mice (Fig. II.3B).

Histological sections of the sternum and radius revealed that the defects in endochondral ossification in the mutants resulted from a failure in chondrocyte hypertrophy (Fig. II.3C). Von Kossa staining showed that the sternum and radius of *Mef2c*$^{loxP/KO}$*; twist2-Cre* mice were completely devoid of trabeculated bone (Fig. II.3C). However, weak von Kossa staining was seen at the midpoint of the mutant radius and in the surrounding bone collar of the mutants, indicative of a few chondrocytes in the late stages of hypertrophic differentiation. Bone collar formation is secondary to chondrocyte hypertrophy, and therefore did not occur in the mutant sternum, where chondrocyte hypertrophy failed to take place (Fig. II.3C). In the mutant radius, a disorganized bone collar was present only near the midpoint of the bone where residual hypertrophic chondrocytes were present (Fig. II.3C).

Deletion of *Mef2c* with *Col2-Cre*

To distinguish whether the skeletal defects in *Mef2c*$^{loxP/KO}$*; twist2-Cre* mice reflected a role for MEF2C in chondrocytes or osteoblasts, we specifically deleted *Mef2c* in proliferating chondrocytes using a Cre transgene controlled by the *Col2a1* promoter, called *Col2-Cre*. The resulting mutants were identifiable at birth by shortened limbs, an

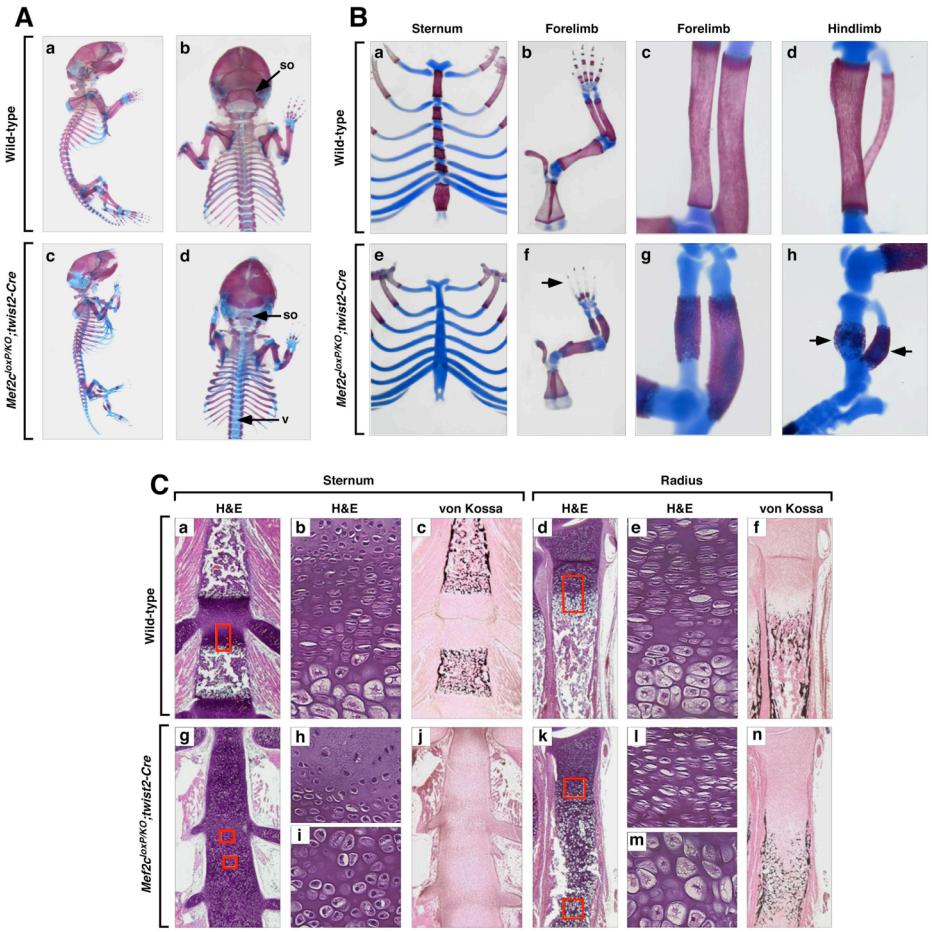

Figure II.3. Failure in endochondral ossification following conditional deletion of *Mef2c* using *Twist2-Cre*. (A) Alizarin red and Alcian blue staining of P1 wild-type or *Mef2c*$^{loxP/KO}$*; twist2-Cre* whole skeletons in lateral (a and c) or dorsal views (b and d). Arrows in panels b and d indicate the supraoccipital bone (so) and vertebral bodies (v), which fail to ossify in *Mef2c*$^{loxP/KO}$*; twist2-Cre* mice. (B) Alizarin red and Alcian blue staining of P1 wild-type or *Mef2c*$^{loxP/KO}$*; twist2-Cre* bones of the sternum, forelimb, or hindlimb, as indicated. Many phalangeal bones of the forelimb fail to ossify in the mutant (arrow in panel f). Arrows indicate the tibia and fibula in panel h, in which ossification is severely disrupted. Bones of the *Mef2c*$^{loxP/KO}$*; twist2-Cre* mice contain excessive cartilage, and bone collars are disorganized. (C) Histologic sections of P1 wild-type and *Mef2c*$^{loxP/KO}$*; twist2-Cre* sternum and radius stained with H&E or by von Kossa's method. The sternum of *Mef2c*$^{loxP/KO}$*; twist2-Cre* mice does not contain hypertrophic chondrocytes, while the radius is filled with cartilage that has undergone limited hypertrophic differentiation. Panels b, e, h, i, l and m show enlargments of the boxed regions panels in a, d, g or k.

absence of ossification of the sternum (Fig. II.4A) and a failure in chondrocyte hypertrophy (Fig. II.4B) similar to the defects seen in *Mef2c*$^{loxP/KO}$*; twist2-Cre* mice.

Mef2c$^{loxP/KO}$*; col2-Cre* mice survived to adulthood and remained distinguishable from wild-type littermates by their waddling gait due to their shortened limbs. Bone and

cartilage staining of skeletons of three month-old mutant mice highlighted the truncation of all long bones of the limbs (Fig. II.4C). The structures of the distal ribs, radius, and sternabrae were also distorted by disorganized cartilaginous remnants of the growth plate and aberrant ossification (Fig. II.4D), demonstrating the requirement for MEF2C in timely chondrocyte maturation.

Chondrocyte deletion of *Mef2c* and *Mef2d*

Our earlier finding that deletion of one *Mef2d* allele exacerbated the bone defects in $Mef2c^{+/-}$ mice suggested that these two *Mef2* genes acted cooperatively to control chondrocyte hypertrophy. Because $Mef2c^{+/-}$; $Mef2d^{+/-}$ mice were not viable, it was necessary to generate a conditional *Mef2d* allele in order to examine possible redundant functions of MEF2C and MEF2D in the developing skeleton. As shown in Figure II.4A (i - l), homozygous deletion of both genes using *Col2-Cre* resulted in a skeletal phenotype more severe than that of $Mef2c^{loxP/KO}$; *Col2-Cre* mice in which nearly all mineralized endochondral skeletal elements were missing.

Requirement of MEF2C for activation of the gene program for chondrocyte hypertrophy and vascularization

To precisely define the molecular defects resulting from the absence of MEF2C expression in the endochondral skeleton, we analyzed numerous markers of skeletal development in the radius (Fig. II.5) and sternum (Fig. II.6) of $Mef2c^{loxP/KO}$; *twist2-Cre* mice at E14.5 and P1. At both stages, *Col2a1*, a marker of proliferating chondrocytes, failed to be down-regulated in mutant chondrocytes (Fig. II.5A and B). *Col10a1*, which

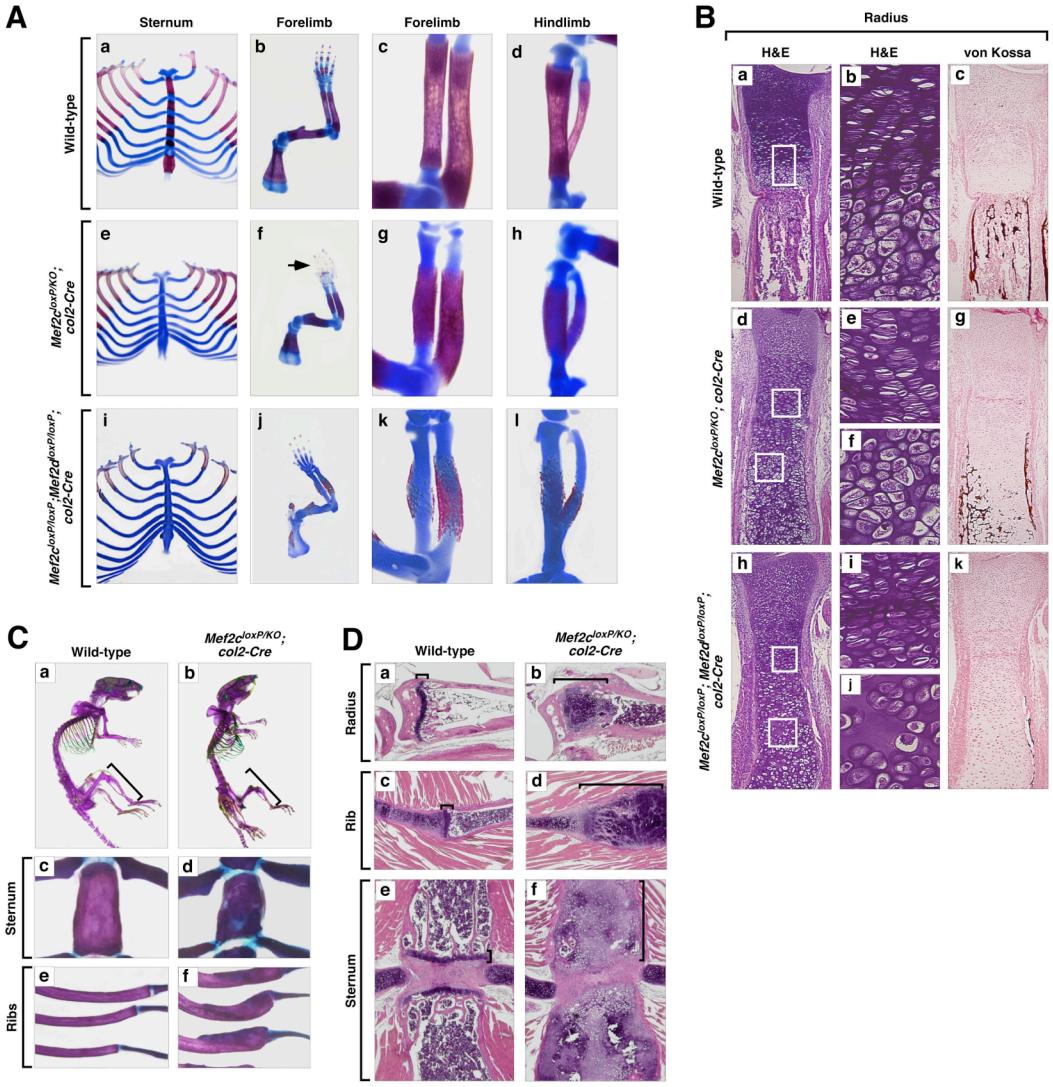

Figure II.4 Failure in endochondral ossification following conditional deletion of *Mef2c* and *Mef2d* using *Col2-Cre*. (A) Alizarin red and Alcian blue staining of P1 wild-type, *Mef2c*$^{loxP/KO}$*; col2-Cre*, or *Mef2c*$^{loxP/loxP}$*; Mef2d*$^{loxP/loxP}$*; col2-Cre* bones of the sternum, forelimb or hindlimb, as indicated. Bones of the *Mef2c*$^{loxP/KO}$*; col2-Cre* mice contain large amounts of cartilage, and bone collars are disorganized. Many phalangeal bones of the hand fail to ossify in the mutant (arrow in panel f). In *Mef2c/Mef2d* double mutants, there is almost a complete absence of bone formation. (B) Histologic sections of P1 wild-type, *Mef2c*$^{loxP/KO}$*; col2-Cre, and Mef2c*$^{loxP/loxP}$*; Mef2d*$^{loxP/loxP}$*; col2-Cre* sternum and radius stained with H&E or by von Kossa's method. The radius of the mutant is filled with cartilage that has undergone only limited hypertrophic differentiation and no mineralization. Panels b, e, f, i, and j show enlargements of the boxed regions of the adjacent panels a, d, or h. Note more severe defects in *Mef2c/Mef2d* double mutants than in *Mef2c* mutants (compare g and j). (C) Alizarin red and Alcian blue staining of three month old wild-type or *Mef2c*$^{loxP/KO}$*; col2-Cre* bones of the whole skeleton (a and b), sternum (c and d), or ribs (e and f). The limbs of the *Mef2c*$^{loxP/KO}$*; col2-Cre* skeleton are shortened. Brackets in panels a and b correspond to the length of the wild-type tibia. The sternum and ribs of the *Mef2c*$^{loxP/KO}$*;col2-Cre* skeleton contain large cartilaginous growth plate remnants that distort the bone architecture. (D) Histologic sections of three month old wild-type and *Mef2c*$^{loxP/KO}$*; col2-Cre* radius (a and b), ribs (c and d) and sternum (e and f) stained with H&E. The radius and ribs of the *Mef2c*$^{loxP/KO}$*; col2-Cre* skeleton contain large cartilaginous growth plate remnants, and the sternum is filled with partially ossified cartilage. Brackets indicate the position and length of the remaining growth plate cartilages.

is expressed in a specific zone of hypertrophic chondrocytes of normal bones, was not expressed in the radius or sternum of *Mef2c*$^{loxP/KO}$*; twist2-Cre* mutant mice at E14.5, and at P1 we detected only diffuse *Col10a1* expression in a few residual hypertrophic chondrocytes scattered throughout the length of the radius (Fig. II.5A and B), suggesting a severe developmental delay in the timing and extent of chondrocyte hypertrophy. There was no detectable expression of *Col1a1*, a marker of ossification, in the radius or sternum of the mutants at these stages. Similarly, *osteocalcin*, a marker of osteoblasts, was not detected within the endochondral skeleton of mutant mice, consistent with the failure in endochondral ossification.

Runx2, which is normally expressed at high levels in prehypertrophic and hypertrophic chondrocytes and osteoblasts, failed to be up-regulated in endochondral skeletal elements of *Mef2c*$^{loxP/KO}$*; twist2-Cre* mutant mice at P1 (Fig. II.5B), although *Runx2* expression was detected in the bone collar of the mutant. *Ihh* is expressed in prehypertrophic chondrocytes and induces *PTHrP* expression in adjacent chondrocytes, resulting in a delay in chondrocyte hypertrophy (St-Jacques et al., 1999; Vortkamp et al., 1996). In mutant mice, *Ihh* was expressed diffusely in prehypertrophic chondrocytes, but did not show the normally localized expression to the prehypertrophic zone (Fig. II.5B). The diffuse expression of *Ihh* likely reflects, at least in part, the failure in chondrocyte hypertrophy, which typically results in the organization in chondrocytes into a distinct prehypertrophic cell layer. The *PTHrP receptor (Ppr)* was expressed in prehypertrophic chondrocytes of wild type and mutant skeletal elements. *VEGF* is normally up-regulated in hypertrophic chondrocytes of the growth plate, where it stimulates cartilage vascularization (Zelzer et al., 2004). *VEGF* failed to be up-regulated in endochondral

cartilage of *Mef2c*$^{loxP/KO}$*; twist2-Cre* mice, and there was a complete absence of vascularization as assayed by staining for endomucin (Fig. II.5B). In contrast, the perichondrium and surrounding tissue were normally vascularized in the mutant. Thus, MEF2C is required specifically in endochondral cartilage for *VEGF* expression and blood vessel invasion.

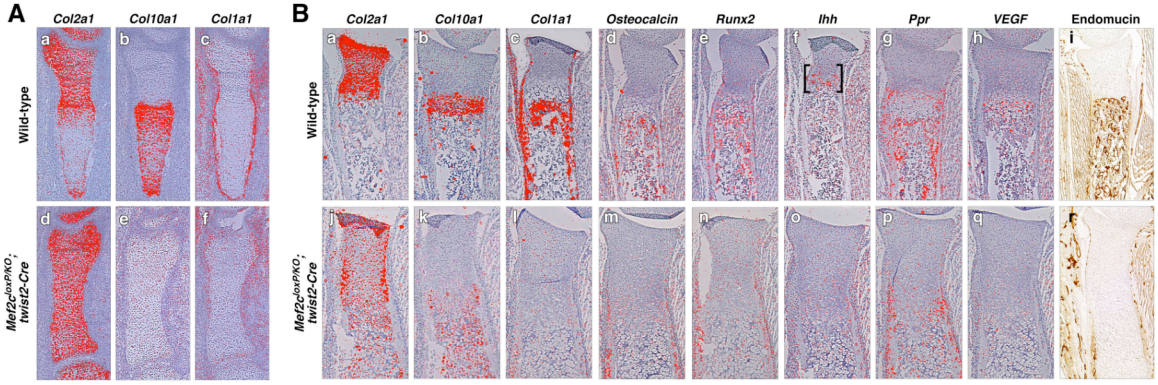

Figure II.5 Detection of markers of bone development in wild-type and *Mef2c*$^{loxP/KO}$*; twist2-Cre* mouse sterna. Transcripts for the indicated markers of bone development were detected by *in situ* hybridization to sections of the radius of wild-type (top row) and *Mef2c*$^{loxP/KO}$*; twist2-Cre* (bottom row) mice at E14.5 (A) and P1 (B). Endomucin expression was detected by immunostaining. Brackets in panel f show the region of prehypertrophic chondrocytes.

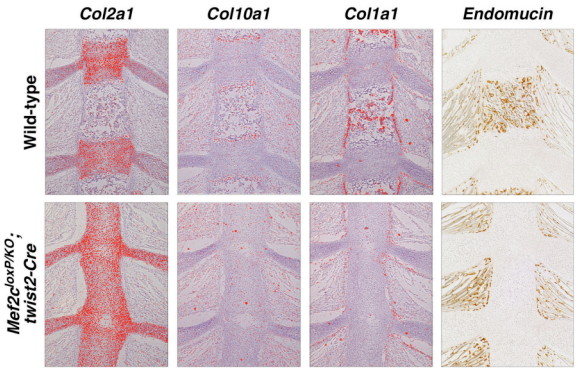

Figure II.6 Detection of markers of bone development in wild-type and *Mef2c*$^{loxP/KO}$*; twist2-Cre* mouse radii. Transcripts for the indicated markers of bone development were detected by *in situ* hybridization to sections of the sternum of wild-type (top row) and *Mef2c*$^{loxP/KO}$*; twist2-Cre* (bottom row) mice at P1. Endomucin expression was detected by immunostaining.

Blockade to chondrocyte hypertrophy by dominant negative MEF2C

The residual chondrocyte hypertrophy and ossification seen in *Mef2c; Mef2d* mutant mice could reflect partial functional redundancy with *Mef2a* or incomplete deletion of

these conditional alleles. As an independent means of inactivating the multiple MEF2 factors expressed in developing endochondral cartilage, we generated transgenic mice that expressed a fusion protein of the MEF2C DNA binding domain and the Engrailed repressor in proliferating chondrocytes under control of the *Col2al* promoter. This MEF2C-Engrailed fusion protein inactivates all MEF2 proteins by preventing DNA binding and creating transcriptionally inactive heterodimers with wild-type MEF2 proteins. Ossification in nearly every region of the endochondral skeleton was blocked in MEF2C-Engrailed transgenic mice, while formation of cartilage-independent membranous bones was unaffected (Fig. II.7). All endochondral bones of these transgenic mice were also hypoplastic, resulting in shortening of the limbs, spine, pelvis and deformation of the rib cage. In the most strongly affected animals, the endochondral bones at the base of the skull, the hyoid bone, limbs, sternum, and pelvis remained entirely cartilaginous (Fig. II.7A, B and D and data not shown). Milder defects were observed in transgenic mice carrying fewer copies of the transgene (data not shown). Histologic sections of the sternum and forelimb demonstrated that chondrocyte hypertrophy in these transgenic mice was completely absent (Fig. II.7C).

Excessive ossification in response to MEF2C-VP16

To determine if MEF2 was sufficient to induce chondrocyte hypertrophy and bone formation, we generated transgenic mice that expressed a super-active MEF2C-VP16 fusion protein under control of the *Col2al* promoter. In contrast to the MEF2C-Engrailed transgenic mice, expression of MEF2C-VP16 in endochondral cartilage of transgenic mice resulted in premature endochondral ossification at E18.5, with consequent

foreshortening of the limbs (Fig. II.7). This phenotype of excessive ossification was especially apparent in the sternum and vertebrae (Fig. II.7B). Growth plates separating the sternebrae were prematurely ossified, resulting in complete ossification along the length of the sternum (Fig. II.7Bh). In contrast to normal vertebrae at E18.5, which contain a cartilaginous growth plate surrounding the vertebral body (Fig. II.7Ba), the entire vertebra was ossified, due to premature fusion of the growth plates between the vertebral body and the lateral vertebral processes (Fig. II.7Bg). Growth plate cartilages of the limbs were also inappropriately ossified in MEF2C-VP16 transgenic mice, resulting in distortion of the forelimb (Fig. II.7Bi). Inappropriate ossification in MEF2C-VP16 transgenic mice was also prominent in the base of the skull, where premature fusion of the endochondral growth plates resulted in deformation of the cranial vault (Fig. II.7Dc). In contrast, formation of cartilage-independent membranous bones was unaffected. Histologic examination of the sternum and forearm confirmed that growth plate maturation was accelerated, particularly in the sternum where nearly all chondrocytes in the growth plate were consumed by premature differentiation (Fig. II.7Cf).

Activation of the *Col10a1* promoter by MEF2C

The bone abnormalities resulting from *Mef2c* deletion and MEF2C-Engrailed expression suggested that MEF2 was required for activation of a hypertrophic gene program in chondrocytes. Analysis of the promoter region of the *Col10a1* gene, the prototypical marker of chondrocyte hypertrophy (Gebhard et al., 2004), revealed several evolutionarily conserved sequences resembling MEF2 binding sites (Fig. II.8A), and gel

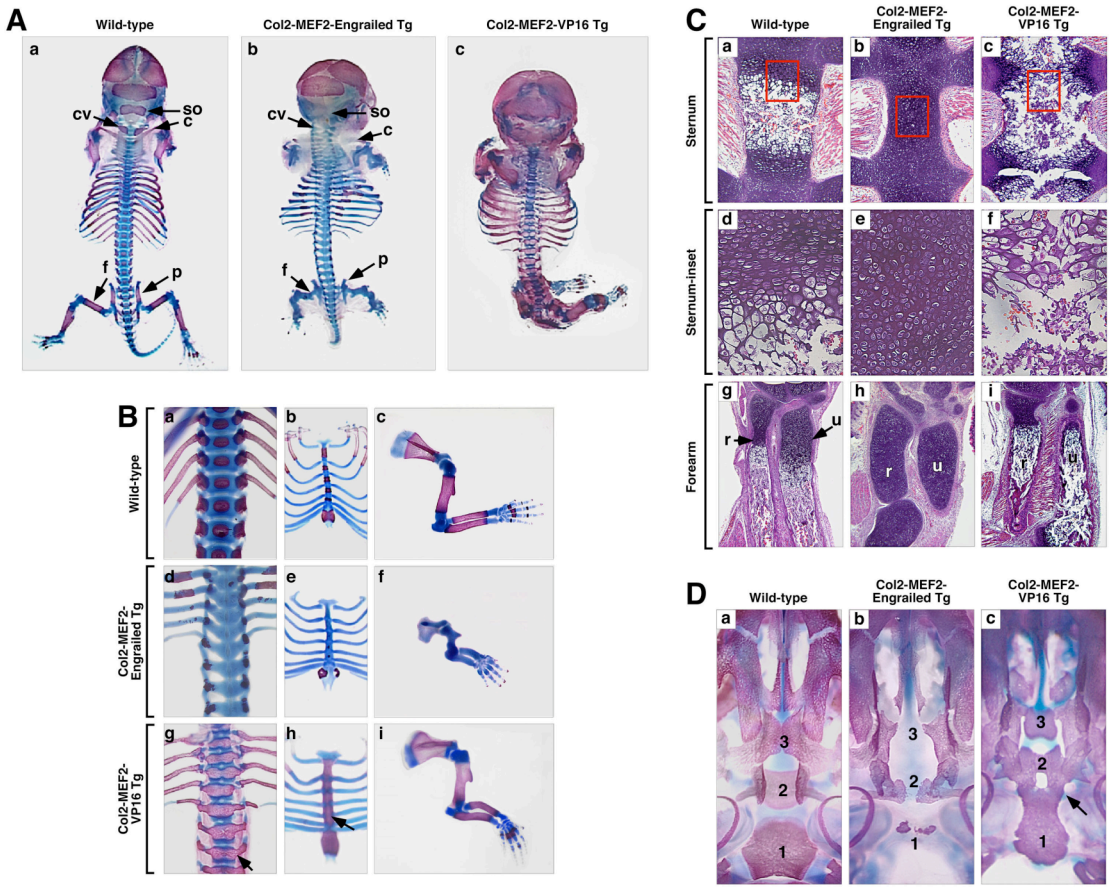

Figure II.7 Regulation of bone development by dominant negative and activating forms of MEF2C. (A) Alizarin red and Alcian blue staining of wild-type (a), Col2-MEF2C-Engrailed transgenic (b) and Col2-MEF2C-VP16 transgenic (c) E18.5 embryos depicting dorsal view of whole skeletons. Arrows indicate the supraoccipital bone (so), first cervical vertebrae (cv), clavicle (c), femur (f) and pelvis (p). (B) Alizarin red and Alcian blue staining of wild-type (a, b and c), Col2-MEF2C-Engrailed transgenic (d, e and f) and Col2-MEF2C-VP16 transgenic (g, h and i) E18.5 embryos depicting spine (a, d and g), sternum (b, e and h) and arm (c, f and i). Elements of the endochondral skeleton remain cartilaginous in Col2-MEF2C-Engrailed transgenic embryos, and endochondral skeletal elements of Col2-MEF2C-VP16 transgenic embryos are prematurely ossified (arrows in g and h). (C) Sections of wild-type (a, d, and g), Col2-MEF2C-Engrailed transgenic (b, e, and h) and Col2-MEF2C-VP16 transgenic (c, f, and i) E18.5 embryos stained with H&E depicting the sternum (panels a - f) or forearm (panels g, h and i) of the indicated embryos. The radius (r) and ulna (u) are indicated in panels g, h and i. Panels d to f are enlargements of the boxed regions of panels a to c. Chondrocytes in the sternum and radius of Col2-MEF2C-Engrailed transgenic embryos fail to initiate hypertrophic differentiation, conversely in Col2-MEF2C-VP16 transgenic embryos, chondrocyte hypertrophic differentiation is accelerated and has consumed nearly all growth plate chondrocytes. (D) Alizarin red and Alcian blue staining of wild-type (a), Col2-MEF2C-Engrailed transgenic (b) and Col2-MEF2C-VP16 transgenic (c) E18.5 embryos depicting the ventral skull. The endochondral basioccipital (1), basisphenoid (2) and presphenoid (3) bones are indicated. These bones fail to ossify in Col2-MEF2C-Engrailed transgenic embryos, and prematurely fuse in Col2-MEF2C-VP16 transgenic embryos (arrow in c).

mobility shift assays confirmed that MEF2 bound these sites (Fig. II.8C). Transfection assays also showed that MEF2 could activate the *Col10a1* promoter, and mutation of the

MEF2 sites eliminated MEF2 responsiveness (Fig. II.8B). As previously reported (Gebhard et al., 2004), the 5' flanking region of the *Col10a1* gene was able to direct the expression of a lacZ reporter in hypertrophic chondrocytes of developing endochondral bones of transgenic mice, in a pattern that recapitulated the endogenous expression pattern of the *Col10a1* gene (Fig. II.8D and E). Mutation of the MEF2 DNA binding sites in the promoter diminished expression in hypertrophic chondrocytes *in vivo*. These results identify MEF2 as a direct activator of chondrocyte gene expression and a critical control point in regulating chondrocyte hypertrophy *in vivo*.

Genetic antagonism between *Mef2c* and *Hdac4*

The decreased ossification observed in *Mef2c* mutant mice contrasts with the precocious and ectopic ossification of endochondral cartilage in mice lacking HDAC4, a MEF2 co-repressor (Vega et al., 2004b). Thus, we wondered whether the repressive effects of HDAC4 on bone development might be mediated, at least in part, by MEF2. Consistent with this notion, expression of a constitutively nuclear HDAC4 blocked activation of the *Col10a1* promoter by MEF2C (Fig. II.8B).

To test for potential genetic interactions between *Mef2c* and *Hdac4 in vivo*, we investigated whether deletion of one *Mef2c* allele might diminish the excessive and ectopic ossification of endochondral cartilage seen in *Hdac4* null mice (Vega et al., 2004b). Indeed, deletion of one *Mef2c* allele in *Hdac4*$^{-/-}$ mice normalized ossification of the chondrocostal cartilage and sternum (Fig. II.8F). Conversely, deletion of one copy of the *Hdac4* gene in the *Mef2c*$^{+/-}$ background partially restored ossification of the sternum and increased ossification in the xiphoid process, and deletion of both copies of *Hdac4* in

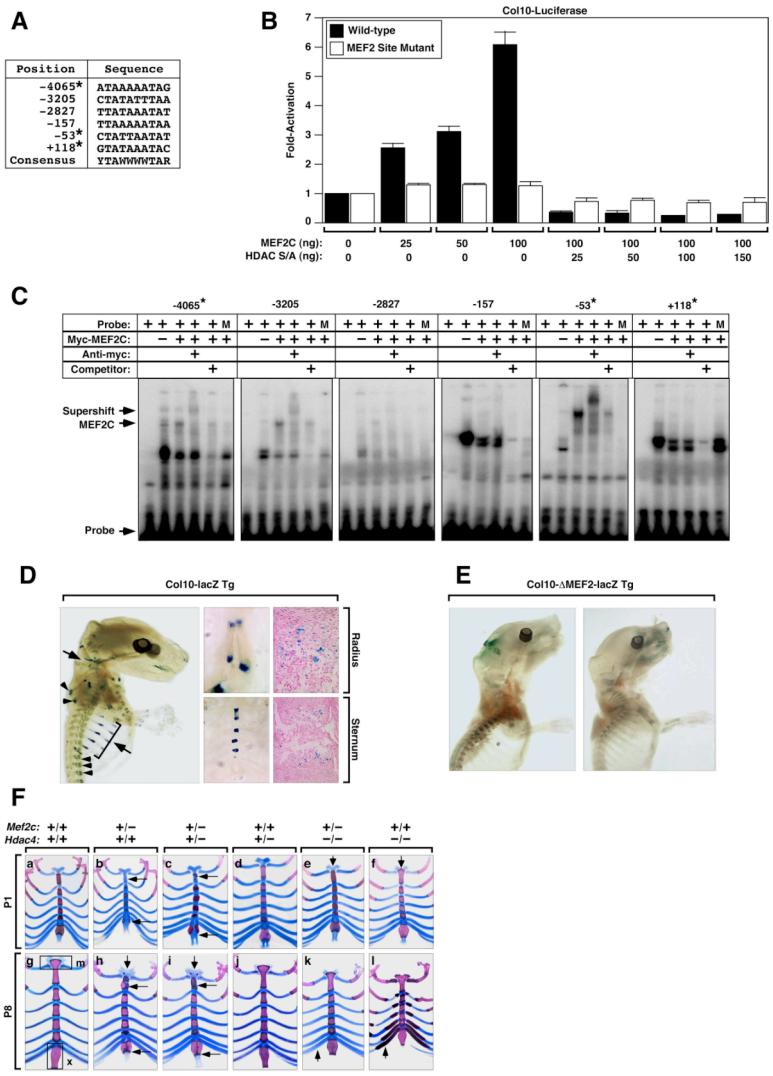

Figure II.8 Regulation of the *Col10a1* promoter by MEF2. (A) Comparison of potential MEF2 binding sites in the *Col10a1* promoter to the MEF2 biding consensus. All of the selected sites match the core TAWWWWTA of the MEF2 binding consensus. MEF2 binding sites conserved between the mouse and human genomes are indicated (*). (B) COS-7 cells were transfected with a luciferase reporter controlled by the wild-type *Col10a1* upstream region or the same region in which the MEF2 sites were disrupted by point mutations and increasing amounts of MEF2C-myc or a constitutively nuclear HDAC4 mutant (HDAC S/A), as indicated. (C) Electromobility shift assays of MEF2 binding to sites in the *Col10a1* promoter. Oligonucleotides containing MEF2 sites from the *Col10a1* promoter were labeled with ^{32}P and assayed for MEF2C-myc binding. MEF2C was supershifted with an anti-myc antibody (Anti-myc) or competed with 100 molar excess of the *Srpk3* MEF2 binding site (cold competitor) and compared to reticulocyte lysate that did not contain MEF2C (-) or binding of a labeled probe containing the corresponding MEF2 site disrupted by point mutations (M). MEF2 binding sites conserved between the mouse and human genomes are indicated (*). (D) b-galactosidase staining of E18.5 mice transgenic for Col10-lacZ. Note strong expression of the transgene in the growth plates. H&E sections of the radius and sternum show specific expression of the transgene in hypertrophic chondrocytes. (E) Mutation of the MEF2 binding sites in the Col10-lacZ transgene diminishes the expression of β-galactosidase in hypertrophic chondrocytes, demonstrating the requirement of MEF2 factors in the activation of the Col10-lacZ transgene. (F) Opposing influences of MEF2C and HDAC4 on mineralization of sternal and rib cartilage. Anterior views of the sternum and ribs of mice stained for bone (red) and cartilage (blue) at P1 (a to f) and P8 (g to l). Genotypes are indicated at the top. The manubrium (m) and xiphoid process (x) are identified in panel g. Arrows mark sites of ossification that are altered by the balance of *Mef2c* and *Hdac4*.

the presence of a heterozygous *Mef2c* allele resulted in a nearly normal pattern of ossification in the sternum (Fig. II.8F). Similar rescue of normal ossification was seen in endochondral bones of the skull and the hyoid bone (data not shown). These findings demonstrate that ossification of endochondral cartilage depends on the balance between transcriptional activation by MEF2C and repression by HDAC4.

DISCUSSION

The results of this study reveal the following new insights into the molecular basis of bone development and the role of MEF2C in this process. 1) MEF2C is a necessary early regulator of chondrocyte hypertrophy and subsequent growth plate maturation. The extent of chondrocyte hypertrophy and bone formation *in vivo* directly reflects the level of MEF2C transcriptional activity in chondrocytes, as shown by the perturbation of these processes with even a heterozygous *Mef2c* mutation. 2) MEF2C is sufficient to induce chondrocyte hypertrophy and bone formation *in vivo* as revealed by the stimulation of these processes by MEF2C-VP16 *in vivo*. 3) MEF2D augments the pro-hypertrophic actions of MEF2C in chondrocytes. 4) MEF2C is a direct regulator of *Col10a1* transcription and is required for appropriate temporal and spatial expression of the genetic program of chondrocyte development, including expression of *Runx2* and *VEGF* in endochondral cartilage. 5) Chondrocyte hypertrophy and bone formation depend on the balance between the opposing actions of MEF2C and HDAC4. We conclude that MEF2C is a key regulator of chondrocyte development that orchestrates multiple steps in the transcriptional program for bone formation, as schematized in Figure II.9.

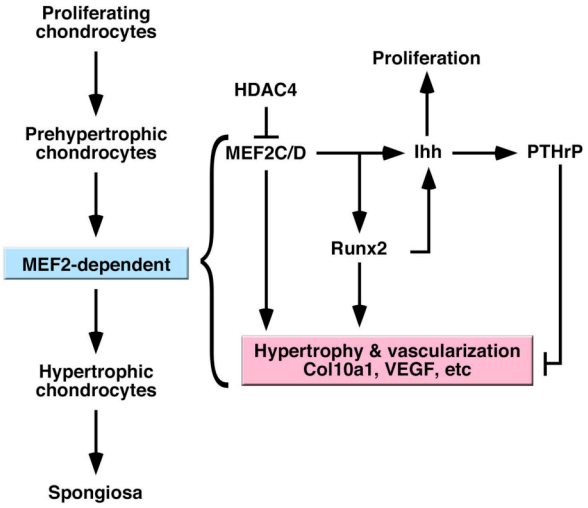

Figure II.9 A model for transcriptional regulation of bone development by MEF2C and HDAC4. HDAC4 repression in chondrocytes is mediated by MEF2 and Runx transcription factors. MEF2 factors function to regulate chondrocyte hypertrophy, while Runx factors are required for both chondrocyte hypertrophy and osteoblast development.

Control of chondrocyte hypertrophy by MEF2C

Growth of endochondral bone requires a tightly regulated sequence of developmental steps in which proliferating chondrocytes in the growth plate exit the cell cycle and undergo hypertrophy. Hypertrophic chondrocytes secrete a calcified extracellular matrix and undergo apoptosis. Osteoblasts then invade the cartilaginous skeleton and deposit bone on the mineralized cartilaginous spicules of the primary spongiosa. Lengthwise bone growth is driven by the dynamics of chondrocyte proliferation, differentiation and hypertrophy within the growth plates (Olsen et al., 2000). *Mef2c* is expressed in prehypertrophic and hypertrophic chondrocytes and its specific deletion from this cell population impairs hypertrophy with consequent short-limb dwarfism. Deletion of *Mef2d* exacerbates the bone defects associated with a *Mef2c* mutation, and expression of a dominant negative MEF2C-Engrailed fusion protein in endochondral cartilage prevents hypertrophy and ossification. The importance of MEF2C as a regulator of chondrocyte hypertrophy and bone formation is underscored by the ability of the super-activating

MEF2C-VP16 fusion protein to promote precocious ossification of endochondral bones and dwarfism due to premature growth plate fusion.

Runx2 mutant mice also display defects in chondrocyte hypertrophy and ossification, but the phenotypes of *Runx2* and *Mef2c* mutant mice differ in several important respects that highlight the distinct functions of these genes. For example, only a relatively small subset of chondrocytes display defects in hypertrophy in *Runx2* mutant mice, whereas osteoblasts are missing in these mice, resulting in an absence of membranous and endochondral ossification (Komori et al., 1997). Deletion of *Mef2c* from multiple mesodermal lineages, including chondrocytes and osteoblasts, with *Twist2-Cre* or specifically from chondrocytes with *Col2-Cre* results in similar phenotypes, supporting the conclusion that MEF2C functions primarily to regulate chondrocyte hypertrophy. We interpret the differences between the *Mef2c* and *Runx2* mutant phenotypes to indicate a primary role of MEF2C in hypertrophy of endochondral cartilage.

How does MEF2 regulate chondrocyte hypertrophy and bone development? Many of the actions of MEF2 on these processes undoubtedly reflect the direct activation of downstream target genes, such as the *Col10a1* gene, a specific marker for chondrocyte hypertrophy, which serves as a direct transcriptional target of MEF2. It is noteworthy that *Runx2* expression was also dramatically diminished in the endochondral cartilage of *Mef2c* mutant mice, suggesting that MEF2C is required, either directly or indirectly, for *Runx2* expression and that some of the defects of *Mef2c* mutant mice may be attributable to diminished expression of *Runx2*. MEF2C is also essential for normal expression of *VEGF* within the endochondral cartilage, which regulates angiogenesis in the late stages

of chondrocyte development. In addition, *Ihh* fails to be up-regulated in pre-hypertrophic chondrocytes of *Mef2c* mutant mice. Ihh plays multiple roles in endochondral bone development by enhancing chondrocyte proliferation (Long et al., 2001; St-Jacques et al., 1999) and stimulating PTHrP synthesis, thereby regulating a negative feedback loop to govern the timing of hypertrophy (St-Jacques et al., 1999; Vortkamp et al., 1996). The failure of *Ihh* to be up-regulated in pre-hypertrophic chondrocytes of *Mef2c* mutant mice could contribute to the truncations of endochondral bones in these animals. MEF2C, therefore, influences numerous interwoven steps of signaling and gene activation during bone development.

Control of bone development by the balance of MEF2C and HDAC4

Impairment of chondrocyte hypertrophy resulting from deletion of *Mef2c* or expression of MEF2C-Engrailed in endochondral cartilage is the opposite of the phenotype resulting from genetic deletion of *Hdac4* (Vega et al., 2004b), which results in premature ossification and fusion of the growth plates. Conversely, the premature and ectopic ossification of endochondral bones resulting from expression of MEF2C-VP16 is similar to, but more severe than, that of *Hdac4* null mice. Altering the balance between the opposing actions of MEF2C and HDAC4 can dictate the extent of chondrocyte hypertrophy and ossification in predictable ways. Failure of endochondral ossification resulting from heterozygosity of *Mef2c*, for example, can be rescued in a dose-dependent manner by removal of *Hdac4* alleles, whereas the premature and ectopic ossification in *Hdac4* mutant mice can be reversed by deletion of a *Mef2c* allele. The rescue of the

Hdac4 mutant phenotype with a heterozygous *Mef2c* allele provides the strongest genetic evidence to date for the opposing actions of MEF2 and class II HDACs *in vivo*.

Misregulation of signaling pathways that influence growth plate dynamics results in dwarfisms and bone deformations due to either accelerated maturation of the growth plate cartilage, characteristic of achondroplasia, or delayed or absent chondrocyte maturation, characteristic of many chondrodysplastic syndromes (Kronenberg, 2003; Zelzer and Olsen, 2003). Our results demonstrate that growth plate dynamics can be modified by the balance of MEF2C and its repressor, HDAC4. The realization that bone formation is controlled by the partnership of MEF2C and HDAC4 suggests possibilities for therapeutically manipulating endochondral bone growth by modulating the signaling pathways that govern the association of HDAC4 with MEF2C. Moreover, our results suggest that HDAC inhibitors currently in clinical trials for cancer, neurodegenerative diseases and other disorders, may also promote bone formation.

Commonalities of developmental processes controlled by MEF2 and class II HDACs

MEF2 transcription factors are well known regulators of skeletal muscle differentiation and fiber type switching, as well as cardiovascular development, heart growth and neuronal development (McKinsey et al., 2002). Class II HDACs play key roles in each of these processes by governing MEF2 transcriptional activity. The results of the present study indicate that these seemingly unrelated processes of cell differentiation, tissue growth and remodeling share an underlying commonality with the regulatory mechanisms that control bone development. Specificity in each case is dictated by the association of MEF2 and class II HDACs with other cell type-specific and signal-

responsive transcriptional regulators. Given the importance of MEF2 for vascular development (Lin et al., 1998) and bone formation, it will be of interest to determine whether the developmental mechanism described here is also operative in the settings of vascular calcification, which is among the most common cardiovascular disorders.

METHODS

Creation of a conditional *Mef2c* mutant allele

Genomic regions of the *Mef2c* locus were isolated from 129SvEv genomic DNA by high-fidelity PCR (Roche Expand Long Template PCR System or Roche High Fidelity PCR System) and cloned into pGKneoF2L2DTA (Hoch and Soriano, 2006). A 4.6kb genomic sequence (5' targeting arm) upstream of *Mef2c* exon 2, bounded by an upstream BamHI site and a downstream NcoI site, was cloned upstream of the 5' loxP sequence in pGKneoF2L2DTA. A 1.8kb genomic sequence (3' targeting arm) downstream of *Mef2c* exon 2, bounded by an upstream EcoRV site and a downstream HindIII site, was cloned downstream of the 3' loxP sequence. A 1.1kb region (conditional knockout region) corresponding approximately to the region deleted in the *Mef2c* knockout allele (Lin et al., 1997) was cloned between the 5' loxP sequence and the 5' FRT sequence. The resulting vector was verified by DNA sequencing and restriction mapping. The vector was linearized at the SacII site upstream of the 5' targeting arm and electroporated into 129SvEv derived ES cells. Cells were then treated with G418, and negative selection was accomplished by the Diphtheria toxin A cassette (DTA) in the pGKneoF2L2DTA vector. Resistant colonies were screened by Southern blot analysis using probe sequences isolated from 129SvEv DNA by high-fidelity PCR and cloned into pCRII-

TOPO (Invitrogen). Southern blot analysis detected the presence of the EcoRI site adjacent to the 5' loxP site and the SacI site in the neomycin resistance cassette to verify recombination of the 5' and 3' arms, resulting in the *Mef2c*$^{neo\text{-}loxP}$ allele. Chimeric male mice generated by blastocyst injection with targeted ES cells transmitted the mutant allele through the germline yielding mice heterozygous for this *Mef2c*$^{neo\text{-}loxP}$ allele. Mice heterozygous for this mutation were bred to mice expressing FLPe recombinase in the germline (Rodriguez et al., 2000) in order to remove the neomycin resistance cassette. F1 progeny from these matings were genotyped by Southern blot analysis or PCR to detect the recombined allele (*Mef2c*^{loxP}), and genotyping of subsequent mice was performed by PCR. Sequences of DNA oligonucleotides used for PCR, DNA sequencing, genotyping, and Southern probe sequences and plasmids are available on request. Mice bearing a conditional *Mef2d* null allele are described elsewhere (Kim et al., 2008).

Transgenic mice

Chondrocyte-specific transgenes were constructed by subcloning either an in-frame fusion of the MEF2C DNA binding domain and the Engrailed repressor or an in-frame fusion of MEF2C and the VP16 activation domain, between a 3-kb fragment of the *Col2a1* promoter and its 3-kb chondrocyte-specific enhancer region (Zhou et al., 1998). Linearized transgenic constructs were injected into the pronuclei of fertilized oocytes. Embryos were harvested and analyzed for changes in skeletal development. The severity of the skeletal phenotype in these mice correlated with transgene copy number.

Tissue culture and transfection

COS-7 cells were grown in DMEM with 10% FBS. Fugene 6 (Roche) was used for transient transfection according to the manufacturer's instructions. A reporter plasmid containing 4.5 kb of the *Col10a1* locus was generated by PCR and cloned into pGL3-basic (Promega). Expression constructs for MEF2C, HDAC4 and Runx2 have been previously described (McKinsey et al., 2000; Vega et al., 2004b). Plasmids were co-transfected with 10 ng of a CMV-β-galactosidase reporter plasmid to control for transfection efficiency.

Electromobility shift assays

MEF2C was translated *in vitro* in a coupled transcription-translation T7 reticulocyte lysate system (Promega). *In vitro* binding analysis was performed as previously described (Wang et al., 2001), using oligonucleotide fragments that contained a MEF2-binding site from the *Col10a1* promoter, and competed with a MEF2 binding site from the *Srpk3* promoter (Nakagawa et al., 2005). Oligonucleotide sequences are available on request.

Tissue specific deletion of *Mef2c*

To generate mice that lack MEF2C in specific tissues, mice heterozygous for the null allele of *Mef2c* were mated to mice bearing the designated Cre transgene or knock-in. The resulting mice were mated to mice homozygous for the $Mef2c^{loxP}$ allele to produce conditional null mice. Mesoderm deletion of *Mef2c* was performed using the *Twist2-Cre* knock-in (Yu et al., 2003). Chondrocyte deletion was performed using *Col2-Cre* (Long

et al., 2001). All animal experimental procedures were reviewed and approved by the Institutional Animal Care and Use Committees at the University of Texas Southwestern Medical Center.

Cartilage and bone staining

Euthanized mice were skinned, eviscerated, and fixed overnight in 100% ethanol. Adult animals were additionally incubated overnight in acetone to clear fatty tissues. All specimens were then stained using Alcian blue for 48 hours. Soft tissues were removed by incubation in 2% KOH as needed, and specimens were stained with Alizarin red for 30 to 90 minutes as needed. Tissues were cleared in 1% KOH, 20% glycerol and photographed in 50% ethanol, 50% glycerol. Staining reagents were prepared as described previously (McLeod, 1980).

Histology

Tissues were fixed in 10% phosphate-buffered formalin at 4°C. Samples were then embedded in paraffin, sectioned at 5 μm, and stained with hematoxylin and eosin or with von Kossa's method. Briefly, sections were deparaffinized and immersed in 5% silver nitrate solution for 30 minutes while exposed to a 100W light bulb. Slides were rinsed in distilled water and immersed in 5% sodium thiosulfate for three minutes. Slides were rinsed again in distilled water and counterstained with nuclear fast red for 5 minutes.

β–galactosidase staining of transgenic mouse bones

Transgenic embryos were collected at E18.5 and stained as described in Zhou et al, 1995. Samples were skinned, eviscerated and fixed in PBS supplemented with 4% paraformaldehyde for 30 minutes on ice. Samples were then washed three times, each for 30 minutes, in PBS supplemented with 2mM $MgCl_2$, 0.2% NP40, and 0.1% deoxycholic acid. Samples were then stained in the dark for 48 hours in PBS supplemented with 2mM $MgCl_2$, 0.2% NP40, 0.1% deoxycholic acid, 5mM potassium ferrocyanide, 5mM potassium ferricyanide and 1mg/ml X-gal. Stained samples were then fixed overnight in PBS supplemented with 4% paraformaldehyde. For photography, fixed samples were dehydrated into methanol by 30 minute washes each in PBS with 25% (v/v) methanol, PBS with 50% methanol, PBS with 75% methanol and 100% methanol and cleared in 2:1 (v/v) benzyl alcohol:benzyl benzoate for approximately 4 hours.

***In situ* hybridization**

Tissue samples were fixed overnight in DEPC-treated 4% paraformaldehyde. Riboprobes were labeled with ^{35}S-UTP using the MAXIscript *in vitro* transcription kit (Ambion, Austin, Texas*). In situ* hybridization of sectioned tissues was performed as previously described (Vega et al., 2004b).

ACKNOWLEDGEMENTS

This research was conducted in collaboration with Michael Arnold.

Chapter III

MEF2 in Stress-Dependent Cardiac Remodeling

The adult heart responds to excessive neurohumoral signaling and workload by a pathological growth response characterized by hypertrophy of cardiomyocytes and activation of a fetal program of cardiac gene expression, which culminate in diminution of pump function, ventricular dilatation and wall thinning, fibrosis and sudden death. Myocyte enhancer factor-2 (MEF2) transcription factors serve as targets of the signaling pathways that drive pathological cardiac remodeling, but whether MEF2 factors are required for heart disease in vivo has not been determined. MEF2A and MEF2D are the primary MEF2 factors expressed in the adult heart. Mice lacking MEF2A are prone to sudden death from arrhythmias, accompanied by abnormalities in expression of genes encoding contractile proteins and metabolic enzymes. We show that mice lacking MEF2D are viable, but are resistant to cardiac hypertrophy, fetal gene activation and fibrosis in response to pressure overload and chronic adrenergic stimulation. Conversely, forced over-expression of MEF2D is sufficient to drive the fetal gene program and pathological remodeling of the heart. These results reveal a unique and important function for MEF2D in stress-dependent cardiac growth and reprogramming of gene expression in the adult heart.

INTRODUCTION

Acute or chronic injury to the adult heart activates a pathological response characterized by hypertrophic growth of cardiomyocytes, assembly of additional sarcomeres to enhance contractility, and activation of a fetal cardiac gene program, ultimately causing ventricular wall thinning, chamber dilation, heart failure and sudden death (Czubryt and Olson, 2004; Frey et al., 2004; Frey and Olson, 2003). A variety of abnormalities cause pathological hypertrophy and heart failure, including hypertension, myocardial infarction, endocrine disorders and inherited mutations in structural and contractile proteins of cardiomyocytes. These insults have been shown to activate a complex set of interwoven signaling pathways that culminate in the nucleus to activate various transcription factors, including nuclear factor of activated T-cells (NFAT), GATA and MEF2 factors, that drive the expression of fetal cardiac and stress response genes (Frey and Olson, 2003; McKinsey and Olson, 2005). There has been great interest in deciphering the molecular mechanisms responsible for transcriptional reprogramming of the failing heart and in "transcriptional" therapies for enhancing cardiac function (Backs and Olson, 2006; McKinsey and Olson, 2005).

Members of the MEF2 family of MADS (MCM1, Agamous, Deficiens, serum response factor) box transcription factors function as stress-dependent regulators of gene expression and have been implicated in multiple aspects of striated muscle development and disease (Black and Olson, 1998). The four vertebrate MEF2 factors, MEF2A, -B, -C and -D, display overlapping expression patterns in embryonic and adult tissues (Edmondson et al., 1994; Martin et al., 1994; Molkentin et al., 1996), and loss-of-function studies in mice have revealed distinct functions for the *Mef2a* and *Mef2c* genes

in the developing heart. Mice lacking *Mef2a* survive until the perinatal period when they succumb to lethal cardiac arrhythmias accompanied by abnormalities in expression of contractile protein and metabolic genes (Naya et al., 2002). Mice lacking *Mef2c* die during early embryogenesis from a spectrum of cardiovascular defects (Lin et al., 1997). However, despite the key roles of MEF2 factors as regulators of cardiac gene expression during development, relatively little is known of their functions in the adult heart.

Using transgenic mice harboring a MEF2-dependent reporter gene, we showed previously that hypertrophic stimuli augment MEF2 activity in the adult heart (Passier et al., 2000). Stress-activated signaling pathways that drive pathological cardiac remodeling stimulate the transcriptional activity of MEF2 through multiple mechanisms. Activation of calcium/calmodulin-dependent protein kinase and protein kinase D stimulates MEF2 activity by promoting the phosphorylation and nuclear export of class II histone deacetylases, which function as MEF2 co-repressors (McKinsey et al., 2000; Vega et al., 2004a). MAPK signaling leads to the phosphorylation of MEF2 and stimulation of transcriptional activity, and calcineurin promotes MEF2 activity through multiple mechanisms (Wu et al., 2001; Yang et al., 1999; Youn et al., 2000).

The major MEF2 isoforms in the adult heart are MEF2A and D, which form heterodimers (Molkentin et al., 1995; Naya et al., 2002). The lethal phenotype of *Mef2a* null mice indicates that MEF2D alone cannot support normal postnatal cardiac function (Naya et al., 2002). Whether MEF2A can support cardiac function in the absence of MEF2D and whether MEF2D may also be essential in the adult heart has not been determined.

To define the potential functions of MEF2D in the heart, we generated mice with a *Mef2d* loss-of-function mutation. In contrast to the lethal cardiac phenotypes resulting from genetic deletion of *Mef2a* or *Mef2c*, we show that mice lacking *Mef2d* are viable, but display an impaired response to stress signals that normally lead to cardiac hypertrophy, fibrosis and fetal gene activation. Conversely, forced over-expression of MEF2D in the heart is sufficient to evoke severe cardiomyopathy. These findings demonstrate that MEF2D plays a key role in mediating stress-dependent gene expression in the adult heart.

RESULTS

Generation of *Mef2d* null mice

Because *Mef2a* and *Mef2c* null mice are not viable (Lin et al., 1997; Naya et al., 2002), we generated a conditional *Mef2d* null allele, called $Mef2d^{loxP}$, in order to determine the functions of *Mef2d* in the adult heart. The conditional allele contained loxP sites flanking the third exon, which encodes the MADS and MEF2-specific domains that mediate DNA binding, dimerization and cofactor interactions (Fig. III.1A). Deletion of the corresponding region between the loxP sites of *Mef2a* or *Mef2c* results in a null allele (Lin et al., 1997; Naya et al., 2002).

To determine the complete loss-of-function phenotype of *Mef2d*, we initially deleted the gene using a *Meox2-Cre* transgene, which expresses Cre recombinase in epiblast-derived tissues as early as embryonic day 5 (Tallquist and Soriano, 2000). Unexpectedly, mice homozygous for this deletion were viable and showed no obvious phenotypic abnormalities. Complete deletion of the genomic region between the two

loxP sites was confirmed by Southern blot and PCR of genomic DNA (Fig. III.1B and C). By RT-PCR of RNA from adult heart, we found that exon 2 was spliced to exon 4 in the mutant allele, resulting in an in-frame deletion within the coding region of the *Mef2d* mRNA (Fig. III.1D). Western blot analysis of cardiac extracts confirmed that the mutant MEF2D protein lacking the MADS and MEF2 domains was expressed at a level comparable to the wild type protein (Fig. III.1E).

To confirm that the residual MEF2 protein did not function as a dominant negative mutant, we coexpressed it with the wild type protein in transfected COS-7 cells and monitored expression of a MEF2-dependent luciferase reporter. As shown in Figure III.2, the MEF2DΔ(18-96) protein was devoid of transcriptional activity and showed no dominant negative effect on wild type MEF2A protein.

We analyzed numerous adult tissues including skeletal muscle, heart, liver, thymus, spleen and brain of *Mef2d* mutant mice and observed no histological abnormalities. *Mef2d* mutant mice also appeared normal by other criteria, including behavior, weight, fertility, and lifespan. We conclude that MEF2D is not required for viability in mice. Quantification of *Mef2a* and *Mef2c* mRNA expression in *Mef2d* mutant hearts showed no compensatory up-regulation of these genes (Fig. III.1F).

Mef2d null mice are resistant to cardiac remodeling and fibrosis in response to pressure overload

To investigate whether MEF2D was required for pathological remodeling of the heart in response to pressure overload, we performed thoracic aortic constriction (TAC) on adult mice. As shown in Figure III.3A, the hearts of wild type and *Mef2d*$^{-/-}$ mice were

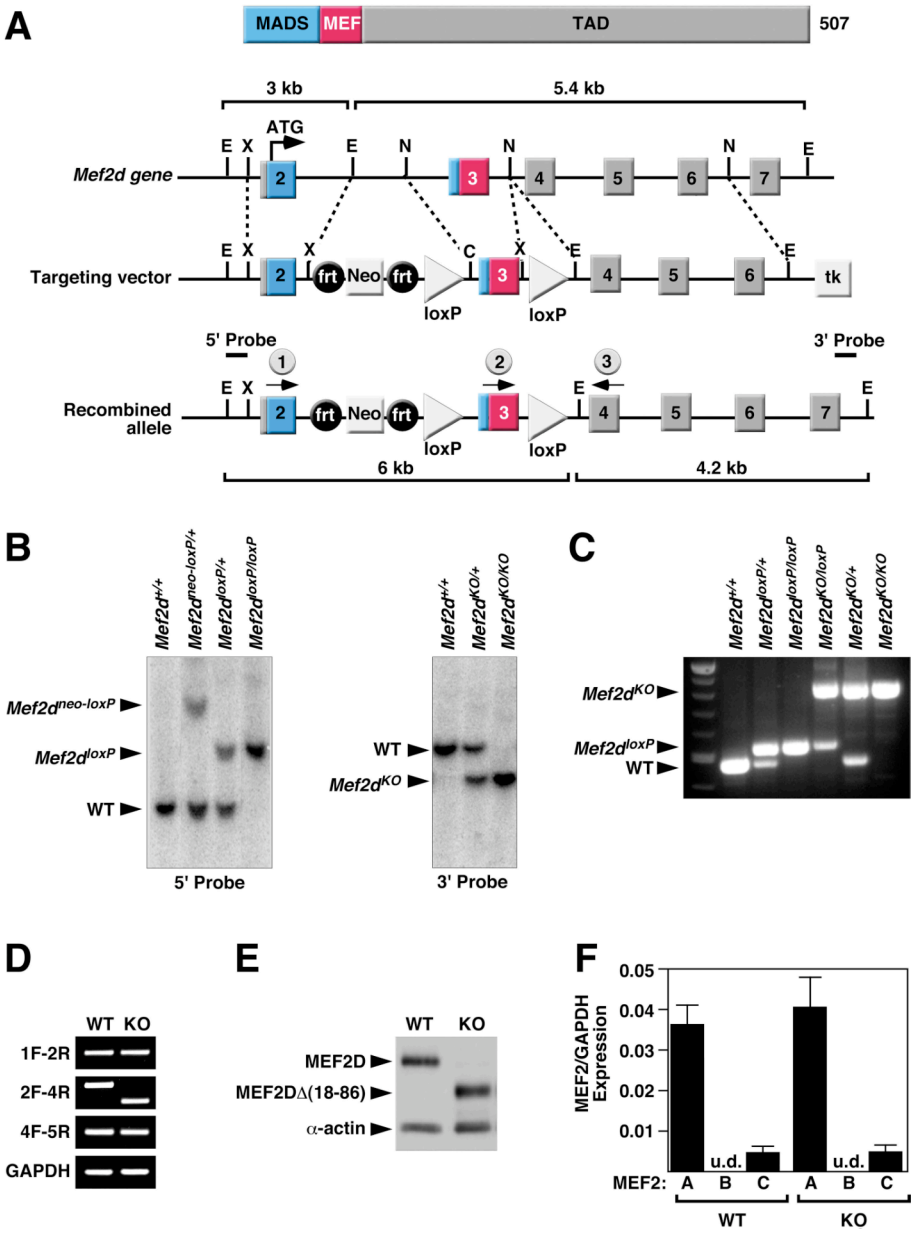

Figure III.1 Generation of mice with a conditional *Mef2d* mutation. (A) Schematic representation of the mouse *Mef2d* locus and targeting strategy. Positions of 3' and 5' probes used for Southern blots are shown. The positions of the PCR primers used for genotyping mutant alleles are marked with arrows (labeled 1, 2, 3 and circled). C, ClaI, E, EcoRI, N, NcoI, X, XhoI. (B) Southern blot analysis of *Mef2d* mutant alleles. Genomic DNA was digested with EcoRI and hybridized to a 5' probe in the left panel and to a 3' probe in the right panel. WT, wild type allele; $Mef2d^{neo\text{-}loxP}$, conditional allele; $Mef2d^{loxP}$, conditional allele with the Neo cassette removed; $Mef2d^{KO}$, null allele. (C) PCR genotyping to distinguish different *Mef2d* alleles. The positions of the primers that produce these PCR products are labeled (1, 2, 3) and circled on panel A. (D) Expression of WT and mutant Mef2d (KO) detected by RT-PCR. Mef2d mutant allele lacks exon 3, which encodes the MADS and MEF2-specific domains. GAPDH was detected as a loading control. Labels on the left side of the panel indicate location and direction of primers used for RT-PCR. (E) Western blot analysis to detect WT and mutant MEF2D (KO) proteins. The mutant MEF2D protein is truncated due to deletion of exon 3. α-actin protein was used as a loading control. (F) Expression level of Mef2 in WT and Mef2d mutant (KO) mice detected by quantitative PCR. Error bars indicate ±SEM. u.d., undetectable.

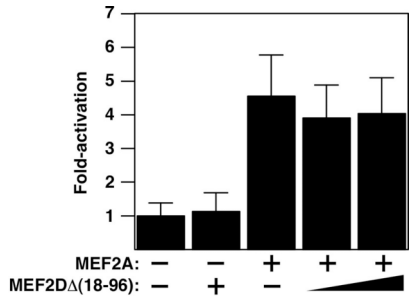

Figure III.2 Transcriptional activity of MEF2DΔ(18-96). COS-7 cells were cotransfected with a MEF2-dependent luciferase reporter and expression vectors of MEF2A and MEF2DΔ(18-96) to demonstrate that presence of mutant MEF2D protein has minimal influence on MEF2 activity. Error bars indicate one standard deviation.

comparable in size at baseline. Following TAC for 21 days, wild type mice showed a 59% increase in heart weight/tibia length (HW/TL). In contrast, *Mef2d* mutant mice showed only a 27% increase in HW/TL (Fig. III.3A). Based on histological sections less cardiac remodeling is observed in *Mef2d* mutant mice compared to wild type mice (Fig. III.3B). Consistent with these findings, following pressure overload we observed a 34.7 ± 0.25% increase in cross sectional area of cardiomyocytes in wild type mice, in comparison to only a 11.5 ± 0.40% increase in mutant mice (Fig. III.3C).

Pressure overload hypertrophy in wild type mice is accompanied by extensive fibrosis of the ventricular wall, as detected by Masson's trichrome staining (Fig. III.3B). Remarkably, there was virtually no ventricular fibrosis in *Mef2d* mutant mice. These findings were corroborated by morphometric analysis of picrosirius red stained sections of wild type and mutant hearts showing that *Mef2d* mutant mice had much less fibrosis after pressure overload compared to wild type mice (Fig. III.3D).

Functional analysis of hearts of *Mef2d* null mice

The response to cardiac stress of *Mef2d* mice was assessed by echocardiography. At baseline there were no significant differences seen in the left ventricular end-diastolic

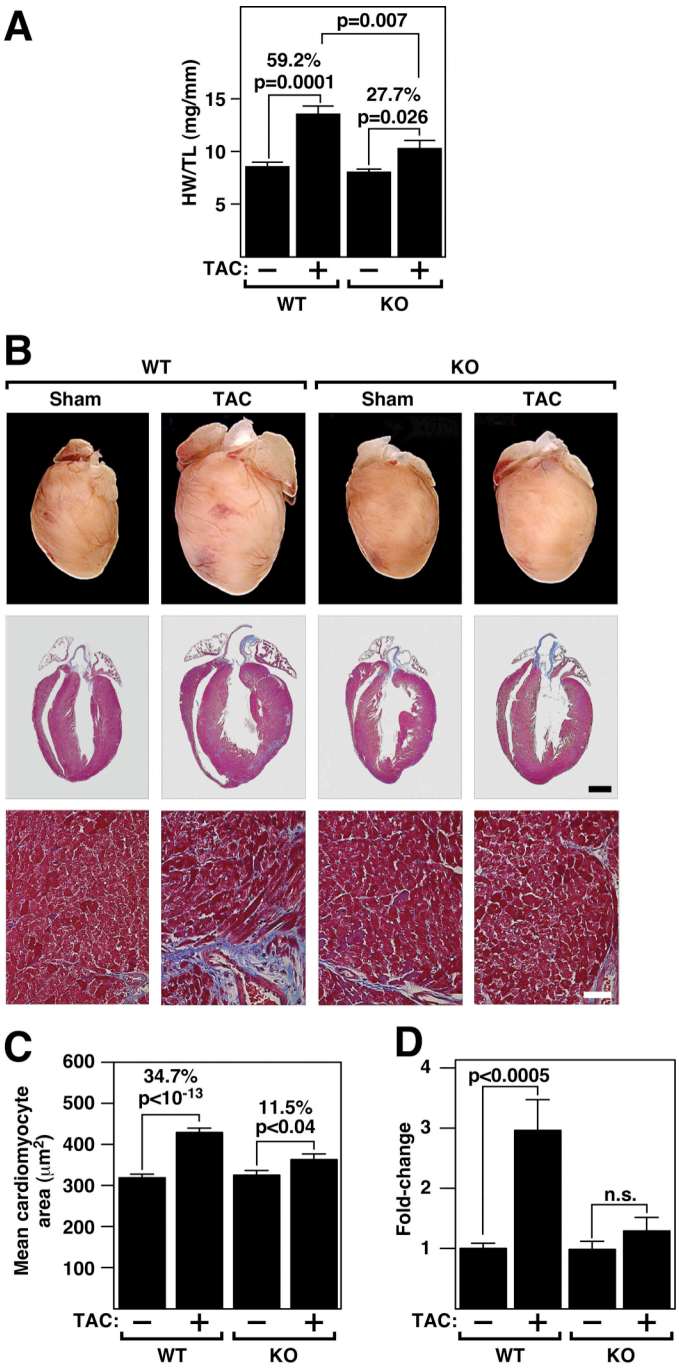

Figure III.3 Blunted hypertrophy of *Mef2d* mutant mice following TAC. (A) Heart weight/tibia length (HW/TL) ratios (±SEM) of WT and *Mef2d* mutant (KO) mice were determined 21 days after TAC. (B) Hearts from WT and *Mef2d* mutant (KO) mice subjected to either a sham operation or pressure overload (TAC) are shown at the top. Histological sections stained with Masson's trichrome are shown on the bottom. Masson's trichrome staining of WT and *Mef2d* mutant hearts indicates lack of fibrosis in *Mef2d*$^{-/-}$ hearts in response to pressure overload by TAC. Scale bar = 1 mm (middle panel) and 40 mm (bottom panel). (C) Mean cross sectional area of cardiomyocyte (±SEM) in WT and *Mef2d* mutant (KO) mice was measured 21 days after TAC. (D) Using morphometric analysis of picrosirius red stained heart sections, the amount of myocardial fibrosis was assessed. Fibrosis is apparent in the hearts of WT mice. In contrast, virtually no fibrosis is detected in the hearts of *Mef2d* mutant (KO) mice. Values indicate fold-changes of fibrosis in each group compared to a group of sham-operated WT mice (±SEM).

diameter (LVIDd) or heart rate (HR), and only minimal differences seen in the left ventricular end-systolic diameter (LVIDs) and fractional shortening (FS) in wild type and mutant *Mef2d* mice (Fig. III.4A and Table III.1). Three weeks after TAC surgery, wild type mice showed a dramatic increase in LVIDd accompanied by a pronounced reduction in cardiac contractility, as indicated by a decreased FS. In contrast, *Mef2d* mutant animals were largely resistant to left ventricular dilation and its concomitant decrease in contractility (Fig. III.4A and B). Additionally, compared to *Mef2d* mutant animals, wild type animals experienced a significant reduction in HR following TAC, which is indicative of the pathological state of the heart. These data demonstrate that in response to pressure overload *Mef2d* mutant hearts are resistant to cardiac remodeling and functional deterioration.

A

	LVIDd (mm)	LVIDs (mm)	FS (%)	HR (min^{-1})	AWd (mm)	PWd (mm)
WT Sham	2.10 ± 0.06	0.28 ± 0.03	83.98 ± 0.81	681.70 ± 10.50	0.83 ± 0.02	0.60 ± 0.03
WT TAC	3.41 ± 0.30	2.09 ± 0.34	41.63 ± 7.10	587.56 ± 31.72	0.69 ± 0.04	0.77 ± 0.04
KO Sham	2.14 ± 0.05	0.50 ± 0.04	75.62 ± 1.68	668.49 ± 5.60	0.80 ± 0.05	0.70 ± 0.05
KO TAC	2.87 ± 0.14	0.98 ± 0.17	65.03 ± 3.64	685.14 ± 21.81	0.95 ± 0.03	0.88 ± 0.01

B

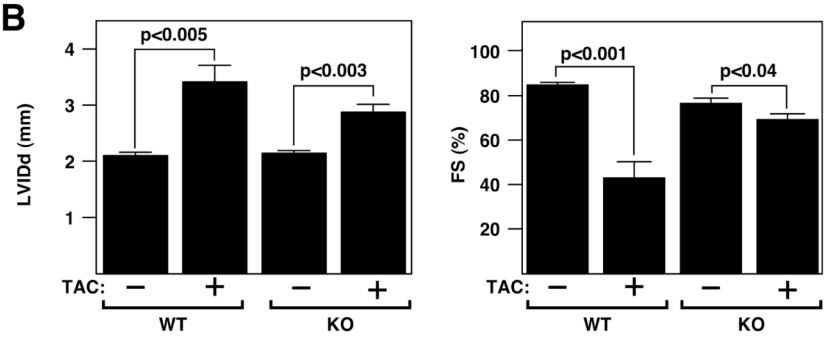

Figure III.4 Echocardiographic analysis of *Mef2d* mutant mice following TAC. (A) Echocardiographic data (±SEM) indicate less left ventricular remodeling in the *Mef2d* mutant (KO) mice in response to TAC compared to WT littermates (n= 5 to 7 per group). LVIDd, left ventricular end-diastolic diameter; LVIDs, left ventricular end-systolic diameter; FS, fractional shortening; HR, heart rate; AWd, anterior wall thickness in diastole; PWd, posterior wall thickness in diastole. (B) *Mef2d* mutant (KO) mice display less left ventricular dilation during diastole and a less pronounced decrease in FS in response to TAC than WT mice.

Echocardiogram		Fetal gene expression	
Parameters	p values	Parameters	p values
LVIDd	<0.7	ANP	<1.0
LVIDs	<0.005	BNP	<0.08
FS	<0.005	Myh6	<1.0
HR	<0.3	Myh7	<0.4
AWd	<0.6	Acta1	<0.09
PWd	<0.2	Ctgf	<0.5
		Col1a2	<0.9
		Col3a1	<0.5
		Mef2a	<0.7

Table III.1 Statistical analysis between wild type and *Mef2d* mutant mice at baseline.

Fetal gene activation is blunted in *Mef2d* null mice in response to pressure overload

MEF2D was required not only for hypertrophic growth and fibrosis in response to pressure overload, but was also essential for fetal gene activation, a prototypical consequence of cardiac stress. As shown in Figure III.5, up-regulation of the hypertrophic gene markers, *atrial natriuretic peptide* (*ANP*), *brain natriuretic peptide* (*BNP*), *myosin, heavy polypeptide 7, cardiac muscle, beta* (*Myh7*), and *actin, alpha 1, skeletal muscle* (*Acta1*) was severely blunted in mutant mice. Also, induction of *connective tissue growth factor* (*Ctgf*), *procollagen, type I, alpha 2* (*Col1a2)*, and *procollagen, type III, alpha 1* (*Col3a1*), which are up-regulated during cardiac fibrosis, was compromised in *Mef2d*$^{-/-}$ mice. Baseline expression of several fetal cardiac genes was also diminished in *Mef2d*$^{-/-}$ mice, suggesting that MEF2D is required for their normal expression in the absence of stress (Fig. III.5 and Table III.1). This data is consistent with Masson's trichrome and picrosirius red staining, and supports the conclusion that cardiac hypertrophy and fibrosis induced by pressure overload are suppressed in *Mef2d*$^{-/-}$ mice.

We also observed a decrease in *Mef2a* and *Mef2d* expression level following TAC, however previous reports showed that MEF2 activity is increased following cardiac

remodeling (Passier et al., 2000; Zhang et al., 2002). We believe that the decrease in MEF2 expression may represent a compensatory mechanism to diminish pathological signaling via MEF2 in the heart.

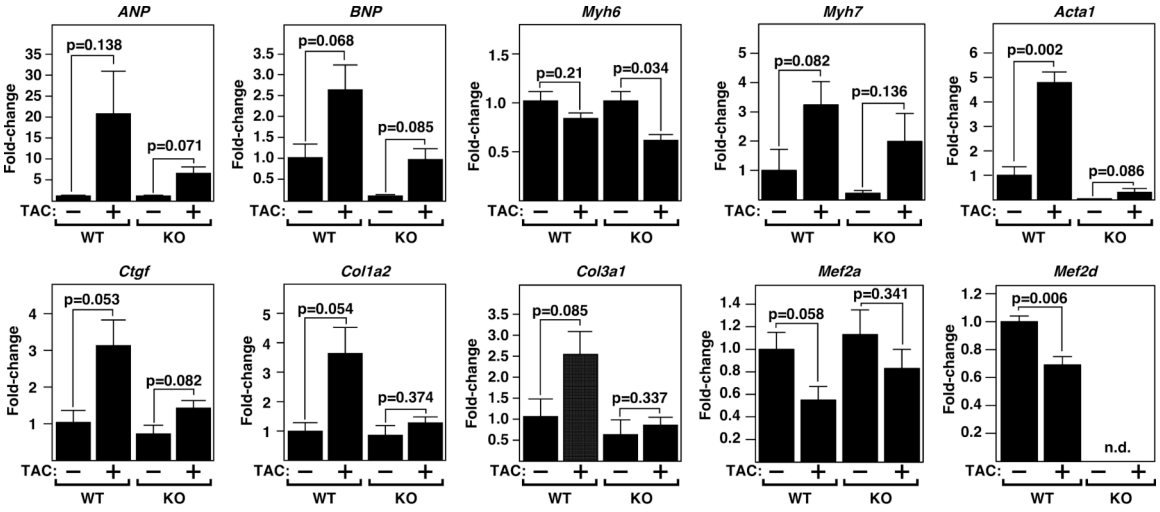

Figure III.5 Resistance of *Mef2d* mutant mice to fetal gene activation following TAC. Expression of cardiac hypertrophic markers, fibrosis markers, *Mef2a*, and *Mef2d* in WT and *Mef2d* mutant (KO) hearts was detected by quantitative PCR 21 days after TAC (n=3 to 5 per group). Values indicate relative expression level to a WT sham-operated group (±SEM). *ANP, atrial natriuretic peptide; BNP, brain natriuretic peptide; Myh6, myosin, heavy polypeptide 6, cardiac muscle, alpha; Myh7, myosin, heavy polypeptide 7, cardiac muscle, beta; Acta1, actin, alpha 1, skeletal muscle; Ctgf, connective tissue growth factor; Col1a2, procollagen, type I, alpha 2; Col3a1, procollagen, type III, alpha 1;* n.d., non-determined.

Mef2d null mice are resistant to cardiac remodeling in response to β-adrenergic stimulation

We also investigated if MEF2D was necessary for cardiac remodeling in response to chronic β-adrenergic stimulation. Isoproterenol (ISO), a β-adrenergic receptor agonist, was administered over 7 days to mice using osmotic minipumps (8.8 mg/kg·day). Compared to wild type mice, which showed a 26% increase in HW/TL (p=0.0008), mutant mice showed only a 17% increase in HW/TL (Fig. III.6A and B). This finding

suggests that MEF2D acts within signaling pathways activated by not only pressure overload, but also β-adrenergic stimulation.

Echocardiography confirmed that ISO administration resulted in a more pronounced increase in left ventricular wall thickness in wild type mice compared to *Mef2d* mutant mice, indicative of cardiac hypertrophy (Fig. III.6C). In addition, the wild type animals experienced more left ventricular remodeling in response to ISO, as shown by more left ventricular dilation and a decrease in contractility (Fig. III.6C and D).

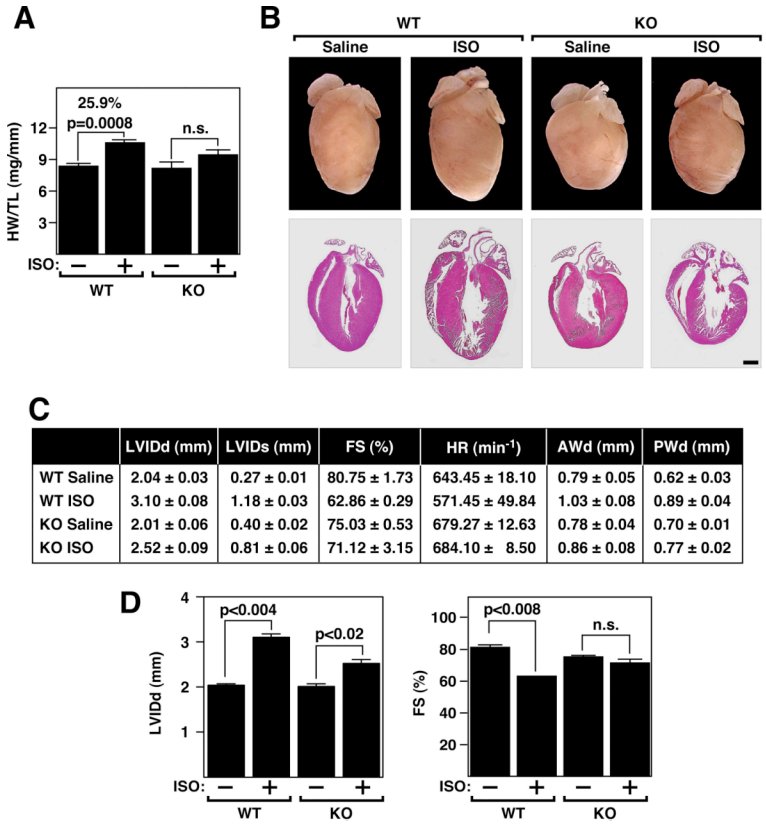

C

	LVIDd (mm)	LVIDs (mm)	FS (%)	HR (min^{-1})	AWd (mm)	PWd (mm)
WT Saline	2.04 ± 0.03	0.27 ± 0.01	80.75 ± 1.73	643.45 ± 18.10	0.79 ± 0.05	0.62 ± 0.03
WT ISO	3.10 ± 0.08	1.18 ± 0.03	62.86 ± 0.29	571.45 ± 49.84	1.03 ± 0.08	0.89 ± 0.04
KO Saline	2.01 ± 0.06	0.40 ± 0.02	75.03 ± 0.53	679.27 ± 12.63	0.78 ± 0.04	0.70 ± 0.01
KO ISO	2.52 ± 0.09	0.81 ± 0.06	71.12 ± 3.15	684.10 ± 8.50	0.86 ± 0.08	0.77 ± 0.02

Figure III.6 Decreased hypertrophic response of *Mef2d* mutant mice following β-adrenergic stimulation. (A) WT and *Mef2d* mutant (KO) mice were chronically infused with either saline vehicle or isoproterenol (ISO) (8.8 mg/kg·day) for 7 days and sacrificed for assessment of cardiac remodeling. Heart weight/tibia length (HW/TL) ratios (±SEM) are shown as bar graphs (n=7 to 9 per group). n.s., non-significant. (B) Whole hearts of WT and *Mef2d* mutant (KO) mice treated with either saline vehicle or ISO (8.8 mg/kg·day) are shown at the top. Hearts were sectioned and stained with H&E as seen on bottom. Scale bar = 1 mm. (C) *Mef2d* mutant (KO) animals show less LV remodeling compared to WT in response to ISO treament (n=3 to 4 per group). All values are shown as mean ±SEM. LVIDd, left ventricular end-diastolic diameter; LVIDs, left ventricular end-systolic diameter; FS, fractional shortening; HR, heart rate; AWd, anterior wall thickness in diastole; PWd, posterior wall thickness in diastole. (D) Representative bar graphs indicating less left ventricular dilation and a decrease in FS in *Mef2d* mutant (KO) mice compared to WT mice in response to ISO treatment. n.s., non-significant.

Forced expression of MEF2D causes severe cardiomyopathy

To determine whether MEF2D is sufficient to induce pathological cardiac remodeling, we generated transgenic mice in which the αMHC transgene directed cardiac-specific expression of MEF2D. Three independent stable transgenic mouse lines (Lines 1, 2 and 3) were established that expressed MEF2D approximately 18- 15- and 2.5-fold higher, respectively, in the heart than the wild type protein based on Western blot analysis (Fig. III.7A). We focused on transgenic line 2, which at 8 weeks of age showed extensive fibrosis, atrial enlargement and thrombi, as well as severely congested lungs and liver, which are clear signs of cardiomyopathy (Fig. III.7B).

Fetal cardiac genes as well as *Ctgf*, a marker of fibrosis, were dramatically up-regulated in transgenic lines 1 and 2 and were up-regulated to a lesser extent in line 3, consistent with the lower level of MEF2D expression in this line (Fig. III.7C). MEF2D over-expression in transgenic lines 1 and 2 also caused a diminution in expression of *myosin, heavy polypeptide 6, cardiac muscle, alpha* (*Myh6*) and up-regulation of *Myh7*, a hallmark of pathological cardiac remodeling and reduced cardiac contractility. We conclude that MEF2D is sufficient to induce cardiac remodeling and cardiomyopathy.

DISCUSSION

The results of this study demonstrate that MEF2D plays a unique and important role as a mediator of stress-dependent pathological remodeling of the adult heart. In the absence of MEF2D activity, hypertrophy, chamber dilatation, fibrosis and fetal gene activation were profoundly blunted following pressure overload or chronic adrenergic stimulation. Conversely, elevating MEF2D activity by transgenic over-expression, is sufficient to

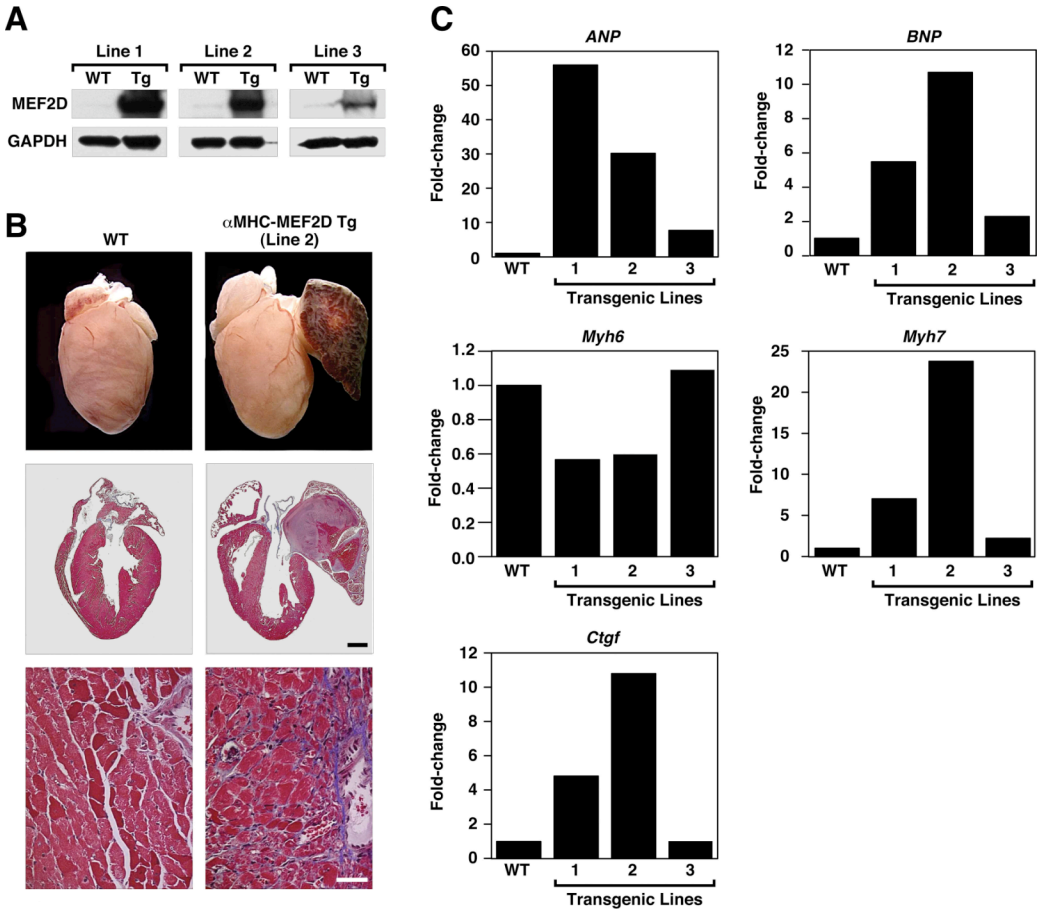

Figure III.7 Pathological cardiac remodeling induced by overexpression of MEF2D. (A) Proteins were extracted from ventricles of aMHC-MEF2D transgenic mouse lines at 6 weeks to 8 weeks of age for Western blot analysis using an antibody against MEF2D. GAPDH was detected as a loading control. (B) Hearts were dissected from aMHC-MEF2D male mice (Line 2) and WT littermates at 8 weeks of age. Note the enlarged left atrium in the aMHC-MEF2D heart. The lower panels are histological sections stained with Masson's trichrome to detect fibrosis. Scale bar = 1 mm (middle panel) and 40 mm (bottom panel). (C) Expression level of various hypertrophy and fibrosis markers was evaluated by quantitative PCR in each transgenic line. Note the correlation between expression level of MEF2D (panel A) and that of hypertrophy and fibrosis markers. *ANP, atrial natriuretic peptide; BNP, brain natriuretic peptide; Myh6, myosin, heavy polypeptide 6, cardiac muscle, alpha; Myh7, myosin, heavy polypeptide 7, cardiac muscle, beta; Ctgf, connective tissue growth factor.*

substitute for stress signals and drive pathological cardiac remodeling. The viability of *Mef2d* null mice contrasts with the early embryonic lethality of *Mef2c* null mice and perinatal lethality of *Mef2a* null mice, pointing to distinct functions for each MEF2 isoform at different stages of heart development.

Signaling pathways leading to cardiac remodeling

Our results indicate that MEF2D is a critical component of the signaling pathways through which pressure overload and adrenergic signaling drive cardiac remodeling and fetal gene activation. In this regard, prior studies showed that MEF2 regulates an array of genes involved in ion handling, extracellular matrix remodeling, and metabolism during pathological cardiac remodeling (van Oort et al., 2006; Xu et al., 2006). Some of these genes are direct targets of MEF2, whereas others are regulated indirectly by MEF2 through protein-protein interactions with other transcription factors and through subordinate MEF2-regulated transcription factors. Recent studies pointing to the importance of stress-inducible microRNAs in the cardiac remodeling response reveal an additional layer of potential regulation by MEF2 (van Rooij et al., 2006; van Rooij et al., 2007).

Forced expression of MEF2A or C in transgenic mice has been shown previously to cause dilated cardiomyopathy and fetal gene activation with little or no hypertrophy (van Oort et al., 2006; Xu et al., 2006). Over-expression of MEF2 or expression of a superactive MEF2-VP16 chimeric protein in primary cardiomyocytes also evokes a phenotype of myocyte elongation and sarcomere disorganization (van Oort et al., 2006; Xu et al., 2006). Similarly, our results show that over-expression of MEF2D causes ventricular dilation and fibrosis in transgenic mice.

Expression of a dominant negative MEF2 mutant protein in the adult heart also reduces chamber dilation and improves contractility in the presence of constitutive calcineurin activation (van Oort et al., 2006). Notably, dominant negative MEF2 results in a minimal block to hypertrophy, suggesting that MEF2 function is required primarily

for late stages of pathological cardiac remodeling. Since MEF2 associates with both NFAT and GATA factors, both of which have been shown to mediate pathological cardiac signaling (Liang et al., 2001; Molkentin et al., 1998; Morin et al., 2000; Youn et al., 2000), the blockade to cardiac remodeling by dominant negative MEF2 likely involves the inhibition of multiple downstream transcriptional effectors in addition to endogenous MEF2. The diminution of cardiac remodeling in *Mef2d* mutant mice therefore provides a more direct assessment of the specific contribution of this MEF2 isoform to the cardiac stress response. It will be of interest to examine mice with a cardiomyocyte-specific deletion of *Mef2d* to determine whether the reduction of cardiac remodeling in *Mef2d* mutant mice results exclusively from the lack of MEF2D in cardiomyocytes.

While hypertrophy, fetal gene activation and fibrosis were substantially blunted in *Mef2d* mutant mice, we observed residual hypertrophy and fetal gene activation in these animals. This likely reflects redundant functions of MEF2A, the other major MEF2 factor expressed in the adult heart, as well as other stress-responsive transcription factors such as NFAT, GATA and CAMTA (Liang et al., 2001; Molkentin et al., 1998; Morin et al., 2000).

Myriad functions of *Mef2* genes in vivo

The phenotypes of *Mef2a*, *-c* and *-d* mutant mice reveal unique roles for each of these MEF2 factors at different steps in cardiac development: MEF2C regulates early cardiac morphogenesis (Lin et al., 1997), MEF2A regulates genes involved in contractility and energy metabolism after birth (Naya et al., 2002) and MEF2D serves as a mediator of

stress-dependent gene expression in the adult heart. These unique functions are likely to reflect the distinct expression patterns of the different *Mef2* genes and, possibly, intrinsic differences in the transcriptional activities and protein-protein interactions of the MEF2 factors due to their amino acid sequence differences.

In addition to their functions in the heart, MEF2 factors are expressed in most or all tissues, and are likely to play key roles in diverse gene programs for cell differentiation and stress responsiveness. Conditional gene deletion of *Mef2c*, for example, has revealed important roles for this gene in regulation of skeletal muscle fiber type and resistance to fatigue, as well as in endochondral bone development (Arnold et al., 2007; Potthoff et al., 2007). MEF2 factors also participate in neural and vascular development (Flavell et al., 2006; Lin et al., 1998; Shalizi et al., 2006) and, recently, have been implicated in coronary artery disease, cancer and hepatic fibrosis (Bai et al., 2007; Du et al., 2005; Wang et al., 2003; Wang et al., 2004). Thus, strategies to modulate the MEF2 activity in adult tissues may be therapeutically beneficial in the settings of a variety of diseases.

METHODS

Generation of *Mef2d* mutant mice

The mouse *Mef2d* genomic locus was isolated from a 129SvEv mouse BAC library. A 1.3 kb genomic DNA fragment (short arm) that includes exon 2 and flanking introns was digested with XhoI and EcoRI restriction enzymes. The EcoRI restriction site of this genomic DNA fragment was blunted and subcloned into the XhoI site located upstream of the FRT-flanked neomycin resistance cassette of the pDelboy targeting vector. A 1.2

kb genomic DNA fragment (the deleted region) that encoded exon 3 was digested by NcoI restriction enzyme, blunted and inserted in between loxP sites of the targeting vector via ClaI and XhoI restriction sites. A 3.3 kb genomic fragment (long arm) that encodes exons 4-6 was digested and blunt-end cloned into the EcoRI restriction site downstream of the loxP sites in the targeting vector. This EcoRI site was not destroyed by the blunt cloning and was used for screening for positive recombination by Southern blots analysis (Fig. 1A).

The *Mef2d* targeting vector was linearized by digestion with NotI and electroporated into 129SvEv derived embryonic stem (ES) cells. Following positive-negative selection with G418 and FIAU, resistant colonies were screened by Southern blot analysis of EcoRI digested DNA using 5' and 3' probes (Fig. 1A and B). Three correctly targeted clones were expanded and injected into C57BL/6 blastocysts, which were transferred to the uterus of pseudopregnant females. High percentage chimeric male mice ($Mef2d^{neo\text{-}loxP/+}$) were bred into a C57BL/6 background to obtain germline transmission. Heterozygous $Mef2d^{neo\text{-}loxP}$ mice were intercrossed with hACTB::FLPe transgenic mice (Rodriguez et al., 2000) to remove the neomycin resistance cassette. Southern analysis and PCR were performed to confirm the removal of the neomycin resistance cassette in the genome of $Mef2d^{loxP/+}$ mice. To obtain mice with a *Mef2d* null allele, the intercross of $Mef2d^{loxP/+}$ mice to *Meox2-Cre* transgenic mice (Tallquist and Soriano, 2000) was performed. Southern blot analysis and PCR were performed to confirm mice with *Mef2d* heterozygous or homozygous null ($Mef2d^{KO}$) alleles (Fig. 1B and C). All experiments on mice were conducted in 129SvEv/C57Bl6 mixed background.

Southern blot analysis and PCR genotyping

DNA sequences for PCR primers and Southern blot probes are available upon request. In brief, tail genomic DNA was digested with EcoRI and analyzed using a standard Southern blot protocol. The PCR reaction contained 1 μl of tail DNA as template, Taq polymerase (Promega) with 2 mM $MgCl_2$ in a final volume of 25 ul. An annealing temperature of 70ºC was used and the PCR products were electrophoresed on a 2% agarose gel.

RNA analysis

Total RNA was purified from isolated heart ventricles with TRIzol reagent (Invitrogen) according to the manufacturer's instructions. Two micrograms of RNA was used as template to synthesize cDNA using random hexamers. Quantitative PCR was performed using Taqman probes purchased from ABI. RT-PCR primer and quantitative PCR probe information is available upon request.

Histology

Hearts were fixed in 4% paraformaldehyde in phosphate-buffered saline, embedded in paraffin, and sectioned at 5 μm intervals. H&E staining, Masson's trichrome staining, and picrosirius red staining were performed using standard procedures.

Measurements of mean cardiomyocyte area and myocardial fibrosis

Cardiomyocyte size was assessed on H&E stained sections using ImageJ software (National Institutes of Health). About 100 to 150 randomly chosen cardiomyocytes from

each group (n=2 to 3) were analyzed to measure cross sectional cardiomyocyte area. ImageJ software (National Institutes of Health) was used to measure the amount of myocardial fibrosis on picrosirius red stained sections. About 30 to 50 randomly chosen frames from each group (n=2 to 3) were analyzed.

Transthoracic echocardiography

Cardiac function and heart dimensions were evaluated by two-dimensional echocardiography on conscious mice using a Vingmed System (GE Vingmed Ultrasound) and a 11.5-MHz linear array transducer. M-mode tracings were used to measure anterior and posterior wall thicknesses at end diastole and end systole. Left ventricular internal diameter (LVID) was measured as the largest anteroposterior diameter in either diastole (LVIDd) or systole (LVIDs). The data were analyzed by a single observer blinded to mouse genotypes. Left ventricular FS was calculated according to the following formula: FS (%) = [(LVIDd - LVIDs)/LVIDd] x 100.

Statistical analysis

Gene expression was normalized to GAPDH expression level and calculated as relative change. Differences in morphological, physiological, and biochemical parameters between groups were analyzed by 2-sided Student's *t* test using Microsoft Excel 2002. Non-significant (n.s.) difference indicates a p value bigger than 0.05.

Thoracic aortic constriction and isoproterenol administration

Male mice (8- to 12-week-old) either underwent a sham operation or were subjected to TAC as described (Hill et al., 2000). Peri-operative mortalities (within 24 hours of surgery) were similar (about 10%) in wild type and mutant mice subjected to TAC. There was no excess mortality during follow-up in any of the 4 groups (Sham or TAC, wild type or mutant mice). Hearts were isolated 21 days following TAC for assessment of cardiac hypertrophy. Isoproterenol (Sigma) (8.8 mg/kg·day) or saline vehicle was administered using miniosmotic pumps (Model 2001, Alzet) subcutaneously implanted on the back of 8- to 10-week-old male mice. Cardiac hypertrophy was evaluated by measuring heart weight and tibia length of sacrificed mice 7 days after pump implantation.

Generation of transgenic mice

A cDNA encoding mouse FLAG-tagged MEF2D was cloned into a plasmid containing the αMHC transgene and human GH (hGH) poly(A)$^+$ signal (Gulick et al., 1991), and transgenic mice were generated by standard techniques. Genotyping was performed by PCR analysis using genomic DNA and transgenic expression of MEF2D in the heart was confirmed by Western blot analysis using mouse anti-MEF2D antibody (1:1000, BD transduction laboratories) and mouse anti-GAPDH antibody (1:5000, Chemicon).

ACKNOWLEDGEMENTS

Dillon Phan generated the conditional *Mef2d* mutant allele.

Chapter IV

Yap in Heart Development

Yes-associated protein (Yap) is a transcriptional coactivator whose role in cancer development and tissue size control has been recently identified. We report that Yap is also an essential regulator of cardiac function and angiogenesis, revealing a previously unidentified role of Yap. Mice lacking Yap in cardiomyocytes develop lethal cardiomyopathy and die by five months of age. The mutant mice show impaired cardiac contractility, misregulation of cardiac remodeling genes, and fibrosis likely due to impaired cardiac angiogenesis and myocardial hypoxia as evidenced by downregulation of *Angiopoietin1* (*Angpt1*) and upregulation of *hypoxia inducible factor 1, alpha subunit* (*Hif1*α). Yap and GATA4 coactivate the promoter of *Angpt1*, which encodes an angiogenic factor secreted from cardiomyocytes, identifying Yap as a novel transcriptional coactivator of GATA4. Furthermore, deletion of Yap in other tissues causes extensive hemorrhage and edema implying that loss of Yap results in compromised vascular integrity. Our study demonstrates that Yap plays a critical role in preservation of cardiac function and raises an intriguing possibility that Yap may serve as a global proangiogenic factor.

INTRODUCTION

The heart is the first organ to form during vertebrate development and is responsible for distributing nutrients and oxygen throughout the embryo. Its importance is underscored by the fact that congenital heart disease is the most common human birth defect (Hoffman and Kaplan, 2002). The heart is a dynamic organ that undergoes constant remodeling even after birth. In response to mechanical or neurohormonal stress, the heart undergoes hypertophy, while it becomes atrophic when workload is relieved. The heart balances increased workload by enhancing protein synthesis and increasing the size of cardiomyocytes. In addition, coronary angiogenesis has been suggested to play a protective role in the heart to enable functional compensation against disease-inducing stimuli (Frey and Olson, 2003; Izumiya et al., 2006; Shiojima et al., 2005). When the heart cannot functionally compensate for increased hemodynamic load, it undergoes failure characterized by ventricular dilation, fibrosis, and resultant loss of ventricular contractility. Although various transcriptional regulators controlling these intricate processes have been widely studied, novel molecules and signaling pathways continue to be identified. Moreover, the fact that cardiovascular disease affects an estimated five million Americans, and coronary heart disease is the number one killer of American males and females calls for further understanding of the molecular mechanism behind the disease and development of new therapeutics (Rosamond et al., 2008).

T-box genes encode a family of transcription factors that possess a highly conserved 180-amino acid DNA-binding domain called the T-box. Tbx5 is expressed predominantly in the heart and limb buds during embryonic development. A mutation in the *TBX5* gene causes Holt-Oram syndrome (HOS), an inherited disorder characterized

by congenital heart defects and upper limb abnormalities (Basson et al., 1997; Li et al., 1997). *Tbx5* heterozygous mice generated through homologous recombination show cardiac and forelimb defects similar to those in HOS patients, indicating a conserved molecular mechanism behind the disease and emphasizing the relevance of studying HOS disease in the mouse model system (Bruneau et al., 2001). Recently, we reported that the yes-associated protein (Yap) is a transcriptional coactivator of Tbx5, suggesting the possible involvement of Yap in heart development (Murakami et al., 2005).

Yap is a transcriptional coactivator containing a series of functional domains, including a proline-rich amino terminus, a 14-3-3 binding site, WW domains, SH3 binding motifs, a coiled-coil domain, and a PDZ binding motif (Kanai et al., 2000; Yagi et al., 1999). The *Drosophila* homolog of *Yap*, *Yorkie* (*Yki*), is a major target of the Hippo pathway that controls organ size in the fly. This pathway consists of a series of kinases and adaptor proteins that negatively regulate Yki through its phosphorylation. Hippo (Hpo) interacts with Salvador (Sav) to phorphorylate and activate the complex of Warts (Wts) and Mats, which in turn phorphorylates and inactivates Yki (Fig. IV.1) (Huang et al., 2005). Components of the Hippo pathway, Hippo, Sav, Wts, and Mats, are homologous to mammalian Mst1/2, WW45, Lats1/2, and Mob1, respectively. Their functional conservation is demonstrated by the fact that each mammalian homolog can rescue the corresponding fly mutant (Pan, 2007; Zeng and Hong, 2008). Recent studies in mammalian cells show that Yap and the mammalian Hippo pathway govern cell contact inhibition, organ size control, and tumorigenesis (Camargo et al., 2007; Dong et al., 2007; Zhao et al., 2007). Other groups also have demonstrated an interaction between Yap and various transcription factors such as Tbx5, Runx2, and Tead family

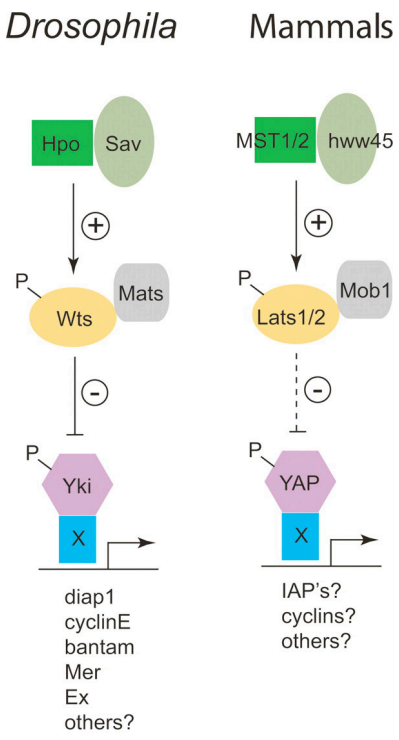

Figure IV.1 The Hippo pathway in *Drosophila* and mammals. The corresponding factors in the pathways in Drosophila and mammals are indicated in matching colors and shapes. (Adapted from Pan, 2006)

members (Murakami et al., 2005; Vassilev et al., 2001; Zaidi et al., 2004). Moreover, global deletion of *Yap* in mice results in early embryonic lethality (Morin-Kensicki et al., 2006). These reports suggest that *Yap* may play an essential role during embryogenesis in addition to cancer development.

To investigate the role of Yap in heart development, we generated mutant mice lacking *Yap* in the heart. In this study, we identify a previously unknown function of Yap as a regulator of angiogenesis. Loss of *Yap* in cardiomyocytes results in lethal cardiomyopathy, impaired cardiac contractility, and dysregulation of cardiac remodeling genes. We also show that Yap coactivates a proangiogenic factor *Angiopoietin1* (*Angpt1*) with GATA4, a transcription factor that has been previously reported to be an important

regulator of cardiac angiogenesis (Heineke et al., 2007). Furthermore, deletion of *Yap* in other tissues leads to embryonic lethality resulting from compromised vascular integrity implying that Yap may serve as a global angiogenic factor, possibly in collaboration with GATA4. These findings demonstrate that Yap acts as an essential regulator of cardiac function and angiogenesis.

RESULTS

Generation of a conditional *Yap* mutant allele

Global deletion of *Yap* results in early embryonic lethality at E8.5 prior to the completion of heart development (Morin-Kensicki et al., 2006). Hence, we generated a conditional *Yap* mutant allele (Yap^{loxP}) through homologous recombination in ES cells and FLPe-mediated excision to study the role of Yap in heart development (Rodriguez et al., 2000). The mutant *Yap* allele contains two loxP sites flanking exon 3, which encodes part of a WW domain, which mediates protein-protein interactions, and deletion of exon 3 leads to a frameshift in exon 4 and exon 5 (Fig. IV.2A).

We confirmed targeting and germline transmission of a conditional *Yap* mutant allele by Southern blot analysis and PCR genotyping (Fig. IV.2B and 2C). To recapitulate the previously published global deletion of *Yap* (Morin-Kensicki et al., 2006), we bred $Yap^{loxP/+}$ mice to mice expressing a CAG-Cre transgene that globally excises the loxP-flanked genomic region in the germline (Sakai and Miyazaki, 1997). $Yap^{loxP/loxP}$; *CAG-Cre* mice, which are equivalent to *Yap* null mice, showed developmental arrest at around E8.5, consistent with the prior description of $Yap^{-/-}$ embryos (Fig. IV.2D) (Morin-Kensicki et al., 2006).

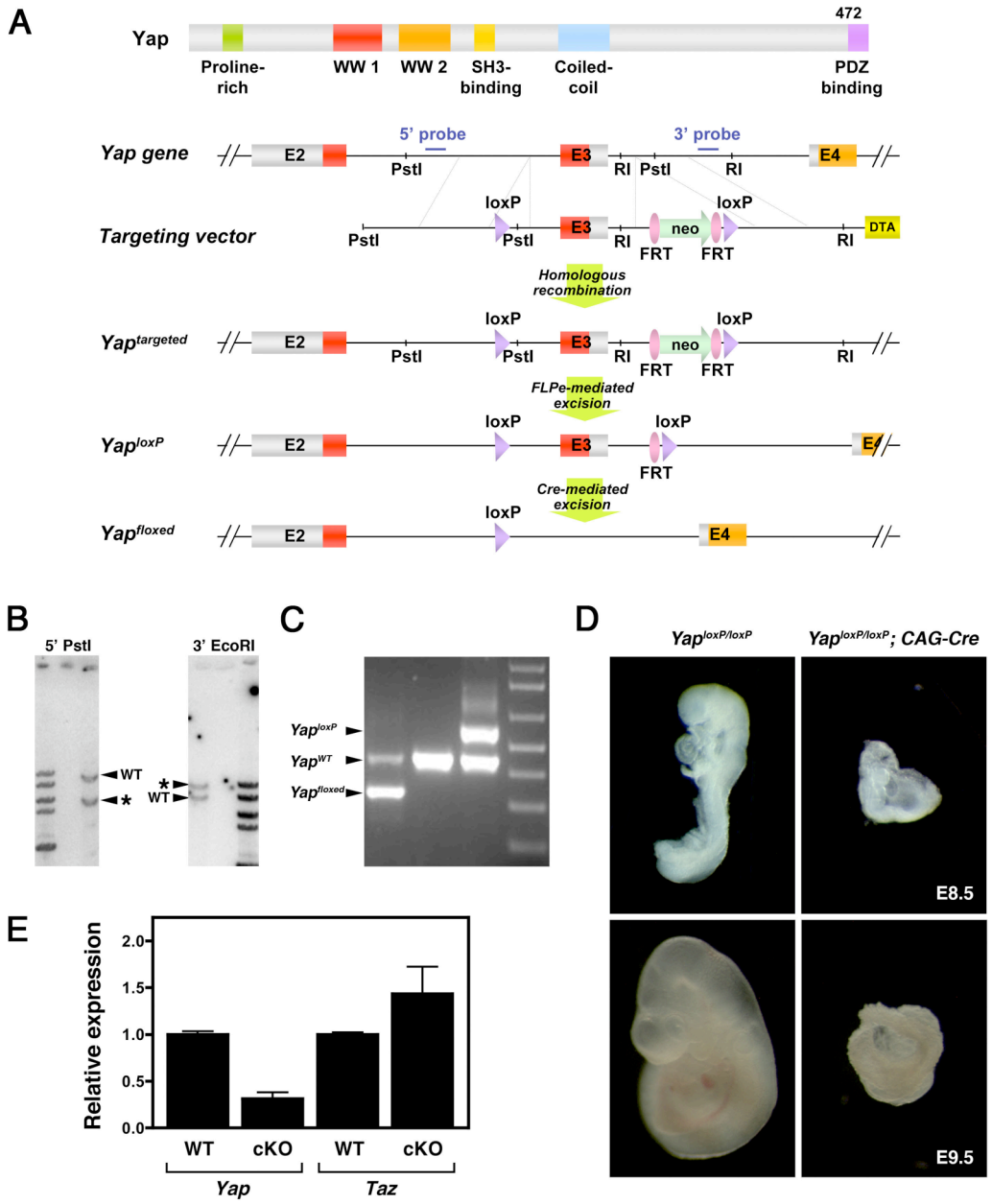

Figure IV.2 Generation of mice with a conditional *Yap* mutation. (A) Schematic representation of the mouse Yap locus and the targeting strategy. Positions of probes for Southern blot analysis are shown as 5' probe and 3' probe. Location of restriction enzymes used for Southern blot analysis are indicated: PstI and RI. Successful homologous recombination in ES cells and recombinase-mediated excisions generates the Yap^{floxed} allele, in which exon 3 is replaced by one loxP site. E, exon; neo, neomycin resistance cassette; RI, EcoRI. (B) Southern blot analysis showing successful ES cell targeting. PstI digestion generates a 9.5 kb band and a 6.2 kb band for the Yap^{WT} (WT) and the $Yap^{targeted}$ (*) allele, respectively. The 3' probe detects an 8 kb band for the wild type allele and a 9.8 kb band for the targeted allele after EcoRI digestion. (C) PCR genotyping to distinguish different *Yap* alleles and to confirm successful excision of Yap exon 3. (D) Global deletion of Yap using CAG-Cre recapitulating the previously reported phenotype of *Yap* null mice. (E) Quantitative PCR analysis demonstrating efficient deletion of Yap in cardiomyocytes. Expression of *Taz*, a gene that shares about 45% amino acid identity, is not changed in *Yap* mutant heart. RNA isolated from left ventricles of 6 week-old males was used for the assay. WT and cKO indicate $Yap^{loxP/loxP}$ and $Yap^{loxP/loxP}$; *αMHC-Cre*, respectively.

Deletion of *Yap* in cardiomyocytes results in lethal cardiomyopathy

We utilized α-myosin heavy chain (αMHC)-Cre transgenic mice to generate a heart-specific deletion of *Yap*, called *Yap$^{loxP/loxP}$; αMHC-Cre*. Transgenic mice harboring αMHC-Cre express Cre recombinase in differentiated cardiomyocytes pre- and postnatally (Agah et al., 1997). We first examined the efficiency of *Yap* deletion in mutant hearts. Quantitative PCR (Q-PCR) on RNA isolated from the left ventricle of *Yap$^{loxP/loxP}$; αMHC-Cre* mice (cKO) confirmed the effective Cre-mediated recombination in vivo (Fig. IV.2E). The residual expression of *Yap* is likely to be due to the presence of *Yap* in fibroblasts.

The transcriptional coactivator with PDZ-binding motif (Taz) protein shares 45% amino acid identity with Yap. We examined the expression of *Taz* to determine if it might be upregulated upon deletion of *Yap*, as a compensatory mechanism, and found that *Taz* expression was not significantly changed in *Yap* mutant hearts (Fig. IV.2E).

Yap mutant mice became lethargic and showed difficulty in breathing before they succumbed to death between three and five months of age (Fig. IV.3A). Hearts from the mutant mice were enlarged and dilated. Histological analysis revealed that the mutant mice exhibited dilated cardiomyopathy accompanied by atrial thrombosis, thinning of ventricular walls, and cardiomyocyte hypertrophy (Fig. IV.3B). Extensive fibrosis of the ventricular wall was detected by Masson's trichrome staining in the mutant heart, suggesting compromised cardiac contractility of *Yap* mutant mice (Fig. IV.3C). These data demonstrate that cardiac deletion of *Yap* results in heart failure and eventual lethality.

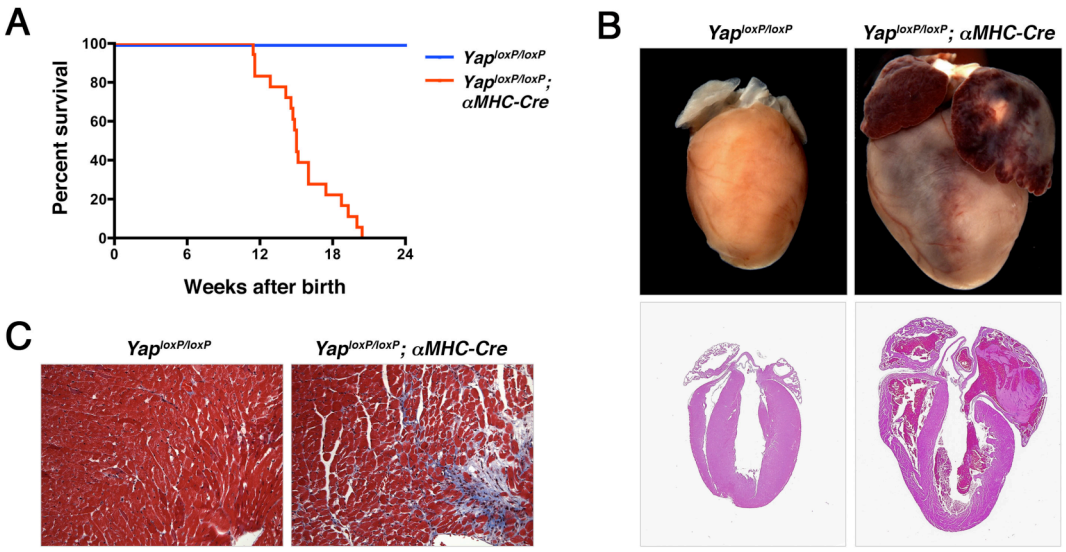

Figure IV.3 Lethal cardiomyopathy resulting from deletion of Yap in heart. (A) Kaplan-Meier survival curve for mice that lack Yap in heart. Loss of Yap in cardiomyocytes leads to lethality at three to five months of age (n = 21 per group). (B) Dilated cardiomyopathy of *Yap*$^{loxP/loxP}$*; αMHC-Cre* mice. Bottom panels are H&E stained sections of hearts showing dilation of ventricular walls and atrial thrombosis. (C) Masson's trichrome staining indicates extensive fibrosis present in *Yap*$^{loxP/loxP}$*; αMHC-Cre* hearts.

Requirement of Yap in maintenance of cardiac function

We performed echocardiography to assess cardiac performance of *Yap* mutant mice at six and twelve weeks of age. As seen in representative echocardiograms, *Yap*$^{loxP/loxP}$*; aMHC-Cre* mice showed reduced cardiac contractility compared to *Yap*$^{loxP/loxP}$ mice. Cardiac function deteriorated progressively with age (Fig. IV.4A). Echocardiography along with histological analysis supports the notion that *Yap* mutant hearts develop ventricular chamber dilation and mild functional deficits at six weeks of age and their contractility is dramatically compromised by twelve weeks of age (Fig. IV.4B).

To examine the molecular changes in *Yap* mutant hearts, we assessed the expression levels of various cardiac remodeling genes, such as *atrial natriuretic peptide* (*ANP*), *brain natriuretic peptide* (*BNP*), *myosin, heavy polypeptide 6, cardiac muscle, alpha* (*Myh6*), *myosin, heavy polypeptide 7, cardiac muscle, beta* (*Myh7*), *actin, alpha 1,*

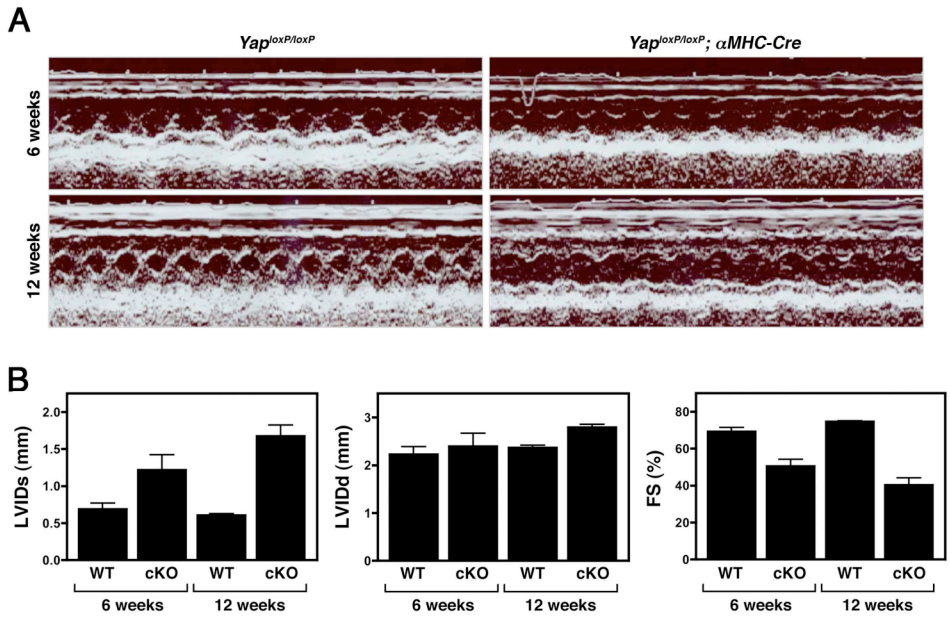

Figure IV.4 Echocardiographic analysis of *Yap*$^{loxP/loxP}$; *αMHC-Cre* mice. (A) Representative echocardiograms showing impaired cardiac contractility upon deletion of Yap in heart. Progressive deterioration of cardiac function is observed with increasing age. (B) *Yap* mutant mice display abnormal LV dilation during systole and diastole compared control mice. In addition, a dramatic decrease in FS is observed in *Yap*$^{loxP/loxP}$*; αMHC-Cre* mice (n = 2 to 6 per group). WT and cKO indicates *Yap*$^{loxP/loxP}$ and *Yap*$^{loxP/loxP}$*; αMHC-Cre* mice, respectively. FS, fractional shortening; LVIDd, left ventricular end-diastolic diameter; LVIDs, left ventricular end-systolic diameter.

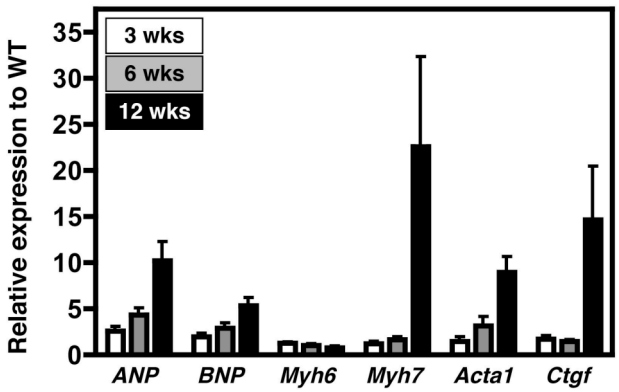

Figure IV.5 Fetal gene activation in *Yap* mutant hearts. Quantitative PCR analysis using RNA isolated from hearts of *Yap*$^{loxP/loxP}$*; αMHC-Cre* mice demonstrates that deletion of *Yap* results in dysregulation of cardiac remodeling genes at 3 weeks, 6 weeks, and 12 weeks of age (n = 2 to 6 per group). Expression level of each gene in *Yap* mutant mice was first normalized to that of GAPDH and shown as a fold-change to the value from control mice (WT). Acta1, actin, alpha 1, skeletal muscle ; ANP, atrial natriuretic peptide ; BNP, brain natriuretic peptide ; Ctgf, connective tissue growth factor; Myh6, myosin, heavy polypeptide 6, cardiac muscle, alpha; Myh7, myosin, heavy polypeptide 7, cardiac muscle, beta.

skeletal muscle (*Acta1*), and *connective tissue growth factor* (*Ctgf*) using Q-PCR. Expression levels of *ANP*, *BNP*, *Myh7*, *Acta1*, and *Ctgf* increased and that of *Myh6* decreased in $Yap^{loxP/loxP}$*; aMHC-Cre* mice with age (Fig. IV.5). This data is consistent with the heart failure phenotype of the mutant mice and demonstrates that Yap is essential for preservation of cardiac performance.

Angpt1 is downregulated in *Yap* mutant hearts

To further investigate the molecular mechanism behind the mutant phenotype and identify how Yap contributes to preserving cardiac function, we performed microarray analysis using RNA isolated from left ventricles of $Yap^{loxP/loxP}$ mice and $Yap^{loxP/loxP}$*; αMHC-Cre* mice. The expression profile of *Yap* mutant hearts showed that deletion of *Yap* in cardiomyocytes led to downregulation of 318 genes and upregulation of 197 genes when a cutoff of two-fold change was applied (data not shown). Yap is a transcriptional coactivator, but its role in regulation of cardiac gene expression has not been studied previously. Hence, we focused on studying cardiac genes that were downregulated in the *Yap* mutant heart to identify potential gene targets of Yap.

One of the most dysregulated genes in cardiomyocytes lacking Yap was *Angpt1*, a secreted angiogenic factor that binds to the endothelial-specific receptor tyrosine kinase (Tek) receptor (Table IV.1). Angiogenic cytokines, such as vascular endothelial growth factor (VEGF) and Angpt1, are secreted by cardiomyocytes and enhance endothelial cell proliferation and vessel formation (Hsieh et al., 2006). *Angpt1* was downregulated by two-fold at 6 weeks of age and three-fold at 12 weeks of age in hearts of $Yap^{loxP/loxP}$*; αMHC-Cre* mice, as confirmed by Q-PCR (Fig. IV.6A). Decreased expression of *Angpt1*

Gene Title	Gene Symbol	Fold-Change
ornithine decarboxylase antizyme 3	Oaz3	0.033
prolactin receptor	Prlr	0.036
aquaporin 4	Aqp4	0.044
pellino 1	Peli1	0.047
phospholipase A2, group V	Pla2g5	0.063
epsin 3	Epn3	0.067
angiopoietin 1	Angpt1	0.072
Inositol polyphosphate-5-phosphatase A	Inpp5a	0.072
aquaporin 4	Aqp4	0.077
vacuolar protein sorting 35	Vps35	0.082
REV3-like, catalytic subunit of DNA polymerase zeta RAD54 like (S. cerevisiae)	Rev3l	0.082
AT rich interactive domain 4A (Rbp1 like)	Arid4a	0.082
coatomer protein complex, subunit gamma 2, antisense 2	Copg2as2	0.095
G-protein-coupled receptor 50	Gpr50	0.102
zinc finger protein 260	Zfp260	0.109
potassium voltage-gated channel, Shal-related family, member 2	Kcnd2	0.125
6-phosphofructo-2-kinase/fructose-2,6-biphosphatase 1	Pfkfb1	0.125
ankyrin repeat domain 6	Ankrd6	0.125
Dachshund 1 (Drosophila)	Dach1	0.125
copine III	Cpne3	0.134
kinesin family member 2A	Kif2a	0.144
Shroom	Shrm	0.144
pleiomorphic adenoma gene-like 1	Plagl1	0.144
potassium voltage-gated channel, Shal-related family, member 2	Kcnd2	0.144
prolactin receptor	Prlr	0.154
cyclin-dependent kinase 6	Cdk6	0.165
fer (fms/fps related) protein kinase, testis specific 2	Fert2	0.177
yes-associated protein 1	Yap1	0.203

Table IV.1 A list of the most downregulated genes in *Yap* mutant hearts. RNA isolated from left ventricles of 6 week-old male mice was used for microarray analysis. Fold-changes of *Angpt1* and *Yap* in $Yap^{loxP/loxP}$; *αMHC-Cre* mice compared to $Yap^{loxP/loxP}$ mice are indicated with red boxes.

implies impaired angiogenesis in the mutant heart, which may result in cardiac ischemia and explain the occurrence of the heart failure in Yap mutant mice. This hypothesis was supported by the fact that *hypoxia inducible factor 1, alpha subunit* (*Hif1α*) was upregulated in the hearts of *Yap* mutant mice (Fig. IV.6B). Hif1α is a basic helix-loop-helix transcription factor that induces adaptive physiological processes under hypoxic conditions. Expression of *Hif1α* increases in mammalian cells during ischemia in an attempt to minimize cellular injury and maintain cardiac output by regulating angiogenesis, metabolism, cell survival, and oxygen delivery (Shohet and Garcia, 2007). Our finding that *Angpt1* was downregulated and *Hif1α* was upregulated in *Yap* mutant

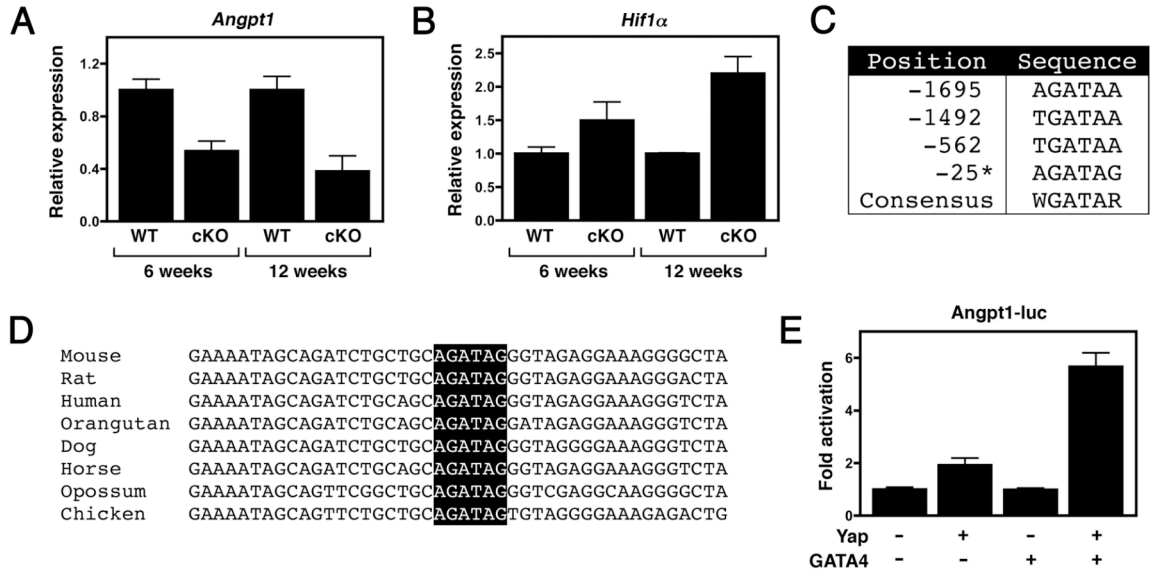

Figure IV.6 Regulation of *Angpt1* by Yap and GATA4. (A) Downregulation of *Angpt1* in hearts of $Yap^{loxP/loxP}$; *αMHC-Cre* mice at six- and twelve-week of age. RNA from left ventricles was isolated, and mRNA expression was examined using Q-PCR (n = 3 to 5 per group). WT and cKO indicate the control mice and the mutant mice, respectively. (B) Q-PCR analysis of *Hif1α* expression level. Upregulation of *Hif1α* in mutant hearts suggests presence of cardiac ischemia upon deletion of *Yap* (n = 3 to 5 per group). (C) Potential GATA4-binding sites in the *Angpt1* promoter. All selected sequences match the GATA4-binding consensus. The position of each site indicates the distance from the transcription start site of *Angpt1*. * denotes the site conserved among mammals. (D) DNA sequences of the potential GATA4-binding site located at 25 bp upstream of the transcription start site of *Angpt1* and their evolutionary conservation is shown. (E) Coactivation of *Angpt1* promoter by Yap and GATA4. COS-7 cells were transfected with plasmids expressing a luciferase reporter (100 ng), Yap (50 ng) and/or GATA4 (50 ng). CMV-β-galactosidase expression vector was used to normalize tranfection efficiency.

hearts suggested that the lack of Yap in cardiomyocytes led to impaired cardiac angiogenesis, myocardial ischemia, and ultimately heart failure.

Regulation of *Angpt1* by Yap and GATA4

To determine whether Yap directly regulates the *Angpt1* gene, we examined the response of the *Angpt1* promoter to Yap. Initial analysis of the *Angpt1* promoter revealed four putative GATA binding sites including one conserved site within 2.3 kb of the transcription start site (Fig. IV.6C and 6D). GATA4 has been previously described as a regulator of angiogenesis in the murine heart (Heineke et al., 2007). Since Yap is a

transcriptional coactivator that interacts with a transcription factor to control expression of its downstream target genes, we investigated whether Yap and GATA4 act together to regulate transcription of *Angpt1*. Transfection of COS-7 cells with expression plasmids of Yap and GATA4 resulted in six-fold activation of a luciferase reporter containing a 2.5 kb upstream region of the *Angpt1* gene, while expression of either factor alone induced minimal activation of the *Angpt1* promoter (Fig. IV.6E). This finding establishes Yap as a novel transcriptional coactivator of GATA4 and raises an intriguing possibility that Yap may play an important role in other processes involving GATA4 functions, such as response to cardiac hypertrophic stimuli.

Yap is necessary for preservation of vascular integrity

The importance of Yap as a regulator of angiogenesis is supported by the fact that deletion of *Yap* in other tissues of the mouse results in compromised vascular integrity in corresponding tissues. Deletion of *Yap* in neural crest cells ($Yap^{loxP/floxed}$; *Wnt1-Cre*) by utilizing *Wnt1-Cre* transgenic mice (Danielian et al., 1998) led to embryonic lethality at E10.5 accompanied by extensive hemorrhage in the forebrain region and the 1st pharyngeal arch region (Fig. IV.7A). Accumulation of blood was evidently shown by histological analysis of mutant embryos (Fig. IV.7B). Immunostaining using an antibody against PECAM, an endothelial cell marker, revealed disrupted vascular organization in the mutant embryo compared to intricately organized vasculature of the wild type embryo (Fig. IV.7C). Moreover, we generated limb bud-specific *Yap* mutant mice ($Yap^{loxP/floxed}$; *Prx1-Cre*) using transgenic mice harboring a Cre recombinase whose expression is driven by the promoter of *Prx1* gene (Logan et al., 2002). These mice showed dramatic edema

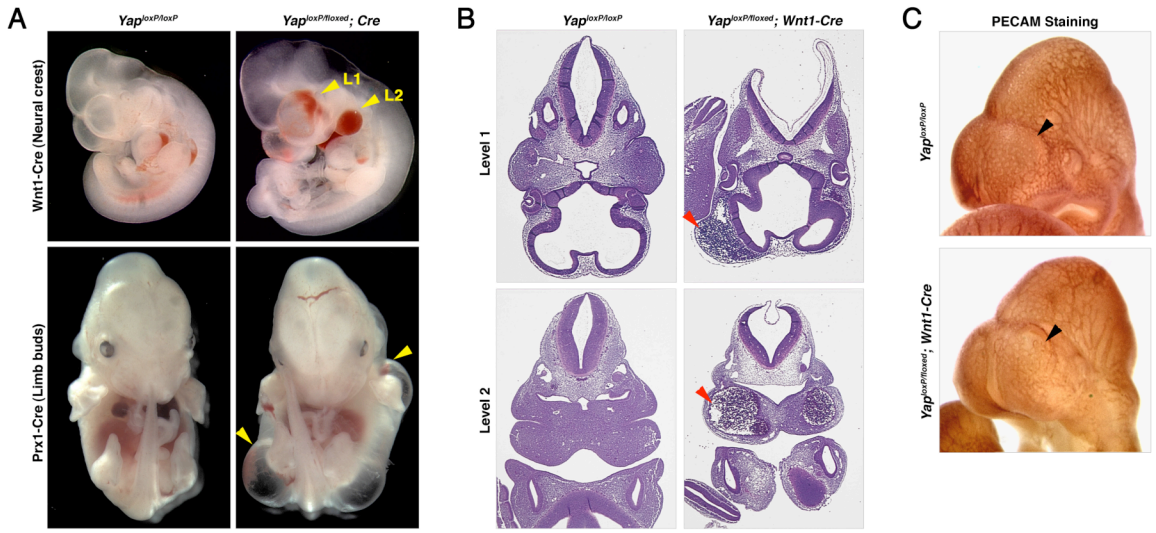

Figure IV.7 Impaired angiogenesis upon deletion of Yap. (A) Hemorrhage and edema of *Yap* mutant embryos are marked with arrowheads. Top two panels show wild type and neural crest-specific *Yap* mutant mouse embryos at E10.5, and bottom two panels show wild type and limb bud-specific *Yap* mutant mouse embryos at E13.5. L1, Level 1; L2, Level 2. (B) H&E sections of E10.5 $Yap^{loxP/loxP}$ and $Yap^{loxP/floxed}$; *Wnt1-Cre* embryos at E10.5. Two different sectioning levels are indicated in panel A as L1 and L2. (C) PECAM stained E10.0 embryos are shown. The arrowheads compare vascular organization in the forebrain region of the wild type and the mutant embryos.

and hemorrhage in the embryonic limbs at E13.5 (Fig. IV.7A). These data corroborate our findings on the potential role of Yap in cardiac angiogenesis and reveal a previously unknown role of Yap as an essential regulator of vessel maintenance.

DISCUSSION

Although *Yap* and its *Drosophila* homolog *Yki* have been extensively studied in tissue size control and tumorigenesis, their roles in cardiogenesis have not been previously described. Results of this study demonstrate that Yap is a critical regulator of cardiac function maintenance and angiogenesis. We show that mice lacking Yap in cardiomyocytes develop lethal cardiomyopathy, which is accompanied by thinning of the myocardium, atrial thrombosis, and fibrosis. Loss of Yap leads to reactivation of the

fetal gene program in the heart and diminished cardiac contractility of mutant mice with age. In addition, we demonstrate that Yap and GATA4 together to control expression of *Angpt1*. Decreased expression of *Angpt1* and increased expression of *Hif1α* in mutant hearts suggest that cardiac deletion of *Yap* results in compromised angiogenesis and cardiac ischemia. We conclude that Yap is essential in preservation of cardiac function and proper regulation of angiogenesis.

Importance of Yap in maintenance of cardiac function and angiogenesis

Cardiac angiogenesis is essential for preservation of cardiac function. Increased capillary density in the heart is tightly tied to the growth of cardiomyoctes during development (Rakusan et al., 1992; Tomanek et al., 1982). Furthermore, the importance of coronary angiogenesis as a protector against cardiac disease-inducing stimuli such as pressure overload has been demonstrated previously (Izumiya et al., 2006; Shiojima et al., 2005). A protective response by the heart to hypoxia involves increased activity of Hif1α, a transcription factor that regulates multiple angiogenic growth factors such as Angpt1, VEGF, and platelet derived growth factor, B polypeptide (Pdgfb) (Hirota and Semenza, 2006; Kelly et al., 2003). *Hif1α* deficient mice show embryonic lethality by E11.0 with vascular defects, underscoring the importance of *Hif1α* in cardiovascular development (Iyer et al., 1998). The upregulation of *Hif1α* in *Yap* mutant hearts suggests the presence of myocardial hypoxia possibly leading to lethal heart failure. We believe that cardiac ischemia of the mutant mice is due to compromised angiogenesis resulting from downregulated expression of *Angpt1*, since Angpt1 performs an important role in maturation of vascular endothelium (Suri et al., 1996). Taken together, these findings

reveal a novel function of Yap as an important regulator of cardiac angiogenesis and performance, suggesting a possible therapeutic application of Yap as a drug target in cardiac ischemia.

Yap has been previously described as a transcriptional coactivator of several transcription regulators of cardiogenesis such as ErbB4, Tead proteins, and Tbx5 (Komuro et al., 2003; Murakami et al., 2005; Vassilev et al., 2001). Mice lacking these proteins all display embryonic lethality resulting from cardiac developmental defects, demonstrating the importance of these molecules in cardiogenesis (Bruneau et al., 2001; Gassmann et al., 1995; Sawada et al., 2008).

We are aware that the phenotype of *Yap* mutant mice is different from mice lacking ErbB4, Tead1, or Tbx5. We believe that this disparity may be due to the presence of highly homologous gene *Taz*, which is a transcriptional coactivator whose binding partners include Tbx5, Runx2, and Pparγ (Hong et al., 2005; Murakami et al., 2005). 30-50 % of mice lacking die by the age of weaning of unknown cause while the rest develop glomerulocystic kidney disease in the adulthood (Hossain et al., 2007). Although Taz and Yap may perform some distinct roles as evidenced by different phenotypes resulting from deletion of each gene (Hossain et al., 2007; Morin-Kensicki et al., 2006), the fact that they share 45% amino acid identity and several protein motifs such as a WW domain, a PDZ-binding motif, and a 14-3-3 binding motif suggests some redundancy between the two factors (Kanai et al., 2000).

We utilized αMHC-Cre transgenic mice and mice harboring conditional mutant alleles of *Taz* and *Yap* to generate mice lacking both Taz and Yap in cardiomyocytes. Deletion of both Taz and Yap in heart leads to perinatal lethality, different from the early

$Taz^{loxP/loxP}; Yap^{loxP/loxP}$ ⊗ $Taz^{loxP/loxP}; Yap^{loxP/+}; \alpha MHC\text{-}Cre$	$Taz^{loxP/loxP}; Yap^{loxP/+}$	$Taz^{loxP/loxP}; Yap^{loxP/loxP}$	$Taz^{loxP/loxP}; Yap^{loxP/+}; \alpha MHC\text{-}Cre$	$Taz^{loxP/loxP}; Yap^{loxP/loxP}; \alpha MHC\text{-}Cre$	Total
# of animals @ P10	32	34	29	0	95
%	33.7	35.8	30.5	0	100
Expected %	25	25	25	25	100

Table IV.2 Perinatal lethality of mice lacking Taz and Yap in the heart. The actual numbers and expected numbers of offsprings from $Taz^{loxP/loxP}; Yap^{loxP/+}; \alpha MHC\text{-}Cre$ and $Taz^{loxP/loxP}; Yap^{loxP/loxP}$ intercrosses are shown. No viable $Taz^{loxP/loxP}; Yap^{loxP/loxP}; \alpha MHC\text{-}Cre$ animal was observed at P10.

embryonic lethality of *ErbB4*, *Tead1*, and *Tbx5* mutant mice (Table. IV.2). This data suggests that there may be other transcriptional coactivators in addition to Taz and Yap that act with ErbB4, Tead1, and Tbx5 in the heart. Moreover, the phenotypic difference might be due to the fact that *Taz* and *Yap* were deleted only in cardiomyocytes in our study while ErbB4, Tead1, and Tbx5 were disrupted globally in other studies. We propose that Yap may work with transcription factors, such as ErbB4, Tead1, and Tbx5, to activate a subset of their downstream target genes, while other coactivators participate to control the rest.

Coactivation of GATA4 by Yap

We show that Yap and GATA4 coactivate the *Angpt1* promoter. GATA4 is a zinc finger transcription factor that binds to a WGATAR DNA motif. Its deletion in mice results in lethality at E8.5 due to cardiac bifida and failure of ventral foregut closure (Molkentin et al., 1997). Early cardiac-specific deletion of *Gata4* utilizing a conditional mutant allele causes embryonic lethality with myocardial thinning, abnormal endocardial cushion development, and right ventricular hypoplasia, while cardiac-specific deletion of *Gata4* at a later time point leads to reduced cardiac function and compromised response to

pressure overload (Oka et al., 2006; Zeisberg et al., 2005). Furthermore, a recent report identified a previously unrecognized function of GATA4 as a regulator of cardiac angiogenesis, highlighting the importance of GATA4 in numerous aspects of cardiac development and disease (Heineke et al., 2007). Our finding that Yap is a GATA4 coactivator suggests that Yap may work with GATA4 in other processes as well as cardiac angiogenesis. For example, Yap may be critical in modulating stress-dependent cardiac remodeling upon pressure overload or exercise. In addition, the function of GATA4 as a global regulator of angiogenesis has been suggested by the fact that GATA4 infection induces angiogenesis in quadriceps muscle (Heineke et al., 2007). Hence, Yap may also serve as a global proangiogenic factor along with GATA4. Our observation of compromised vascular integrity in various tissues upon deletion of *Yap* supports this hypothesis. Analysis of composite mutant mice of *Yap* and *Gata4* will demonstrate the relevance of the interaction between the two factors in vivo and reveal how they cooperate to regulate various processes.

Other possible mechanisms of Yap activity

Although we propose that the primary mechanism of Yap in the heart is to co-activate the *Angpt1* gene with GATA4, we recognize that there are other possible mechanisms of Yap. Further analysis of the *Angpt1* promoter sequence revealed Tead binding sites, in addition to the GATA binding sites (Fig. IV.8A and 8B). The Tead family of transcription factors is composed of four members (Tead1, -2, -3, -4) and shares a DNA binding motif called a TEA domain (Kaneko and DePamphilis, 1998). *Tead1* mutant mice are embryonic lethal at E11.5 accompanied by thin ventricular walls and defective trabeculation, implicating

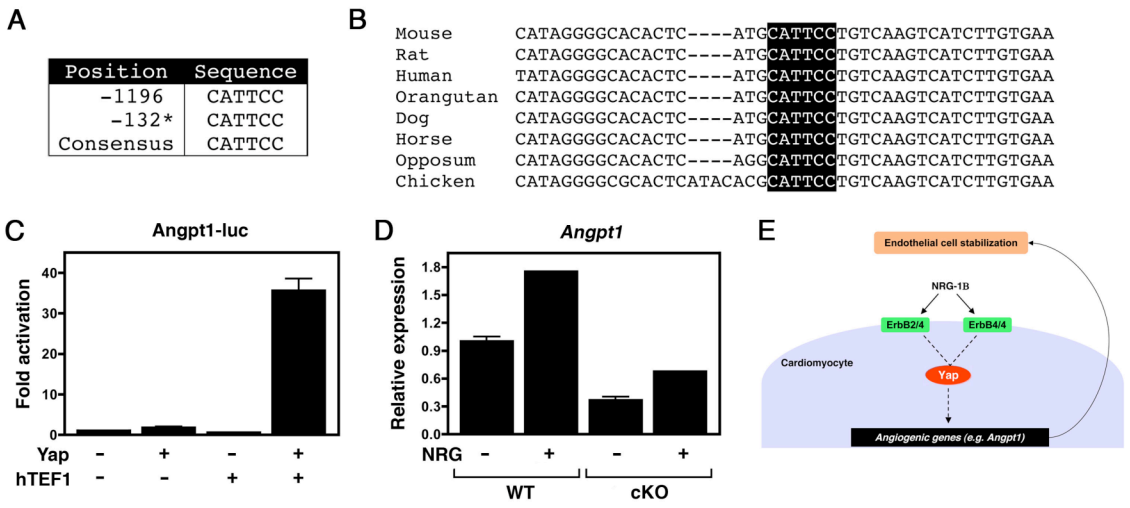

Figure IV.8 Possible alternative mechanisms of Yap activity. (A) Potential Tead binding sites in the *Angpt1* promoter. * denotes the site conserved among mammals. (B) Conserved DNA sequences of the Tead binding site and its flanking region are shown. (C) Coactivation of the *Angpt1* promoter by Yap and Tead1. COS-7 cells were transfected with plasmids expressing a luciferase reporter (100 ng), Yap (50 ng), and/or Tead1 (50 ng). CMV-β-galactosidase expression vector was used to normalize transfection efficiency. hTEF1 indicates a human orthorlog of Tead1. (D) RNA was isolated from left ventricles of $Yap^{loxP/loxP}$ (WT) and $Yap^{loxP/loxP}$; *αMHC-Cre* (cKO) mice 8 hours after Neuregulin-1 (NRG) injection and used to measure the level of *Angpt1* expression by Q-PCR. n = 1 for the injected group per genotype. (E) A diagram showing how Yap may act as a downstream factor of the ErbB signaling pathway in cardiomyocytes to regulate *Angpt1* expression.

an essential role of Tead1 in cardiac development (Chen et al., 1994; Sawada et al., 2008). Furthermore, coactivation of Yap and Tead proteins has been previously reported in vitro and in *Drosophila* (Vassilev et al., 2001; Wu et al., 2008; Zhang et al., 2008). We determined whether Yap and Tead1 coactivate the *Angpt1* promoter by cotransfecting COS-7 cells with a luciferase reporter harboring a 2.5 kb upstream region of the *Angpt1* gene and vectors expressing Yap and Tead1. The addition of both Yap and Tead1 dramatically increased the luciferase activity by 35-fold, indicating that the two factors coactivate the *Angpt1* promoter (Fig. IV.8C).

Another possible mechanism of Yap involves the ErbB signaling pathway, a critical regulator of heart development and function. ErbB receptor ligands are

comprised of the EGF family members, such as neuregulin-1 (NRG-1). NRG-1 secreted from the endothelium activates the ErbB4 homodimer or the ErbB2/ErbB4 heterodimer on cardiomyocytes (Brutsaert, 2003; Garratt et al., 2003). Mice globally lacking NRG-1, ErbB2, or ErB4 die embryonically with defects in ventricular trabeculation (Gassmann et al., 1995; Lee et al., 1995; Meyer and Birchmeier, 1995). Cardiomyocyte-specific *ErbB2*- and *ErbB4*- deficient mice exhibit dilated cardiomyopathy (Iwamoto et al., 2003; Jackson et al., 2003). Furthermore, some breast cancer patients treated with trastuzumab, a monoclonal antibody against ErbB2, develop cardiac dysfunction (Slamon et al., 2001). Based on the fact that activation of ErbB receptors leads to *Angpt1* upregulation (Nakaoka et al., 2007), that Yap associates physically and functionally with ErbB proteins (Komuro et al., 2003), and that disruption of the ErbB signaling pathway results in heart failure (similar to the phenotype of cardiac-specific *Yap* deficient mice), we tested whether upregulation of *Angpt1* following activation of the ErbB pathway was compromised in the *Yap* mutant mice. To activate the ErbB pathway, we injected NRG-1 (5 μg/100 μl PBS) into the inferior vena cava of *Yap* mutant mice and measured the expression level of *Angpt1* in the heart by Q-PCR 8 hours after injection. Our preliminary data showed a minimal increase in *Angpt1* expression in the Yap mutant heart compared to wild type mice, suggesting that Yap may mediate ErbB receptor activation of *Angpt1* in cardiomyocytes (Fig. IV.8D and 8E). Further studies are in progress to test this hypothesis.

Based on the microarray data and the *Yap* mutant phenotype we are investigating the role of Yap in other functional processes, such as protein trafficking and water transport. The most downregulated genes in the *Yap* mutant hearts include a water-

selective channel *aquaporin 4* and several factors involved in protein trafficking, such as *vacuolar protein sorting 35*, *coatomer protein complex*, and *copine 3* (Table IV.1). We are planning to confirm misregulation of these genes by Q-PCR to explore these candidates as potential Yap target genes.

Future directions

To corroborate our model that Yap regulates cardiac angiogenesis by controlling *Angpt1* expression, we will perform further studies to show compromised angiogenesis in *Yap* mutant mice by performing PECAM staining on the $Yap^{loxP/loxP}$*; aMHC-Cre* mutant heart and comparing the cardiac capillary density to the hearts of $Yap^{loxp/loxP}$ mice. We anticipate observing fewer capillaries in the mutant heart. Using a gain of function approach we will use recombinant adenovirus expressing Yap to examine if Yap is sufficient to induce angiogenesis in vitro. We will perform an in vitro angiogenesis assay using HUVECs overlaying cardiomyocytes that are infected with adenovirus expressing Yap. In addition, we plan to mutate the GATA binding sites in the *Angpt1* promoter to confirm that disrupting the GATA binding sites abolishes activation of the *Angpt1* promoter by Yap and GATA4. Finally, we plan to demonstrate genetic interaction between *Yap* and *Gata4* in vivo by generating and analyzing the composite mutant mice ($Gata4^{+/-}$*;* $Yap^{loxP/loxP}$*; aMHC-Cre*).

Implications

Yap has been identified as an oncogene in various cancer systems such as liver cancer model and breast cancer cell lines (Guo et al., 2006; Zender et al., 2006). Moreover,

overexpression of Yap in the liver is sufficient to induce cancer development (Dong et al., 2007). Our finding of Yap as a potential proangiogenic factor implies that Yap may contribute to acceleration of tumorigenesis by promoting angiogenesis in addition to stimulating cell proliferation. Neovascularization is a critical step for tumor progression since a tumor cannot grow beyond a certain size or metastasize without forming new blood vessels. Without neovascularization oxygen and nutrients become limited in tumor cells that are distant from blood vessels (Carmeliet and Jain, 2000). Thus, it will be interesting to see if inhibition of Yap activity in tumors can lead to impaired neovascularization and tumor progression. Our finding suggests a possible novel therapeutic approach to alter angiogenesis by modulating Yap activity.

METHODS

Creation of a conditional *Yap* mutant allele

The *Yap* targeting vector was constructed using pGKneoF2L2DTA harboring two loxP sites encompassing a neomycin resistance cassette flanked by two FRT sites (Hoch and Soriano, 2006). Targeting arm sequences were isolated from 129SvEv genomic DNA by PCR. 5' targeting arm (5 kb), 3' targeting arm (4 kb), and the knockout arm (2 kb) were cloned into the vector using NotI, SmaI, and EcoRV, respectively. The sequence-verified targeting vector was linearized and electroporated into 129SvEv-derived ES cells. Targeting of the mutant allele was screened through Southern blot analysis. 5' probe detects a 6 kb fragment in addition to the wild type 9 kb fragment in the presence of *Yap* targeted allele after PstI digestion. Similarly, EcoRI digestion produces a 10 kb DNA fragment in addition to the wild type 8 kb fragment if homologous recombination

occurred. Targeted ES cells were injected into blastocysts to generate chimeric mice. High-percentage chimeric males were bred with mice expressing FLPe recombinase to remove the neomycin resistance cassette, producing Yap^{loxP} alleles (Rodriguez et al., 2000). PCR genotyping using a forward primer upstream of 5' loxP site, a first reverse primer located in the knockout arm, and a second reverse primer downstream of 3' loxP site produces 600 bp, 457 bp, and 338 bp bands for Yap^{loxP}, Yap^{WT}, and Yap^{floxed} alleles, respectively. Primer sequences for targeting vector construction, Southern probes, and PCR genotyping are available upon request. All animal experimental procedures were reviewed and approved by the Institutional Animal Care and Use Committees of the University of Texas Southwestern Medical Center.

Histology

Hearts were fixed in 4% paraformaldehyde in phosphate-buffered saline, embedded in paraffin, and sectioned at 5 μm intervals. H&E staining and Masson's trichrome staining were performed using standard procedures.

Transthoracic echocardiography

Cardiac function and heart dimensions were evaluated by two-dimensional echocardiography on conscious mice. M-mode tracings were used to measure anterior and posterior wall thicknesses at end diastole and end systole. Left ventricular internal diameter (LVID) was measured as the largest anteroposterior diameter in either diastole (LVIDd) or systole (LVIDs). The data were analyzed by a single observer blinded to

mouse genotypes. Left ventricular FS was calculated according to the following formula: FS (%) = [(LVIDd - LVIDs)/LVIDd] x 100.

RNA analysis

Total RNA was purified from isolated heart ventricles with TRIzol reagent (Invitrogen) according to the manufacturer's instructions. Two micrograms of RNA was used as template to synthesize cDNA using random hexamers. Quantitative PCR was performed using Taqman probes purchased from Applied Biosystems: Acta1, Mm00808218_g1; ANP, Mm01255748_g1; BNP, Mm00435304_g1; Ctgf, Mm00515790_g1; Myh6, Mm00 4403 54_m1; Myh7, Mm01319006_g1; Taz, Mm00513560_m1; Yap, Mm00494240_m1.

Tissue culture and transfection

COS-7 cells were grown in DMEM with 10% FBS. Fugene 6 (Roche) was used for transient transfection according to the manufacturer's instructions. A reporter plasmids containing 2.5 kb of the *Angpt1* locus were generated by PCR (forward primer, 5'-CCTCTTCCTAGATATCCGTGCGTCCCCATG; reverse primer, 5'-CCGTGCCTCCT GCAAAGCTTGCTCTTCTCTTC) and cloned into pGL3-basic (Promega). Expression constructs for Yap and GATA4 have been previously described (Lu et al., 1999; Murakami et al., 2005). An expression vector for hTEF1 was provided by Esther Creemers. Plasmids were co-transfected with 10 ng of a CMV-β-galactosidase reporter plasmid to control for transfection efficiency.

Whole-mount immunostaining

PECAM antibody (MEC13.3) was purchased from Pharmingen (San Diego, CA). Embryos were fixed in 4% paraformaldehyde/PBS overnight at 4 °C before staining. Briefly, samples were blocked in PBSMT (3% skim milk, 0.5% TritonX-100 in PBS), incubated with a PECAM antibody (10 μg/ml) overnight at 4 °C, and treated with 1:100 dilution of horseradish peroxidase-conjugated goat anti-rat IgG (Kirkegaad and Perry Laboratories Inc., Gaithersburg, MD).

ACKNOWLEDGEMENTS

Masao Murakami generated the conditional *Taz* mutant allele.

Bibliography

Agah, R., Frenkel, P.A., French, B.A., Michael, L.H., Overbeek, P.A., and Schneider, M.D. (1997). Gene recombination in postmitotic cells. Targeted expression of Cre recombinase provokes cardiac-restricted, site-specific rearrangement in adult ventricular muscle in vivo. The Journal of clinical investigation *100*, 169-179.

Akiyama, H., Chaboissier, M.C., Martin, J.F., Schedl, A., and de Crombrugghe, B. (2002). The transcription factor Sox9 has essential roles in successive steps of the chondrocyte differentiation pathway and is required for expression of Sox5 and Sox6. Genes & development *16*, 2813-2828.

Antos, C.L., McKinsey, T.A., Frey, N., Kutschke, W., McAnally, J., Shelton, J.M., Richardson, J.A., Hill, J.A., and Olson, E.N. (2002). Activated glycogen synthase-3 beta suppresses cardiac hypertrophy in vivo. Proceedings of the National Academy of Sciences of the United States of America *99*, 907-912.

Arnold, M.A., Kim, Y., Czubryt, M.P., Phan, D., McAnally, J., Qi, X., Shelton, J.M., Richardson, J.A., Bassel-Duby, R., and Olson, E.N. (2007). MEF2C transcription factor controls chondrocyte hypertrophy and bone development. Developmental cell *12*, 377-389.

Backs, J., Backs, T., Bezprozvannaya, S., McKinsey, T.A., and Olson, E.N. (2008). Histone deacetylase 5 acquires calcium/calmodulin-dependent kinase II responsiveness by oligomerization with histone deacetylase 4. Molecular and cellular biology *28*, 3437-3445.

Backs, J., and Olson, E.N. (2006). Control of cardiac growth by histone acetylation/deacetylation. Circulation research *98*, 15-24.

Bagga, S., Bracht, J., Hunter, S., Massirer, K., Holtz, J., Eachus, R., and Pasquinelli, A.E. (2005). Regulation by let-7 and lin-4 miRNAs results in target mRNA degradation. Cell *122*, 553-563.

Bai, X., Wu, L., Liang, T., Liu, Z., Li, J., Li, D., Xie, H., Yin, S., Yu, J., Lin, Q., *et al.* (2007). Overexpression of myocyte enhancer factor 2 and histone hyperacetylation in hepatocellular carcinoma. J Cancer Res Clin Oncol.

Basson, C.T., Bachinsky, D.R., Lin, R.C., Levi, T., Elkins, J.A., Soults, J., Grayzel, D., Kroumpouzou, E., Traill, T.A., Leblanc-Straceski, J., *et al.* (1997). Mutations in human TBX5 [corrected] cause limb and cardiac malformation in Holt-Oram syndrome. Nature genetics *15*, 30-35.

Bi, W., Huang, W., Whitworth, D.J., Deng, J.M., Zhang, Z., Behringer, R.R., and de Crombrugghe, B. (2001). Haploinsufficiency of Sox9 results in defective cartilage primordia and premature skeletal mineralization. Proceedings of the National Academy of Sciences of the United States of America *98*, 6698-6703.

Black, B.L., and Olson, E.N. (1998). Transcriptional control of muscle development by myocyte enhancer factor-2 (MEF2) proteins. Annual review of cell and developmental biology *14*, 167-196.

Bodmer, R. (1993). The gene tinman is required for specification of the heart and visceral muscles in Drosophila. Development (Cambridge, England) *118*, 719-729.

Bruneau, B.G. (2008). The developmental genetics of congenital heart disease. Nature *451*, 943-948.

Bruneau, B.G., Nemer, G., Schmitt, J.P., Charron, F., Robitaille, L., Caron, S., Conner, D.A., Gessler, M., Nemer, M., Seidman, C.E., *et al.* (2001). A murine model of Holt-Oram syndrome defines roles of the T-box transcription factor Tbx5 in cardiogenesis and disease. Cell *106*, 709-721.

Brutsaert, D.L. (2003). Cardiac endothelial-myocardial signaling: its role in cardiac growth, contractile performance, and rhythmicity. Physiological reviews *83*, 59-115.

Buckingham, M., Meilhac, S., and Zaffran, S. (2005). Building the mammalian heart from two sources of myocardial cells. Nature reviews *6*, 826-835.

Bueno, O.F., Wilkins, B.J., Tymitz, K.M., Glascock, B.J., Kimball, T.F., Lorenz, J.N., and Molkentin, J.D. (2002). Impaired cardiac hypertrophic response in Calcineurin Abeta -deficient mice. Proceedings of the National Academy of Sciences of the United States of America *99*, 4586-4591.

Camargo, F.D., Gokhale, S., Johnnidis, J.B., Fu, D., Bell, G.W., Jaenisch, R., and Brummelkamp, T.R. (2007). YAP1 increases organ size and expands undifferentiated progenitor cells. Curr Biol *17*, 2054-2060.

Carmeliet, P., and Jain, R.K. (2000). Angiogenesis in cancer and other diseases. Nature *407*, 249-257.

Chen, Z., Friedrich, G.A., and Soriano, P. (1994). Transcriptional enhancer factor 1 disruption by a retroviral gene trap leads to heart defects and embryonic lethality in mice. Genes & development *8*, 2293-2301.

Czubryt, M.P., and Olson, E.N. (2004). Balancing contractility and energy production: the role of myocyte enhancer factor 2 (MEF2) in cardiac hypertrophy. Recent progress in hormone research *59*, 105-124.

Danielian, P.S., Muccino, D., Rowitch, D.H., Michael, S.K., and McMahon, A.P. (1998). Modification of gene activity in mouse embryos in utero by a tamoxifen-inducible form of Cre recombinase. Curr Biol *8*, 1323-1326.

Denli, A.M., Tops, B.B., Plasterk, R.H., Ketting, R.F., and Hannon, G.J. (2004). Processing of primary microRNAs by the Microprocessor complex. Nature *432*, 231-235.

Dong, J., Feldmann, G., Huang, J., Wu, S., Zhang, N., Comerford, S.A., Gayyed, M.F., Anders, R.A., Maitra, A., and Pan, D. (2007). Elucidation of a universal size-control mechanism in Drosophila and mammals. Cell *130*, 1120-1133.

Du, Y., Spence, S.E., Jenkins, N.A., and Copeland, N.G. (2005). Cooperating cancer-gene identification through oncogenic-retrovirus-induced insertional mutagenesis. Blood *106*, 2498-2505.

Edmondson, D.G., Lyons, G.E., Martin, J.F., and Olson, E.N. (1994). Mef2 gene expression marks the cardiac and skeletal muscle lineages during mouse embryogenesis. Development (Cambridge, England) *120*, 1251-1263.

Flavell, S.W., Cowan, C.W., Kim, T.K., Greer, P.L., Lin, Y., Paradis, S., Griffith, E.C., Hu, L.S., Chen, C., and Greenberg, M.E. (2006). Activity-dependent regulation of MEF2 transcription factors suppresses excitatory synapse number. Science (New York, NY *311*, 1008-1012.

Frey, N., Katus, H.A., Olson, E.N., and Hill, J.A. (2004). Hypertrophy of the heart: a new therapeutic target? Circulation *109*, 1580-1589.

Frey, N., and Olson, E.N. (2003). Cardiac hypertrophy: the good, the bad, and the ugly. Annual review of physiology *65*, 45-79.

Garratt, A.N., Ozcelik, C., and Birchmeier, C. (2003). ErbB2 pathways in heart and neural diseases. Trends in cardiovascular medicine *13*, 80-86.

Gassmann, M., Casagranda, F., Orioli, D., Simon, H., Lai, C., Klein, R., and Lemke, G. (1995). Aberrant neural and cardiac development in mice lacking the ErbB4 neuregulin receptor. Nature *378*, 390-394.

Gebhard, S., Poschl, E., Riemer, S., Bauer, E., Hattori, T., Eberspaecher, H., Zhang, Z., Lefebvre, V., de Crombrugghe, B., and von der Mark, K. (2004). A highly conserved enhancer in mammalian type X collagen genes drives high levels of tissue-specific expression in hypertrophic cartilage in vitro and in vivo. Matrix Biol *23*, 309-322.

Gossett, L.A., Kelvin, D.J., Sternberg, E.A., and Olson, E.N. (1989). A new myocyte-specific enhancer-binding factor that recognizes a conserved element associated with multiple muscle-specific genes. Molecular and cellular biology *9*, 5022-5033.

Gulick, J., Subramaniam, A., Neumann, J., and Robbins, J. (1991). Isolation and characterization of the mouse cardiac myosin heavy chain genes. The Journal of biological chemistry *266*, 9180-9185.

Guo, J., Kleeff, J., Zhao, Y., Li, J., Giese, T., Esposito, I., Buchler, M.W., Korc, M., and Friess, H. (2006). Yes-associated protein (YAP65) in relation to Smad7 expression in human pancreatic ductal adenocarcinoma. International journal of molecular medicine *17*, 761-767.

Heineke, J., Auger-Messier, M., Xu, J., Oka, T., Sargent, M.A., York, A., Klevitsky, R., Vaikunth, S., Duncan, S.A., Aronow, B.J., *et al.* (2007). Cardiomyocyte GATA4 functions as a stress-responsive regulator of angiogenesis in the murine heart. The Journal of clinical investigation *117*, 3198-3210.

Hill, J.A., Karimi, M., Kutschke, W., Davisson, R.L., Zimmerman, K., Wang, Z., Kerber, R.E., and Weiss, R.M. (2000). Cardiac hypertrophy is not a required compensatory response to short-term pressure overload. Circulation *101*, 2863-2869.

Hill, J.A., and Olson, E.N. (2008). Cardiac plasticity. The New England journal of medicine *358*, 1370-1380.

Hirota, K., and Semenza, G.L. (2006). Regulation of angiogenesis by hypoxia-inducible factor 1. Critical reviews in oncology/hematology *59*, 15-26.

Hoch, R.V., and Soriano, P. (2006). Context-specific requirements for Fgfr1 signaling through Frs2 and Frs3 during mouse development. Development (Cambridge, England) *133*, 663-673.

Hoffman, J.I., and Kaplan, S. (2002). The incidence of congenital heart disease. Journal of the American College of Cardiology *39*, 1890-1900.

Hong, J.H., Hwang, E.S., McManus, M.T., Amsterdam, A., Tian, Y., Kalmukova, R., Mueller, E., Benjamin, T., Spiegelman, B.M., Sharp, P.A., *et al.* (2005). TAZ, a transcriptional modulator of mesenchymal stem cell differentiation. Science (New York, NY *309*, 1074-1078.

Hossain, Z., Ali, S.M., Ko, H.L., Xu, J., Ng, C.P., Guo, K., Qi, Z., Ponniah, S., Hong, W., and Hunziker, W. (2007). Glomerulocystic kidney disease in mice with a targeted inactivation of Wwtr1. Proceedings of the National Academy of Sciences of the United States of America *104*, 1631-1636.

Hsieh, P.C., Davis, M.E., Lisowski, L.K., and Lee, R.T. (2006). Endothelial-cardiomyocyte interactions in cardiac development and repair. Annual review of physiology *68*, 51-66.

Huang, J., Wu, S., Barrera, J., Matthews, K., and Pan, D. (2005). The Hippo signaling pathway coordinately regulates cell proliferation and apoptosis by inactivating Yorkie, the Drosophila Homolog of YAP. Cell *122*, 421-434.

Ikeda, T., Kamekura, S., Mabuchi, A., Kou, I., Seki, S., Takato, T., Nakamura, K., Kawaguchi, H., Ikegawa, S., and Chung, U.I. (2004). The combination of SOX5, SOX6, and SOX9 (the SOX trio) provides signals sufficient for induction of permanent cartilage. Arthritis and rheumatism *50*, 3561-3573.

Iwamoto, R., Yamazaki, S., Asakura, M., Takashima, S., Hasuwa, H., Miyado, K., Adachi, S., Kitakaze, M., Hashimoto, K., Raab, G., *et al.* (2003). Heparin-binding EGF-

like growth factor and ErbB signaling is essential for heart function. Proceedings of the National Academy of Sciences of the United States of America *100*, 3221-3226.

Iyer, N.V., Kotch, L.E., Agani, F., Leung, S.W., Laughner, E., Wenger, R.H., Gassmann, M., Gearhart, J.D., Lawler, A.M., Yu, A.Y., *et al.* (1998). Cellular and developmental control of O2 homeostasis by hypoxia-inducible factor 1 alpha. Genes & development *12*, 149-162.

Izumiya, Y., Shiojima, I., Sato, K., Sawyer, D.B., Colucci, W.S., and Walsh, K. (2006). Vascular endothelial growth factor blockade promotes the transition from compensatory cardiac hypertrophy to failure in response to pressure overload. Hypertension *47*, 887-893.

Jackson, L.F., Qiu, T.H., Sunnarborg, S.W., Chang, A., Zhang, C., Patterson, C., and Lee, D.C. (2003). Defective valvulogenesis in HB-EGF and TACE-null mice is associated with aberrant BMP signaling. The EMBO journal *22*, 2704-2716.

Kanai, F., Marignani, P.A., Sarbassova, D., Yagi, R., Hall, R.A., Donowitz, M., Hisaminato, A., Fujiwara, T., Ito, Y., Cantley, L.C., *et al.* (2000). TAZ: a novel transcriptional co-activator regulated by interactions with 14-3-3 and PDZ domain proteins. The EMBO journal *19*, 6778-6791.

Kaneko, K.J., and DePamphilis, M.L. (1998). Regulation of gene expression at the beginning of mammalian development and the TEAD family of transcription factors. Developmental genetics *22*, 43-55.

Karaplis, A.C., Luz, A., Glowacki, J., Bronson, R.T., Tybulewicz, V.L., Kronenberg, H.M., and Mulligan, R.C. (1994). Lethal skeletal dysplasia from targeted disruption of the parathyroid hormone-related peptide gene. Genes & development *8*, 277-289.

Karsenty, G. (2003). The complexities of skeletal biology. Nature *423*, 316-318.

Kelly, B.D., Hackett, S.F., Hirota, K., Oshima, Y., Cai, Z., Berg-Dixon, S., Rowan, A., Yan, Z., Campochiaro, P.A., and Semenza, G.L. (2003). Cell type-specific regulation of angiogenic growth factor gene expression and induction of angiogenesis in nonischemic tissue by a constitutively active form of hypoxia-inducible factor 1. Circulation research *93*, 1074-1081.

Kim, Y., Phan, D., van Rooij, E., Wang, D.Z., McAnally, J., Qi, X., Richardson, J.A., Hill, J.A., Bassel-Duby, R., and Olson, E.N. (2008). The MEF2D transcription factor mediates stress-dependent cardiac remodeling in mice. The Journal of clinical investigation *118*, 124-132.

Komori, T., Yagi, H., Nomura, S., Yamaguchi, A., Sasaki, K., Deguchi, K., Shimizu, Y., Bronson, R.T., Gao, Y.H., Inada, M., *et al.* (1997). Targeted disruption of Cbfa1 results in a complete lack of bone formation owing to maturational arrest of osteoblasts. Cell *89*, 755-764.

Komuro, A., Nagai, M., Navin, N.E., and Sudol, M. (2003). WW domain-containing protein YAP associates with ErbB-4 and acts as a co-transcriptional activator for the carboxyl-terminal fragment of ErbB-4 that translocates to the nucleus. The Journal of biological chemistry *278*, 33334-33341.

Kronenberg, H.M. (2003). Developmental regulation of the growth plate. Nature *423*, 332-336.

Kuo, C.T., Morrisey, E.E., Anandappa, R., Sigrist, K., Lu, M.M., Parmacek, M.S., Soudais, C., and Leiden, J.M. (1997). GATA4 transcription factor is required for ventral morphogenesis and heart tube formation. Genes & development *11*, 1048-1060.

Lanske, B., Karaplis, A.C., Lee, K., Luz, A., Vortkamp, A., Pirro, A., Karperien, M., Defize, L.H., Ho, C., Mulligan, R.C., *et al.* (1996). PTH/PTHrP receptor in early development and Indian hedgehog-regulated bone growth. Science (New York, NY *273*, 663-666.

Lee, K.F., Simon, H., Chen, H., Bates, B., Hung, M.C., and Hauser, C. (1995). Requirement for neuregulin receptor erbB2 in neural and cardiac development. Nature *378*, 394-398.

Lee, Y., Ahn, C., Han, J., Choi, H., Kim, J., Yim, J., Lee, J., Provost, P., Radmark, O., Kim, S., *et al.* (2003). The nuclear RNase III Drosha initiates microRNA processing. Nature *425*, 415-419.

Lefebvre, V., and Smits, P. (2005). Transcriptional control of chondrocyte fate and differentiation. Birth Defects Res C Embryo Today *75*, 200-212.

Li, Q.Y., Newbury-Ecob, R.A., Terrett, J.A., Wilson, D.I., Curtis, A.R., Yi, C.H., Gebuhr, T., Bullen, P.J., Robson, S.C., Strachan, T., *et al.* (1997). Holt-Oram syndrome is caused by mutations in TBX5, a member of the Brachyury (T) gene family. Nature genetics *15*, 21-29.

Liang, Q., De Windt, L.J., Witt, S.A., Kimball, T.R., Markham, B.E., and Molkentin, J.D. (2001). The transcription factors GATA4 and GATA6 regulate cardiomyocyte hypertrophy in vitro and in vivo. The Journal of biological chemistry *276*, 30245-30253.

Lilly, B., Zhao, B., Ranganayakulu, G., Paterson, B.M., Schulz, R.A., and Olson, E.N. (1995). Requirement of MADS domain transcription factor D-MEF2 for muscle formation in Drosophila. Science (New York, NY *267*, 688-693.

Lim, L.P., Lau, N.C., Garrett-Engele, P., Grimson, A., Schelter, J.M., Castle, J., Bartel, D.P., Linsley, P.S., and Johnson, J.M. (2005). Microarray analysis shows that some microRNAs downregulate large numbers of target mRNAs. Nature *433*, 769-773.

Lin, Q., Lu, J., Yanagisawa, H., Webb, R., Lyons, G.E., Richardson, J.A., and Olson, E.N. (1998). Requirement of the MADS-box transcription factor MEF2C for vascular development. Development (Cambridge, England) *125*, 4565-4574.

Lin, Q., Schwarz, J., Bucana, C., and Olson, E.N. (1997). Control of mouse cardiac morphogenesis and myogenesis by transcription factor MEF2C. Science (New York, NY *276*, 1404-1407.

Logan, M., Martin, J.F., Nagy, A., Lobe, C., Olson, E.N., and Tabin, C.J. (2002). Expression of Cre Recombinase in the developing mouse limb bud driven by a Prxl enhancer. Genesis *33*, 77-80.

Long, F., Zhang, X.M., Karp, S., Yang, Y., and McMahon, A.P. (2001). Genetic manipulation of hedgehog signaling in the endochondral skeleton reveals a direct role in the regulation of chondrocyte proliferation. Development (Cambridge, England) *128*, 5099-5108.

Lu, J., McKinsey, T.A., Nicol, R.L., and Olson, E.N. (2000a). Signal-dependent activation of the MEF2 transcription factor by dissociation from histone deacetylases. Proceedings of the National Academy of Sciences of the United States of America *97*, 4070-4075.

Lu, J., McKinsey, T.A., Zhang, C.L., and Olson, E.N. (2000b). Regulation of skeletal myogenesis by association of the MEF2 transcription factor with class II histone deacetylases. Molecular cell *6*, 233-244.

Lu, J.R., McKinsey, T.A., Xu, H., Wang, D.Z., Richardson, J.A., and Olson, E.N. (1999). FOG-2, a heart- and brain-enriched cofactor for GATA transcription factors. Molecular and cellular biology *19*, 4495-4502.

Lyons, I., Parsons, L.M., Hartley, L., Li, R., Andrews, J.E., Robb, L., and Harvey, R.P. (1995). Myogenic and morphogenetic defects in the heart tubes of murine embryos lacking the homeo box gene Nkx2-5. Genes & development *9*, 1654-1666.

Martin, J.F., Miano, J.M., Hustad, C.M., Copeland, N.G., Jenkins, N.A., and Olson, E.N. (1994). A Mef2 gene that generates a muscle-specific isoform via alternative mRNA splicing. Molecular and cellular biology *14*, 1647-1656.

Mathew, J., Sleight, P., Lonn, E., Johnstone, D., Pogue, J., Yi, Q., Bosch, J., Sussex, B., Probstfield, J., and Yusuf, S. (2001). Reduction of cardiovascular risk by regression of electrocardiographic markers of left ventricular hypertrophy by the angiotensin-converting enzyme inhibitor ramipril. Circulation *104*, 1615-1621.

McFadden, D.G., Barbosa, A.C., Richardson, J.A., Schneider, M.D., Srivastava, D., and Olson, E.N. (2005). The Hand1 and Hand2 transcription factors regulate expansion of the embryonic cardiac ventricles in a gene dosage-dependent manner. Development (Cambridge, England) *132*, 189-201.

McKinsey, T.A., and Olson, E.N. (2005). Toward transcriptional therapies for the failing heart: chemical screens to modulate genes. The Journal of clinical investigation *115*, 538-546.

McKinsey, T.A., Zhang, C.L., Lu, J., and Olson, E.N. (2000). Signal-dependent nuclear export of a histone deacetylase regulates muscle differentiation. Nature *408*, 106-111.

McKinsey, T.A., Zhang, C.L., and Olson, E.N. (2002). MEF2: a calcium-dependent regulator of cell division, differentiation and death. Trends in biochemical sciences *27*, 40-47.

McLeod, M.J. (1980). Differential staining of cartilage and bone in whole mouse fetuses by alcian blue and alizarin red S. Teratology *22*, 299-301.

Merscher, S., Funke, B., Epstein, J.A., Heyer, J., Puech, A., Lu, M.M., Xavier, R.J., Demay, M.B., Russell, R.G., Factor, S., *et al.* (2001). TBX1 is responsible for cardiovascular defects in velo-cardio-facial/DiGeorge syndrome. Cell *104*, 619-629.

Meyer, D., and Birchmeier, C. (1995). Multiple essential functions of neuregulin in development. Nature *378*, 386-390.

Miska, E.A., Karlsson, C., Langley, E., Nielsen, S.J., Pines, J., and Kouzarides, T. (1999). HDAC4 deacetylase associates with and represses the MEF2 transcription factor. The EMBO journal *18*, 5099-5107.

Molkentin, J.D., Black, B.L., Martin, J.F., and Olson, E.N. (1995). Cooperative activation of muscle gene expression by MEF2 and myogenic bHLH proteins. Cell *83*, 1125-1136.

Molkentin, J.D., Firulli, A.B., Black, B.L., Martin, J.F., Hustad, C.M., Copeland, N., Jenkins, N., Lyons, G., and Olson, E.N. (1996). MEF2B is a potent transactivator expressed in early myogenic lineages. Molecular and cellular biology *16*, 3814-3824.

Molkentin, J.D., Lin, Q., Duncan, S.A., and Olson, E.N. (1997). Requirement of the transcription factor GATA4 for heart tube formation and ventral morphogenesis. Genes & development *11*, 1061-1072.

Molkentin, J.D., Lu, J.R., Antos, C.L., Markham, B., Richardson, J., Robbins, J., Grant, S.R., and Olson, E.N. (1998). A calcineurin-dependent transcriptional pathway for cardiac hypertrophy. Cell *93*, 215-228.

Molkentin, J.D., Tymitz, K.M., Richardson, J.A., and Olson, E.N. (2000). Abnormalities of the genitourinary tract in female mice lacking GATA5. Molecular and cellular biology *20*, 5256-5260.

Moretti, A., Caron, L., Nakano, A., Lam, J.T., Bernshausen, A., Chen, Y., Qyang, Y., Bu, L., Sasaki, M., Martin-Puig, S., *et al.* (2006). Multipotent embryonic isl1+ progenitor cells lead to cardiac, smooth muscle, and endothelial cell diversification. Cell *127*, 1151-1165.

Morin, S., Charron, F., Robitaille, L., and Nemer, M. (2000). GATA-dependent recruitment of MEF2 proteins to target promoters. The EMBO journal *19*, 2046-2055.

Morin-Kensicki, E.M., Boone, B.N., Howell, M., Stonebraker, J.R., Teed, J., Alb, J.G., Magnuson, T.R., O'Neal, W., and Milgram, S.L. (2006). Defects in yolk sac vasculogenesis, chorioallantoic fusion, and embryonic axis elongation in mice with targeted disruption of Yap65. Molecular and cellular biology *26*, 77-87.

Murakami, M., Nakagawa, M., Olson, E.N., and Nakagawa, O. (2005). A WW domain protein TAZ is a critical coactivator for TBX5, a transcription factor implicated in Holt-Oram syndrome. Proceedings of the National Academy of Sciences of the United States of America *102*, 18034-18039.

Naiche, L.A., Harrelson, Z., Kelly, R.G., and Papaioannou, V.E. (2005). T-box genes in vertebrate development. Annual review of genetics *39*, 219-239.

Nakagawa, O., Arnold, M., Nakagawa, M., Hamada, H., Shelton, J.M., Kusano, H., Harris, T.M., Childs, G., Campbell, K.P., Richardson, J.A.*, et al.* (2005). Centronuclear myopathy in mice lacking a novel muscle-specific protein kinase transcriptionally regulated by MEF2. Genes & development *19*, 2066-2077.

Nakaoka, Y., Nishida, K., Narimatsu, M., Kamiya, A., Minami, T., Sawa, H., Okawa, K., Fujio, Y., Koyama, T., Maeda, M.*, et al.* (2007). Gab family proteins are essential for postnatal maintenance of cardiac function via neuregulin-1/ErbB signaling. The Journal of clinical investigation *117*, 1771-1781.

Nakashima, K., and de Crombrugghe, B. (2003). Transcriptional mechanisms in osteoblast differentiation and bone formation. Trends Genet *19*, 458-466.

Nakashima, K., Zhou, X., Kunkel, G., Zhang, Z., Deng, J.M., Behringer, R.R., and de Crombrugghe, B. (2002). The novel zinc finger-containing transcription factor osterix is required for osteoblast differentiation and bone formation. Cell *108*, 17-29.

Naya, F.J., Black, B.L., Wu, H., Bassel-Duby, R., Richardson, J.A., Hill, J.A., and Olson, E.N. (2002). Mitochondrial deficiency and cardiac sudden death in mice lacking the MEF2A transcription factor. Nature medicine *8*, 1303-1309.

Nishio, Y., Dong, Y., Paris, M., O'Keefe, R.J., Schwarz, E.M., and Drissi, H. (2006). Runx2-mediated regulation of the zinc finger Osterix/Sp7 gene. Gene *372*, 62-70.

Oka, T., Maillet, M., Watt, A.J., Schwartz, R.J., Aronow, B.J., Duncan, S.A., and Molkentin, J.D. (2006). Cardiac-specific deletion of Gata4 reveals its requirement for hypertrophy, compensation, and myocyte viability. Circulation research *98*, 837-845.

Olsen, B.R., Reginato, A.M., and Wang, W. (2000). Bone development. Annual review of cell and developmental biology *16*, 191-220.

Olson, E.N. (1993). Signal transduction pathways that regulate skeletal muscle gene expression. Molecular endocrinology (Baltimore, Md *7*, 1369-1378.

Olson, E.N., and Srivastava, D. (1996). Molecular pathways controlling heart development. Science (New York, NY *272*, 671-676.

Orkin, S.H., Shivdasani, R.A., Fujiwara, Y., and McDevitt, M.A. (1998). Transcription factor GATA-1 in megakaryocyte development. Stem cells (Dayton, Ohio) *16 Suppl 2*, 79-83.

Otto, F., Thornell, A.P., Crompton, T., Denzel, A., Gilmour, K.C., Rosewell, I.R., Stamp, G.W., Beddington, R.S., Mundlos, S., Olsen, B.R., *et al*. (1997). Cbfa1, a candidate gene for cleidocranial dysplasia syndrome, is essential for osteoblast differentiation and bone development. Cell *89*, 765-771.

Pan, D. (2007). Hippo signaling in organ size control. Genes & development *21*, 886-897.

Passier, R., Zeng, H., Frey, N., Naya, F.J., Nicol, R.L., McKinsey, T.A., Overbeek, P., Richardson, J.A., Grant, S.R., and Olson, E.N. (2000). CaM kinase signaling induces cardiac hypertrophy and activates the MEF2 transcription factor in vivo. The Journal of clinical investigation *105*, 1395-1406.

Potthoff, M.J., Wu, H., Arnold, M.A., Shelton, J.M., Backs, J., McAnally, J., Qi, X., Bassel-Duby, R., and Olson, E.N. (2007). Modulation of myofiber identity and function by histone deacetylase degradation and MEF2 activation. The Journal of clinical investigation *In press*.

Rakusan, K., Flanagan, M.F., Geva, T., Southern, J., and Van Praagh, R. (1992). Morphometry of human coronary capillaries during normal growth and the effect of age in left ventricular pressure-overload hypertrophy. Circulation *86*, 38-46.

Redkar, A., Montgomery, M., and Litvin, J. (2001). Fate map of early avian cardiac progenitor cells. Development (Cambridge, England) *128*, 2269-2279.

Reim, I., and Frasch, M. (2005). The Dorsocross T-box genes are key components of the regulatory network controlling early cardiogenesis in Drosophila. Development (Cambridge, England) *132*, 4911-4925.

Reim, I., Mohler, J.P., and Frasch, M. (2005). Tbx20-related genes, mid and H15, are required for tinman expression, proper patterning, and normal differentiation of cardioblasts in Drosophila. Mechanisms of development *122*, 1056-1069.

Reiter, J.F., Alexander, J., Rodaway, A., Yelon, D., Patient, R., Holder, N., and Stainier, D.Y. (1999). Gata5 is required for the development of the heart and endoderm in zebrafish. Genes & development *13*, 2983-2995.

Risebro, C.A., Smart, N., Dupays, L., Breckenridge, R., Mohun, T.J., and Riley, P.R. (2006). Hand1 regulates cardiomyocyte proliferation versus differentiation in the developing heart. Development (Cambridge, England) *133*, 4595-4606.

Rodriguez, C.I., Buchholz, F., Galloway, J., Sequerra, R., Kasper, J., Ayala, R., Stewart, A.F., and Dymecki, S.M. (2000). High-efficiency deleter mice show that FLPe is an alternative to Cre-loxP. Nature genetics *25*, 139-140.

Rosamond, W., Flegal, K., Furie, K., Go, A., Greenlund, K., Haase, N., Hailpern, S.M., Ho, M., Howard, V., Kissela, B., *et al.* (2008). Heart disease and stroke statistics--2008 update: a report from the American Heart Association Statistics Committee and Stroke Statistics Subcommittee. Circulation *117*, e25-146.

Sakai, K., and Miyazaki, J. (1997). A transgenic mouse line that retains Cre recombinase activity in mature oocytes irrespective of the cre transgene transmission. Biochemical and biophysical research communications *237*, 318-324.

Sawada, A., Kiyonari, H., Ukita, K., Nishioka, N., Imuta, Y., and Sasaki, H. (2008). Redundant roles of Tead1 and Tead2 in notochord development and the regulation of cell proliferation and survival. Molecular and cellular biology *28*, 3177-3189.

Schipani, E., Lanske, B., Hunzelman, J., Luz, A., Kovacs, C.S., Lee, K., Pirro, A., Kronenberg, H.M., and Juppner, H. (1997). Targeted expression of constitutively active receptors for parathyroid hormone and parathyroid hormone-related peptide delays endochondral bone formation and rescues mice that lack parathyroid hormone-related peptide. Proceedings of the National Academy of Sciences of the United States of America *94*, 13689-13694.

Schultheiss, T.M., Xydas, S., and Lassar, A.B. (1995). Induction of avian cardiac myogenesis by anterior endoderm. Development (Cambridge, England) *121*, 4203-4214.

Shalizi, A., Gaudilliere, B., Yuan, Z., Stegmuller, J., Shirogane, T., Ge, Q., Tan, Y., Schulman, B., Harper, J.W., and Bonni, A. (2006). A calcium-regulated MEF2 sumoylation switch controls postsynaptic differentiation. Science (New York, NY *311*, 1012-1017.

Shimoyama, M., Hayashi, D., Takimoto, E., Zou, Y., Oka, T., Uozumi, H., Kudoh, S., Shibasaki, F., Yazaki, Y., Nagai, R., *et al.* (1999). Calcineurin plays a critical role in pressure overload-induced cardiac hypertrophy. Circulation *100*, 2449-2454.

Shiojima, I., Sato, K., Izumiya, Y., Schiekofer, S., Ito, M., Liao, R., Colucci, W.S., and Walsh, K. (2005). Disruption of coordinated cardiac hypertrophy and angiogenesis contributes to the transition to heart failure. The Journal of clinical investigation *115*, 2108-2118.

Shohet, R.V., and Garcia, J.A. (2007). Keeping the engine primed: HIF factors as key regulators of cardiac metabolism and angiogenesis during ischemia. Journal of molecular medicine (Berlin, Germany) *85*, 1309-1315.

Slamon, D.J., Leyland-Jones, B., Shak, S., Fuchs, H., Paton, V., Bajamonde, A., Fleming, T., Eiermann, W., Wolter, J., Pegram, M., *et al.* (2001). Use of chemotherapy plus a

monoclonal antibody against HER2 for metastatic breast cancer that overexpresses HER2. The New England journal of medicine *344*, 783-792.

Smits, P., Li, P., Mandel, J., Zhang, Z., Deng, J.M., Behringer, R.R., de Crombrugghe, B., and Lefebvre, V. (2001). The transcription factors L-Sox5 and Sox6 are essential for cartilage formation. Developmental cell *1*, 277-290.

Srivastava, D., Cserjesi, P., and Olson, E.N. (1995). A subclass of bHLH proteins required for cardiac morphogenesis. Science (New York, NY *270*, 1995-1999.

Srivastava, D., and Olson, E.N. (2000). A genetic blueprint for cardiac development. Nature *407*, 221-226.

Srivastava, D., Thomas, T., Lin, Q., Kirby, M.L., Brown, D., and Olson, E.N. (1997). Regulation of cardiac mesodermal and neural crest development by the bHLH transcription factor, dHAND. Nature genetics *16*, 154-160.

St-Jacques, B., Hammerschmidt, M., and McMahon, A.P. (1999). Indian hedgehog signaling regulates proliferation and differentiation of chondrocytes and is essential for bone formation. Genes & development *13*, 2072-2086.

Suri, C., Jones, P.F., Patan, S., Bartunkova, S., Maisonpierre, P.C., Davis, S., Sato, T.N., and Yancopoulos, G.D. (1996). Requisite role of angiopoietin-1, a ligand for the TIE2 receptor, during embryonic angiogenesis. Cell *87*, 1171-1180.

Takeda, S., Bonnamy, J.P., Owen, M.J., Ducy, P., and Karsenty, G. (2001). Continuous expression of Cbfa1 in nonhypertrophic chondrocytes uncovers its ability to induce hypertrophic chondrocyte differentiation and partially rescues Cbfa1-deficient mice. Genes & development *15*, 467-481.

Tallquist, M.D., and Soriano, P. (2000). Epiblast-restricted Cre expression in MORE mice: a tool to distinguish embryonic vs. extra-embryonic gene function. Genesis *26*, 113-115.

Tomanek, R.J., Searls, J.C., and Lachenbruch, P.A. (1982). Quantitative changes in the capillary bed during developing, peak, and stabilized cardiac hypertrophy in the spontaneously hypertensive rat. Circulation research *51*, 295-304.

van Oort, R.J., van Rooij, E., Bourajjaj, M., Schimmel, J., Jansen, M.A., van der Nagel, R., Doevendans, P.A., Schneider, M.D., van Echteld, C.J., and De Windt, L.J. (2006). MEF2 activates a genetic program promoting chamber dilation and contractile dysfunction in calcineurin-induced heart failure. Circulation *114*, 298-308.

van Rooij, E., Sutherland, L.B., Liu, N., Williams, A.H., McAnally, J., Gerard, R.D., Richardson, J.A., and Olson, E.N. (2006). A signature pattern of stress-responsive microRNAs that can evoke cardiac hypertrophy and heart failure. Proceedings of the National Academy of Sciences of the United States of America *103*, 18255-18260.

van Rooij, E., Sutherland, L.B., Qi, X., Richardson, J.A., Hill, J., and Olson, E.N. (2007). Control of stress-dependent cardiac growth and gene expression by a microRNA. Science (New York, NY *316*, 575-579.

Vassilev, A., Kaneko, K.J., Shu, H., Zhao, Y., and DePamphilis, M.L. (2001). TEAD/TEF transcription factors utilize the activation domain of YAP65, a Src/Yes-associated protein localized in the cytoplasm. Genes & development *15*, 1229-1241.

Vega, R.B., Harrison, B.C., Meadows, E., Roberts, C.R., Papst, P.J., Olson, E.N., and McKinsey, T.A. (2004a). Protein kinases C and D mediate agonist-dependent cardiac hypertrophy through nuclear export of histone deacetylase 5. Molecular and cellular biology *24*, 8374-8385.

Vega, R.B., Matsuda, K., Oh, J., Barbosa, A.C., Yang, X., Meadows, E., McAnally, J., Pomajzl, C., Shelton, J.M., Richardson, J.A., *et al.* (2004b). Histone deacetylase 4 controls chondrocyte hypertrophy during skeletogenesis. Cell *119*, 555-566.

Verdin, E., Dequiedt, F., and Kasler, H.G. (2003). Class II histone deacetylases: versatile regulators. Trends Genet *19*, 286-293.

Vortkamp, A., Lee, K., Lanske, B., Segre, G.V., Kronenberg, H.M., and Tabin, C.J. (1996). Regulation of rate of cartilage differentiation by Indian hedgehog and PTH-related protein. Science (New York, NY *273*, 613-622.

Wang, D.Z., Valdez, M.R., McAnally, J., Richardson, J., and Olson, E.N. (2001). The Mef2c gene is a direct transcriptional target of myogenic bHLH and MEF2 proteins during skeletal muscle development. Development (Cambridge, England) *128*, 4623-4633.

Wang, L., Fan, C., Topol, S.E., Topol, E.J., and Wang, Q. (2003). Mutation of MEF2A in an inherited disorder with features of coronary artery disease. Science (New York, NY *302*, 1578-1581.

Wang, X., Tang, X., Gong, X., Albanis, E., Friedman, S.L., and Mao, Z. (2004). Regulation of hepatic stellate cell activation and growth by transcription factor myocyte enhancer factor 2. Gastroenterology *127*, 1174-1188.

Wegner, M. (1999). From head to toes: the multiple facets of Sox proteins. Nucleic acids research *27*, 1409-1420.

Weir, E.C., Philbrick, W.M., Amling, M., Neff, L.A., Baron, R., and Broadus, A.E. (1996). Targeted overexpression of parathyroid hormone-related peptide in chondrocytes causes chondrodysplasia and delayed endochondral bone formation. Proceedings of the National Academy of Sciences of the United States of America *93*, 10240-10245.

Wilkins, B.J., De Windt, L.J., Bueno, O.F., Braz, J.C., Glascock, B.J., Kimball, T.F., and Molkentin, J.D. (2002). Targeted disruption of NFATc3, but not NFATc4, reveals an

intrinsic defect in calcineurin-mediated cardiac hypertrophic growth. Molecular and cellular biology *22*, 7603-7613.

Wu, H., Rothermel, B., Kanatous, S., Rosenberg, P., Naya, F.J., Shelton, J.M., Hutcheson, K.A., DiMaio, J.M., Olson, E.N., Bassel-Duby, R., *et al.* (2001). Activation of MEF2 by muscle activity is mediated through a calcineurin-dependent pathway. The EMBO journal *20*, 6414-6423.

Wu, S., Liu, Y., Zheng, Y., Dong, J., and Pan, D. (2008). The TEAD/TEF family protein Scalloped mediates transcriptional output of the Hippo growth-regulatory pathway. Developmental cell *14*, 388-398.

Wu, S.M., Fujiwara, Y., Cibulsky, S.M., Clapham, D.E., Lien, C.L., Schultheiss, T.M., and Orkin, S.H. (2006). Developmental origin of a bipotential myocardial and smooth muscle cell precursor in the mammalian heart. Cell *127*, 1137-1150.

Xin, M., Davis, C.A., Molkentin, J.D., Lien, C.L., Duncan, S.A., Richardson, J.A., and Olson, E.N. (2006). A threshold of GATA4 and GATA6 expression is required for cardiovascular development. Proceedings of the National Academy of Sciences of the United States of America *103*, 11189-11194.

Xu, J., Gong, N.L., Bodi, I., Aronow, B.J., Backx, P.H., and Molkentin, J.D. (2006). Myocyte enhancer factors 2A and 2C induce dilated cardiomyopathy in transgenic mice. The Journal of biological chemistry *281*, 9152-9162.

Yagi, R., Chen, L.F., Shigesada, K., Murakami, Y., and Ito, Y. (1999). A WW domain-containing yes-associated protein (YAP) is a novel transcriptional co-activator. The EMBO journal *18*, 2551-2562.

Yang, S.H., Galanis, A., and Sharrocks, A.D. (1999). Targeting of p38 mitogen-activated protein kinases to MEF2 transcription factors. Molecular and cellular biology *19*, 4028-4038.

Yelon, D., Ticho, B., Halpern, M.E., Ruvinsky, I., Ho, R.K., Silver, L.M., and Stainier, D.Y. (2000). The bHLH transcription factor hand2 plays parallel roles in zebrafish heart and pectoral fin development. Development (Cambridge, England) *127*, 2573-2582.

Yoshida, C.A., Yamamoto, H., Fujita, T., Furuichi, T., Ito, K., Inoue, K., Yamana, K., Zanma, A., Takada, K., Ito, Y., *et al.* (2004). Runx2 and Runx3 are essential for chondrocyte maturation, and Runx2 regulates limb growth through induction of Indian hedgehog. Genes & development *18*, 952-963.

Youn, H.D., Chatila, T.A., and Liu, J.O. (2000). Integration of calcineurin and MEF2 signals by the coactivator p300 during T-cell apoptosis. The EMBO journal *19*, 4323-4331.

Yu, K., Xu, J., Liu, Z., Sosic, D., Shao, J., Olson, E.N., Towler, D.A., and Ornitz, D.M. (2003). Conditional inactivation of FGF receptor 2 reveals an essential role for FGF

signaling in the regulation of osteoblast function and bone growth. Development (Cambridge, England) *130*, 3063-3074.

Zaidi, S.K., Sullivan, A.J., Medina, R., Ito, Y., van Wijnen, A.J., Stein, J.L., Lian, J.B., and Stein, G.S. (2004). Tyrosine phosphorylation controls Runx2-mediated subnuclear targeting of YAP to repress transcription. The EMBO journal *23*, 790-799.

Zeisberg, E.M., Ma, Q., Juraszek, A.L., Moses, K., Schwartz, R.J., Izumo, S., and Pu, W.T. (2005). Morphogenesis of the right ventricle requires myocardial expression of Gata4. The Journal of clinical investigation *115*, 1522-1531.

Zelzer, E., Mamluk, R., Ferrara, N., Johnson, R.S., Schipani, E., and Olsen, B.R. (2004). VEGFA is necessary for chondrocyte survival during bone development. Development (Cambridge, England) *131*, 2161-2171.

Zelzer, E., and Olsen, B.R. (2003). The genetic basis for skeletal diseases. Nature *423*, 343-348.

Zender, L., Spector, M.S., Xue, W., Flemming, P., Cordon-Cardo, C., Silke, J., Fan, S.T., Luk, J.M., Wigler, M., Hannon, G.J., *et al.* (2006). Identification and validation of oncogenes in liver cancer using an integrative oncogenomic approach. Cell *125*, 1253-1267.

Zeng, Q., and Hong, W. (2008). The emerging role of the hippo pathway in cell contact inhibition, organ size control, and cancer development in mammals. Cancer cell *13*, 188-192.

Zhang, C.L., McKinsey, T.A., Chang, S., Antos, C.L., Hill, J.A., and Olson, E.N. (2002). Class II histone deacetylases act as signal-responsive repressors of cardiac hypertrophy. Cell *110*, 479-488.

Zhang, L., Ren, F., Zhang, Q., Chen, Y., Wang, B., and Jiang, J. (2008). The TEAD/TEF family of transcription factor Scalloped mediates Hippo signaling in organ size control. Developmental cell *14*, 377-387.

Zhao, B., Wei, X., Li, W., Udan, R.S., Yang, Q., Kim, J., Xie, J., Ikenoue, T., Yu, J., Li, L., *et al.* (2007). Inactivation of YAP oncoprotein by the Hippo pathway is involved in cell contact inhibition and tissue growth control. Genes & development *21*, 2747-2761.

Zhou, G., Lefebvre, V., Zhang, Z., Eberspaecher, H., and de Crombrugghe, B. (1998). Three high mobility group-like sequences within a 48-base pair enhancer of the Col2a1 gene are required for cartilage-specific expression in vivo. The Journal of biological chemistry *273*, 14989-14997.